Supplementary Information

for

Stable Lead-halide Perovskite Quantum Dots as Efficient Visible Light Photocatalysts for Organic Transformations

Sajan Pradhan[†], Deshaj Bhujel[†], Bikram Gurung[†], Debesh Sharma[†], Siddhant Basel[†], Sagarmani Rasaily[†], Surakcha Thapa[†], Sukanya Borthakur[‡], Wai Li Ling[§], Lakshi Saikia[‡], Peter Reiss[§], Anand Pariyar[†] and Sudarsan Tamang[†,*]

[†]Department of Chemistry, School of Physical Sciences, Sikkim University, Sikkim 737102, India.
[‡]Department of Material Science, North East Institute of Science and Technology (NEIST), Assam 785006, India.
[§]Univ. Grenoble Alpes, CEA, CNRS, IRIG, 38000 Grenoble, France.
*stamang@cus.ac.in

Table of Contents

1. General Information

Materials and general considerations: Chemicals, such as Cesium carbonate (Cs_2CO_3, 99.9%, Sigma-Aldrich), lead acetate ($Pb(OAc)_2$ (Sigma-Aldrich), molecular bromine (Br_2, ≥99%, Sigma-Aldrich), oleic acid (OA, technical grade, Sigma-Aldrich), 1-octadecene (ODE, technical grade, Sigma-Aldrich), oleylamine (OLAM, technical grade, Sigma-Aldrich), anhydrous toluene (99.8%, Sigma-Aldrich), and anhydrous hexane (95%, Sigma-Aldrich) were purchased. Degassed OA and OLAM were prepared by heating the OA or OLAM at 120 °C under vacuum overnight and stored in a glovebox. The analytical thin layer chromatography (TLC) was carried out for monitoring the progress of the reactions using silica gel 60 F_{254} precoated plates. Visualizations of the spots were accomplished with a UV lamp or I_2 stain. Silica gel 60–120 mesh size was used for column chromatographic purification using a combination of ethyl acetate and petroleum ether as the eluent for synthesizing starting materials. Unless otherwise mentioned, all of the reactions were carried out in 4 mL vial under open air in appropriate solvents. The starting materials such as 1,4-DHP (**1a-j**)[1], 1,2-DHP (**3a-f**)[2], pyrazolines (**7a-e**)[3] and dihydrobenzothiazole (**5a**–**c**)[4] were prepared by following the earlier reports. Unless otherwise mentioned, all of the commercial reagents were used as received without further purification.

2. Characterization Methods

Nuclear magnetic resonance (**NMR**): ^{1}H NMR, ^{13}C NMR spectra were recorded on a Bruker ASCEND™ (400 MHZ) spectrometer using $CDCl_3$ solvent as an internal reference. Multiplicity was indicated as follows: s (singlet), d (doublet), t (triplet), q (quartet), and m (multiplet).

Blue light LED: A Kessil 160WE Tuna blue LED Light (40W) purchased from Kessil company was used as source of blue light. The maximum absorption wavelength and the illumination intensity of the blue LED Light are 461 nm and 0.363mW/cm^2 at a distance of 100 cm respectively.

Cyclic voltammetry (CV) measurement: The electrochemical data were collected using a BASI INC, USA/EPSILON electrochemistry workstation. The working electrode (Pt disc electrode, 1.6 mm diameter), the counter electrode (Pt wire) and the reference electrode (Ag/AgCl electrode) were used to construct a three-electrode cell employing

tetrabutylammonium perchlorate (TBAP, 0.1 M) as the supporting electrolyte. Before experiments, all solutions were purged with N_2 for 10 min. Experimental conditions: scan range from 1.5V to -1.5V, scan rate of 50 mV s^{-1}. The potentials obtained from CV experiments were converted to the HOMO/LUMO levels assuming the potential of ferrocene/ferrocenium (Fc/Fc^+) redox pair to be –4.80 eV as a reference from the vacuum level. The formal redox potential of Fc/Fc^+ couple (reference) *vs* Ag/AgCl in acetonitrile and 1:4 v/v mixture of acetonitrile and toluene using 0.1 M TBAP as supporting electrolyte were respectively 0.43 and 0.47 V. The energy levels (eV) were estimated from $-E_{HOMO/LUMO} = E^{redox}$ (*vs* Ag/AgCl) + 4.44 eV = E^{redox} (*vs* Fc/Fc^+) + 4.8 eV.[5–7] For model substrates, E_{HOMO} = [-e(E_{ox} -0.43 + 4.8)] eV and for photocatalyst, E_{HOMO} = [-e(E_{ox} -0.47 + 4.8)] eV; E_{LUMO} = [-e(E_{red} -0.47 + 4.8)] eV.

Thermogravimetric analysis (TGA): TGA data was collected from TA Instruments, TGA Q50 Analyzer.

UV-Vis spectrophotometer: The UV-Visible absorption spectra were collected using Perkin Elmer spectrophotometer (scan rate: 480 nm/s) and Agilent Technologies Cary 100 UV-vis.

Vis-NIR spectrofluorometer: The PL spectra of $CsPbBr_3$ NCs were collected using HORIBA Scientific spectrophotometer (Model: PTI-QM 510).

Transmission electron microscopy (**TEM**): TEM images were taken in JEOL-JEM-2100 Plus electron microscope. HRTEM images were obtained using 200 kV electron source. Samples were prepared by drop-casting of nanocrystal solution in hexane on a carbon coated copper grid purchased from EMS, the grids were kept overnight in a vacuum desiccator. The average particle size was measured using 400 particles. The lattice plane was obtained from lattice fringes. Image J software was used for calculations.

Fourier Transform Infrared Spectroscopy (FTIR): FT-IR spectra were obtained using Bruker ALPHA E, 200396.

X-ray Diffractometer (XRD): The purified NCs in hexane were drop-casted on a clean and dry glass slide. The film on glass slide was run under the Rigaku Miniflex II X-Ray diffractometer using Cu Kα (λ= 1.54 Å) as the incident radiation (30 kV and 15 mA).

X-ray Photoelectron Spectroscopy (XPS): XPS samples were fabricated in glovebox on carbon coated silicon wafers to minimize charging. XPS spectra were obtained using Thermo-Scientific ESCALAB Xi^+ spectrometer with Al Kα (1486.7 eV) X-ray source. For high

resolution spectra constant analyser energy (CAE) of 50 eV was used and for survey spectra (CAE) of 100 eV.

3. Experimental Details

$CsPbBr_3$ perovskite NCs synthesis:

Cs-oleate solution (**solution A**) was prepared by dissolving 812.5 mg (2.5 mmol) of Cs_2CO_3 in 20 mL ODE and 2.5 mL OA. The solution was degassed at room temperature for 15 min, followed by degassing at 120 °C under vacuum until the clear solution was obtained. The solution was kept in an inert atmosphere at 100 °C for further use.

Synthesis of $CsPbBr_3$ perovskite NCs (QD1, QD2 and QD3). QD1 was prepared by following our previous report[8] with slight modification and the method has been scaled up by 8 times. In 100 mL three-necked round-bottom flask, 260 mg (0.8 mmol) of lead acetate, 1.6 mL OA, 4 mL of OLAM, 4.8 mmol of Br_2 solution and 32 mL of ODE were mixed and degassed under vacuum at room temperature for 30 min, followed by degassing under vacuum at 120 °C for 30 min. Subsequently, the temperature was maintained at 200 °C under inert (N_2) atmosphere. To this solution, 3.2 mL of Cs-oleate (**solution A**) was quickly injected. The reaction was quenched quickly after 10s by immersing the reaction flask in ice-bath. The bright yellow-green colloidal solution was subjected to centrifugation at 10000 rpm for 10 min to precipitate $CsPbBr_3$ NCs (**QD1**, emission wavelength = 517 nm; edge-length = 9.4 ± 0.4 nm) by adding 40 mL *tert*-butanol or 40 mL dry toluene and the same step was repeated for one more time. While quantum dots of other sizes such as **QD2** (emission wavelength = 521 nm; edge-length = 15.7 ± 0.7 nm) and **QD3** (emission wavelength = 510 nm; edge-length = 7.2 ± 0.5 nm) were prepared by injecting Cs-oleate (**solution A**) at 230 °C and at 175 °C repectively.

Purification: After preparation, the colloidal solution of as-prepared $CsPbBr_3$ QDs (**QD1**) were precipitated and washed for two times**. First Washing**: The colloidal solution of **QD1** were subjected to the centrifugation at 10000 rpm for 10 min to precipitate **QD1** in the form of jelly mass using either tert-butanol or dry toluene**. Second Washing:** The precipitated jelly mass of **QD1** was further dispersed in either tert-butanol or dry toluene followed by performing the same purification step led to the precipitation of **QD1** as a hardened jelly mass. After degassing under reduced pressure, the hardened jelly mass can be crushed into a powdered form (Figure S20).

Synthesis of conventional $CsPbBr_3$ perovskite CQDs (QD4). QD4 was prepared by following earlier report[9,10]. Briefly, in 25 mL three-necked round-bottom flask, $PbBr_2$ (0.069 g, 0.188 mmol), 0.5 mL OA, 0.5 mL of OLAM and 5 mL of ODE were mixed and degassed under vacuum at room temperature for 1 h, followed by degassing under vacuum at 120 °C for 1 h. After complete dissolution of $PbBr_2$, the reaction temperature was increased to 170 °C. To this solution, 0.4 mL of Cs-oleate (**solution A**) was quickly injected. The reaction was quenched quickly after 10s by immersing the reaction flask in ice-bath. The bright yellow-green colloidal solution was subjected to centrifugation at 5000 rpm for 10 min to precipitate $CsPbBr_3$ NCs (**QD4**) by adding 6 mL toluene.

Synthesis of polydisperse bulk-type $CsPbBr_3$ perovskite NCs (PNCs). The bulk $CsPbBr_3$ perovskite (*ca*. 3~100 nm) **(PNCs)** was synthesized by following previous report.[11] The mixture of 4 mL oleic acid and 0.75 mL *n*-octylamine in 250 mL hexane was vigorously stirred at room temperature followed by dropwise addition of 1.0 mmol $PbBr_2$ dissolved in 1.5 mL DMF and 1.0 mmol CsBr dissolved in 1.0 mL H_2O. The formation of emulsion took place and the color of solution turned from clear to slightly white. Next, to break the emulsion 200 mL of acetone was added. The polydisperse $CsPbBr_3$ nanoparticles were finally collected by centrifugation at 7000 rpm for 10 min.

General procedure for oxidative aromatization: To a 4 mL vial, $CsPbBr_3$ perovskite NCs (**QD1**, 1 mg), starting material (0.1 mmol) and 3 mL 1,2-dichloroethane solvent (DCE) were taken under open air at a distance of 6 cm away from light source and subjected to irradiation with blue LED light for appropriate times. The progress of the reaction was monitored by thin layer chromatographic (TLC) technique. Unless otherwise mentioned, after the completion of the reaction, the reaction mixture was passed through short plug of silica gel and concentrated under vacuum to afford the pure aromatized products.

Table S1. Optimization studies for photocatalytic synthesis of pyridine derivatives **1a**[a]

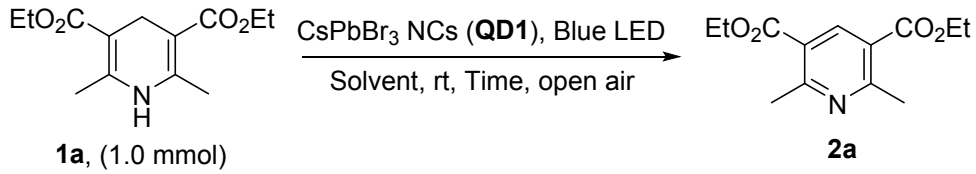

1a, (1.0 mmol) **2a**

Entry	Catalyst	Solvent	Time (min)	Yield (%)
1	**QD1**	DCM	120	85
2[b]	**QD1**	DCM	120	trace

3[c]	-	DCM	120	20
4	**QD1**	**DCE**	**50**	**95**
5	**QD1**	Toluene	150	82
6	**QD1**	$CHCl_3$	90	80
7	**QD1**	1,4-dioxan	120	82
8	**QD1**	THF	90	84
9	**QD1**	ethyl acetate	60	86

[a] Unless noted otherwise, all reactions were carried out with 1.0 mmol of **1a** and 1 mg of **QD1** in 3 mL of appropriate solvent. (b) Reaction was performed in the absence of light. (c) Reaction was conducted without photocatalyst under irradiation with blue LED light.

4. Stability studies and characterization of CQDs

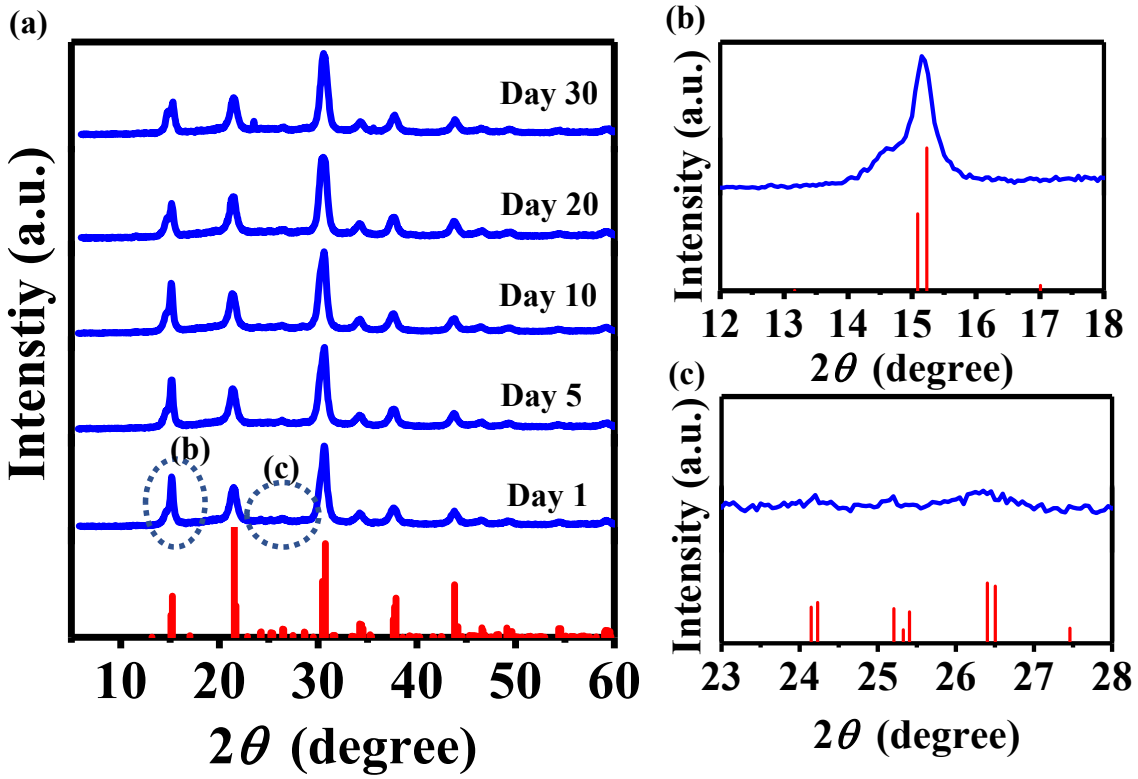

Figure S1. (a) X-ray diffraction patterns of **QD1** displaying stability of the film coated on a glass substrate for at least 30 days in the air under ambient conditions. The red bar indicates orthorhombic (JCPDS 96-451-0746) $CsPbBr_3$ perovskite phase; The dotted circles indicate magnified area around 14 degree (2-theta) in figure (b) and area between ~20 to 30 degree in figure (c).

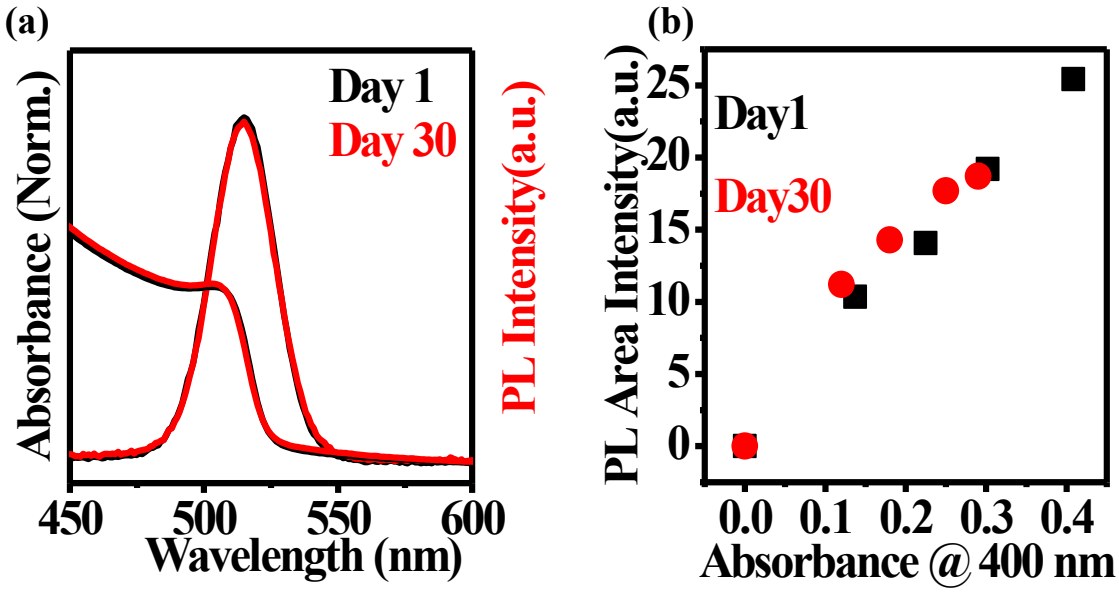

Figure S2. (a) UV-vis absorption and normalised PL (excitation wavelength 400 nm) spectra of **QD1** in hexane measured at day 1 (black) and after storage for 30 days (red); (b) integrated photoluminescence vs. absorbance plot of **QD1** sample of 1st day (black) and 30th day (red).

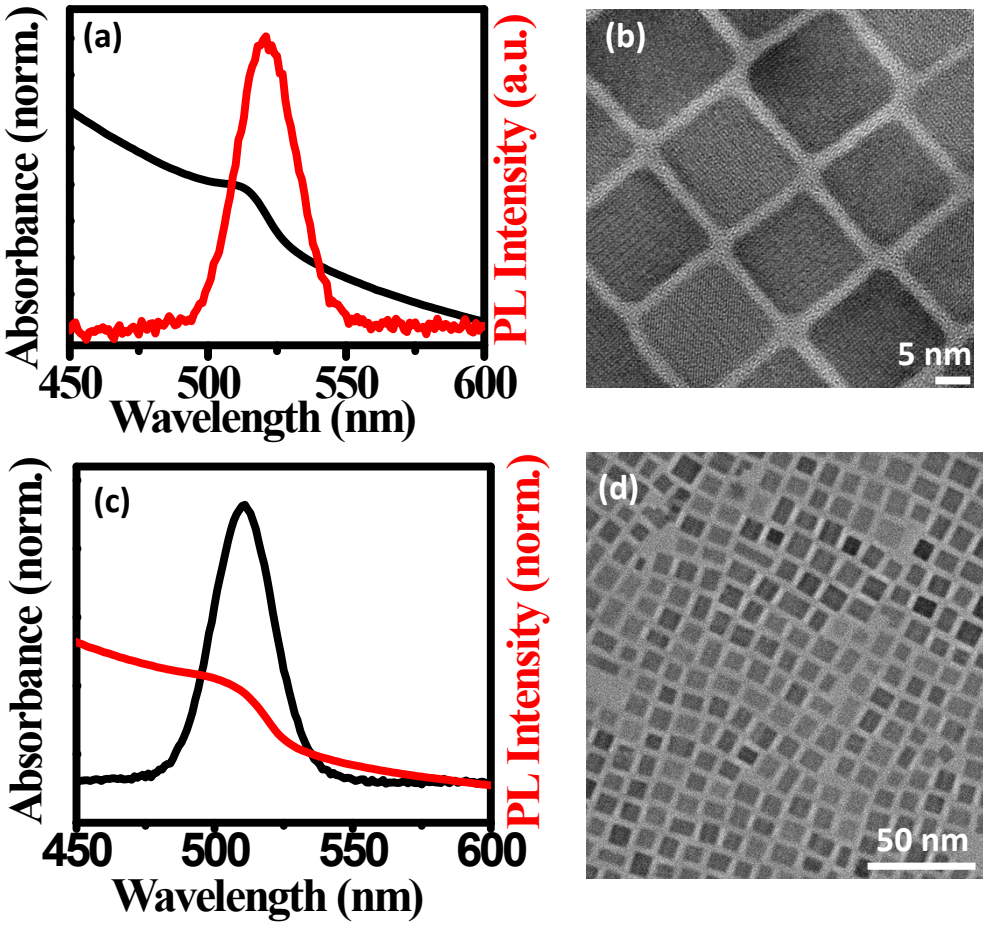

Figure S3. (a) UV-vis absorption and normalised PL spectra of **QD2** dispersed in hexane showing an emission wavelength of 521 nm; (b) TEM image of **QD2** displaying the cubic shape with an average edge length of 15.7 ± 0.7 nm; (c) UV-vis absorption and normalised PL spectra of **QD3** dispersed in hexane showing an emission wavelength of 510 nm; (d) TEM image of **QD3** (cube edge length = 7.2 ± 0.5 nm).

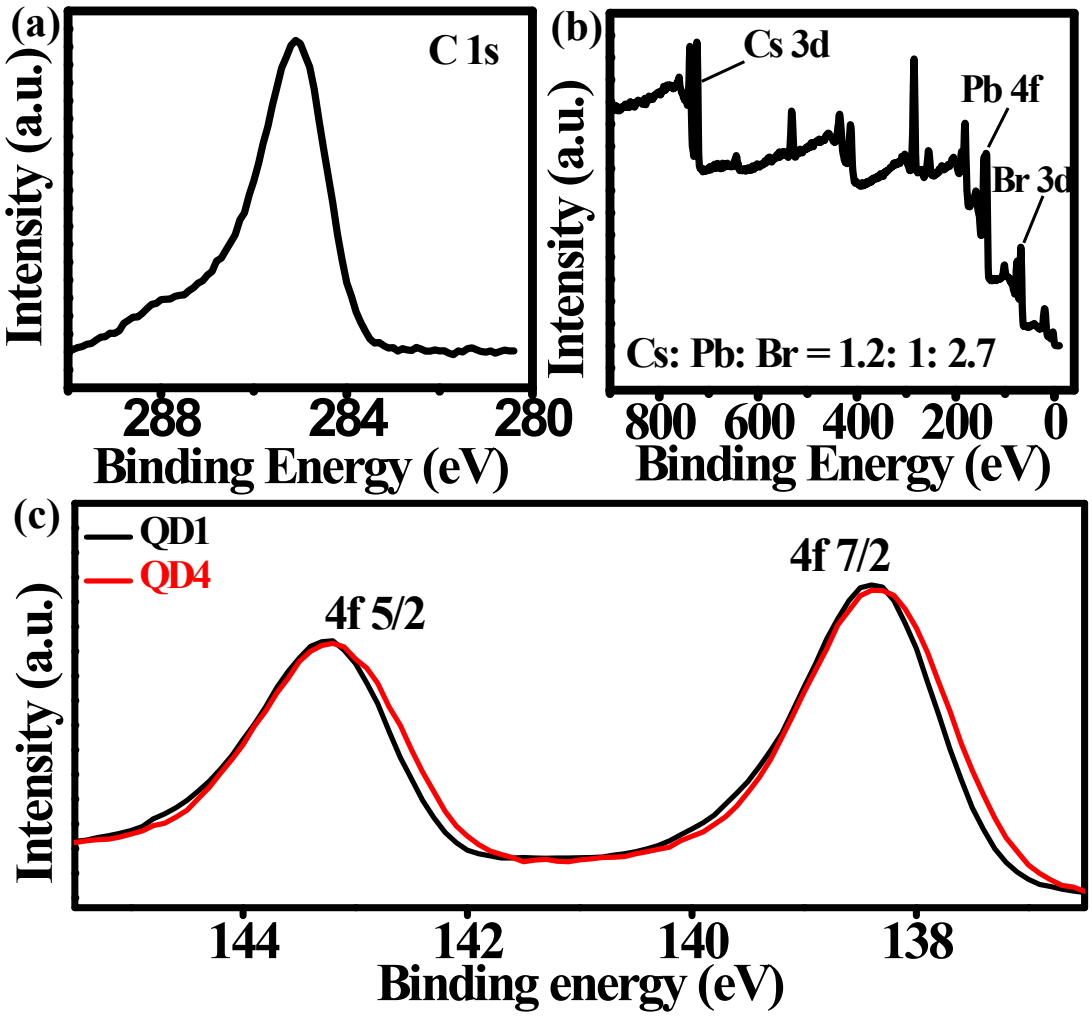

Figure S4. (a) XPS C 1s spectra of **QD1** calibrated at 285.0 eV; (b) XPS survey spectrum of **QD4** (Cs: Pb: Br~1.2: 1: 2.7); (c) The Pb 4f core level spectra of **QD1** (show peaks at 138.39 and 143.25 eV) and **QD4** (show peaks at 138.34 and 143.20 eV) which are assigned to the Pb $4f_{7/2}$ and Pb $4f_{5/2}$ levels.

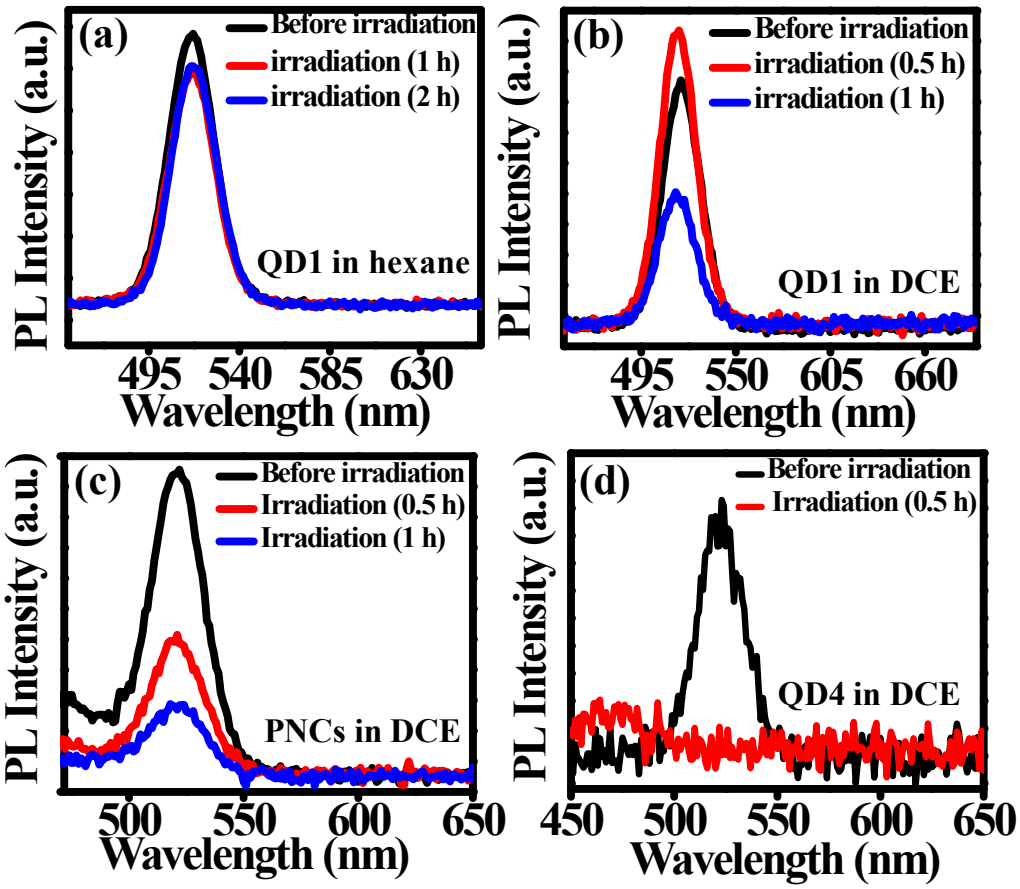

Figure S5. (a) the PL spectra of **QD1** dispersed in hexane before illumination and after irradiation with blue LED for 2 h; (b) the PL spectra of **QD1** dispersed in 1,2-dichloroethane (DCE) before illumination and after irradiation with blue LED for 1 h; (c) the PL spectra of **PNCs** dispersed in 1,2-dichloroethane (DCE) before illumination and after irradiation with blue LED for 1 h; (d) the PL spectra of **QD4** dispersed in 1,2-dichloroethane (DCE) before illumination and after irradiation with blue LED for 0.5 h.

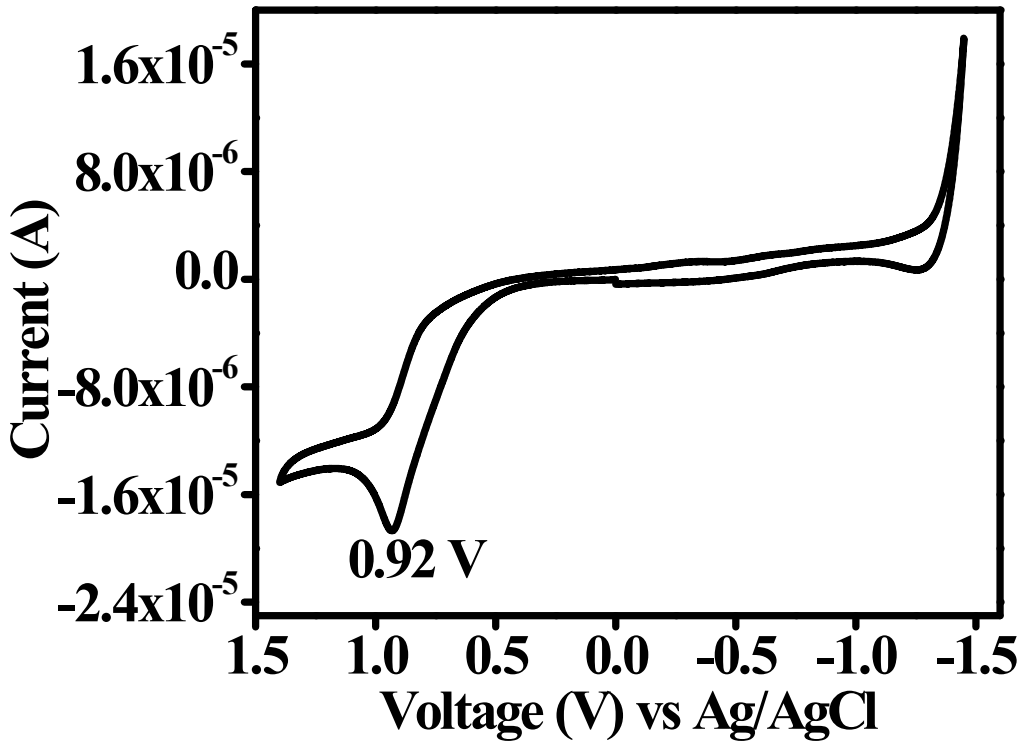

Figure S6. Cyclic voltammogram of diethyl 2,6-dimethyl-1,4-dihydropyridine-3,5-dicarboxylate (**1a**) using TBAP (0.1 M) supporting electrolyte in N_2 saturated CH_3CN. E_{ox} = 0.92 V *vs* Ag/AgCl.

5. Kinetics study for the construction of Hammett plot

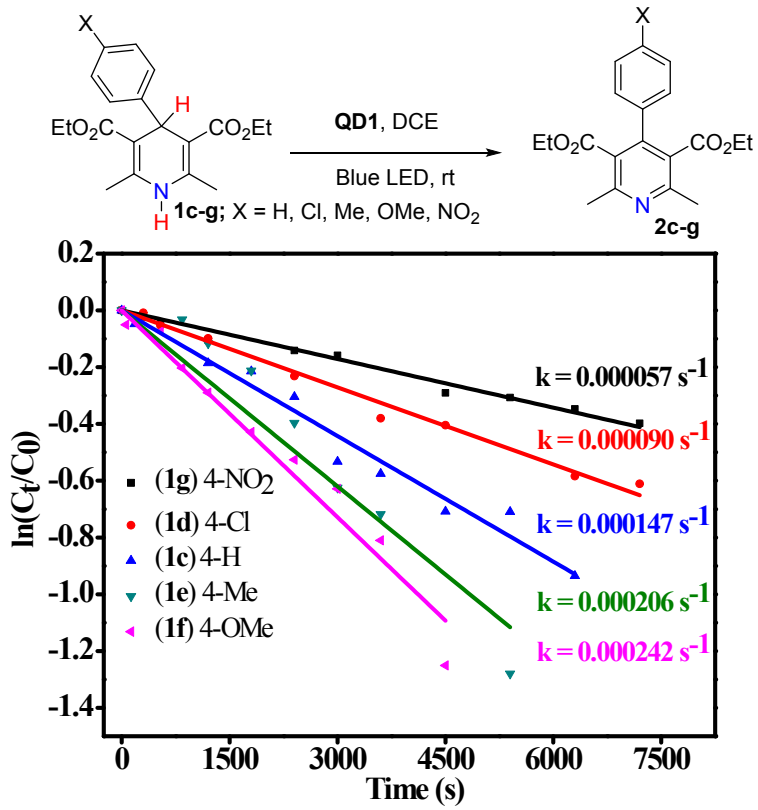

Figure S7. Rate constants of the **QD1** catalysed oxidative aromatization of various *para*-substituted 1,4-aryl-DHP (**1c-g**) obtained through a plot of $\ln(C_t/C_0)$ versus time.

Table S2: Kinetic study of oxidative aromatization of *para*-substituted 1,4-aryl-DHP (**1c-g**) for the construction of Hammett plot

Substituent (1)	**k**	**k_X/k_H**	**$\ln(k_X/k_H)$exp**	**σ**	**σ^+**	**$\sigma^\bullet$**
4-NO_2 (**1g**)	5.71E-05	3.92E-01	-0.949501604	0.778	0.79	0.76
4-Cl (**1d**)	9.05E-05	6.21E-01	-0.488817974	0.227	0.11	0.18
H (**1c**)	1.47E-04	1.01E+00	0	0	0	0
4-Me (**1e**)	2.07E-04	1.40E+00	0.337396874	-0.17	-0.31	0.39
4-OMe (**1f**)	2.43E-04	1.67E+00	0.498669037	-0.268	-0.78	0.42

Table S3: Kinetic study of oxidative aromatization *para*-substituted 1,4-aryl-DHP (**1c-g**) for the construction of Jiang's dual-parameter for Hammett plot. The values of reaction constants were obtained by performing multiple co-efficient linear regression (MCLR).

Substituent (1)	**k**	**k_X/k_H**	**$\ln(k_X/k_H)$exp**	**σ_{mb}**	**$\sigma^{\bullet}_{JJ}$**	**$(-0.885\sigma_{mb}) + (-0.766\sigma^{\bullet}_{JJ})$**
4-NO_2 (**1g**)	5.71E-05	3.92E-01	-0.949501604	0.86	0.36	-1.03686
4-Cl (**1d**)	9.05E-05	6.21E-01	-0.488817974	0.11	0.22	-0.26587
H (**1c**)	1.47E-04	1.01E+00	0	0	0	0
4-Me (**1e**)	2.07E-04	1.40E+00	0.337396874	-0.29	0.15	0.14175
4-OMe (**1f**)	2.43E-04	1.67E+00	0.498669037	-0.77	0.23	0.50527

6. Copies of CV spectra:

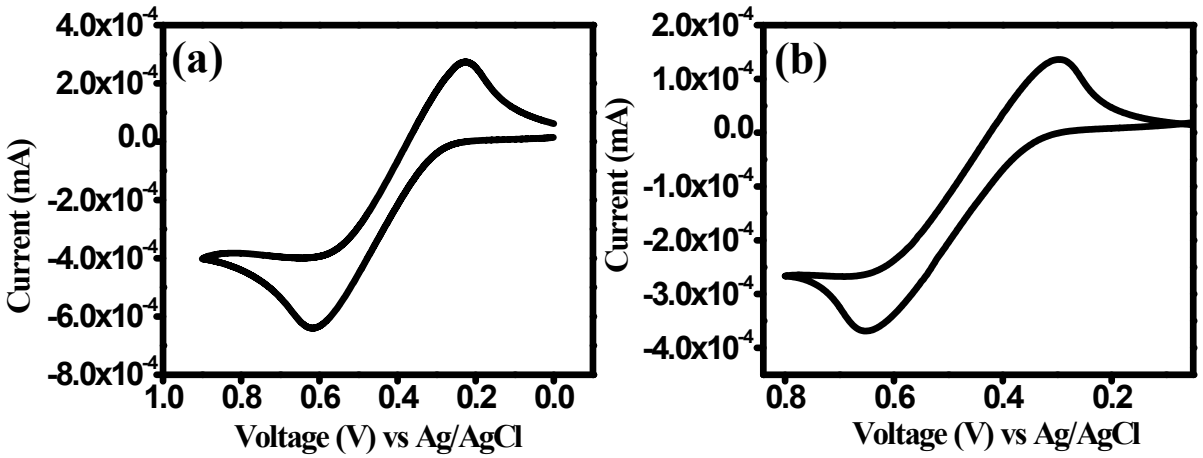

Figure S8. Cyclic voltammogram of ferrocene/ferrocenium (Fc/Fc^+) redox pair using TBAP (0.1 M) supporting electrolyte: (a) in N_2 saturated CH_3CN (solvent system for organic substrate), E_{redox} = 0.43 V *vs* Ag/AgCl and (b) in N_2 saturated 1:4 v/v of CH_3CN and toluene (solvent system for quantum dots), E_{redox} = 0.47 V *vs* Ag/AgCl.

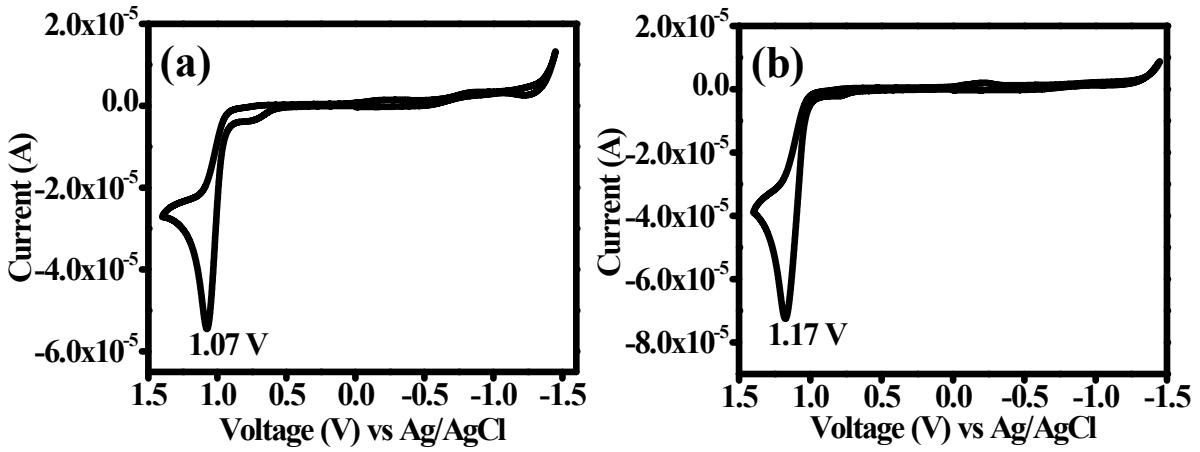

Figure S9. (a) Cyclic voltammogram of diethyl 2,4,6-trimethyl-1,4-dihydropyridine-3,5-dicarboxylate (**1b**) using TBAP (0.1 M) in N_2 saturated CH_3CN. E_{ox} = 1.07 V *vs* Ag/AgCl; (b) Cyclic voltammogram of diethyl 4-(4-chlorophenyl)-2,6-dimethyl-1,4-dihydropyridine-3,5-dicarboxylate (**1d**) using TBAP (0.1 M) in N_2 saturated CH_3CN. E_{ox} = 1.17 V *vs* Ag/AgCl.

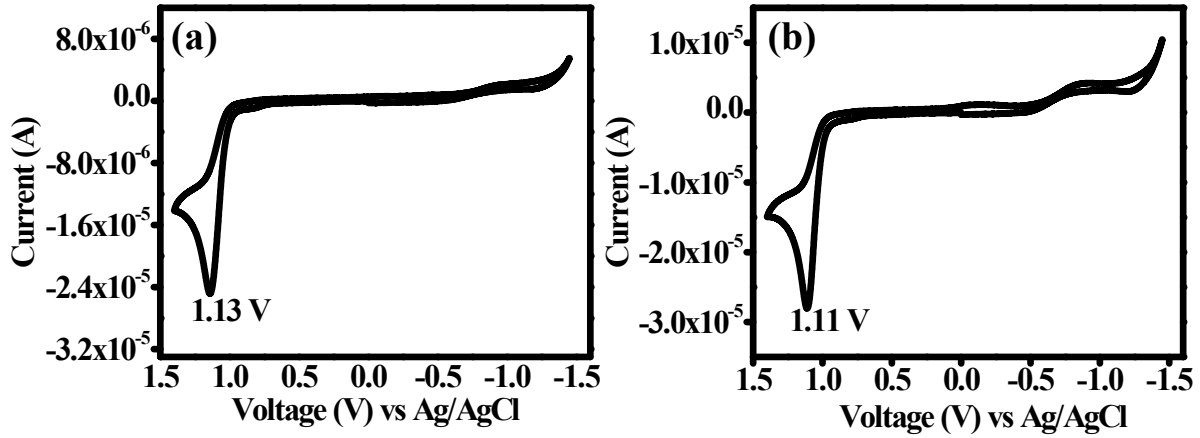

Figure S10. (a) Cyclic voltammogram of diethyl 2,6-dimethyl-4-(*p*-tolyl)-1,4-dihydropyridine-3,5-dicarboxylate (**1e**) using TBAP (0.1 M) in N_2 saturated CH_3CN. E_{ox} = 1.13 V *vs* Ag/AgCl. (b) Cyclic voltammogram of diethyl 4-(4-methoxyphenyl)-2,6-dimethyl-1,4-dihydropyridine-3,5-dicarboxylate (**1f**) using TBAP (0.1 M) in N_2 saturated CH_3CN. E_{ox} = 1.11 V *vs* Ag/AgCl.

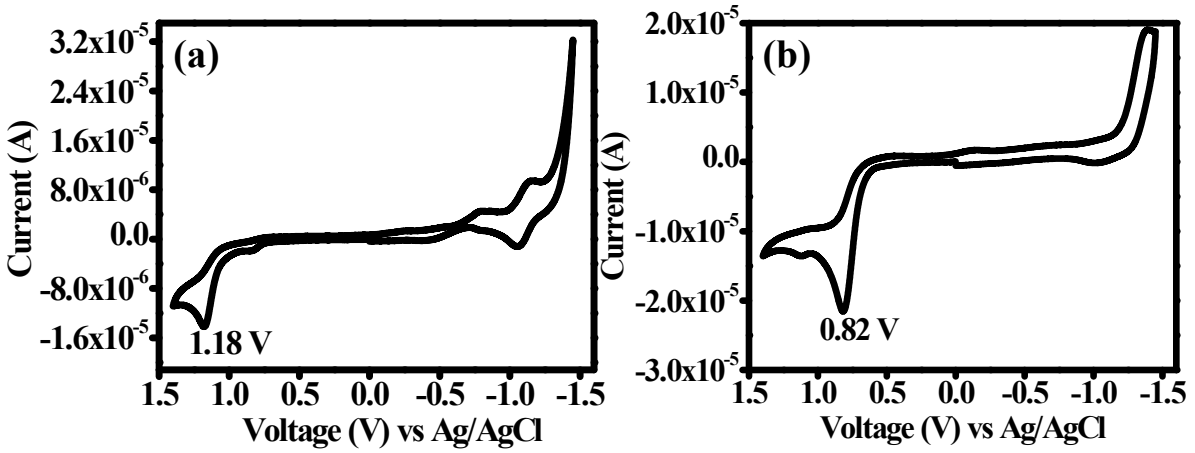

Figure S11. (a) Cyclic voltammogram of diethyl 2,6-dimethyl-4-(4-nitrophenyl)-1,4-dihydropyridine-3,5-dicarboxylate (**1g**) using TBAP (0.1 M) in N_2 saturated CH_3CN. E_{ox} = 1.18 V *vs* Ag/AgCl. (b) Cyclic voltammogram of diethyl 2-(4-chlorophenyl)-4,6-dimethyl-1,2-dihydropyridine-3,5-dicarboxylate (**3b**) using TBAP (0.1 M) in N_2 saturated CH_3CN. E_{ox} = 0.82 V *vs* Ag/AgCl.

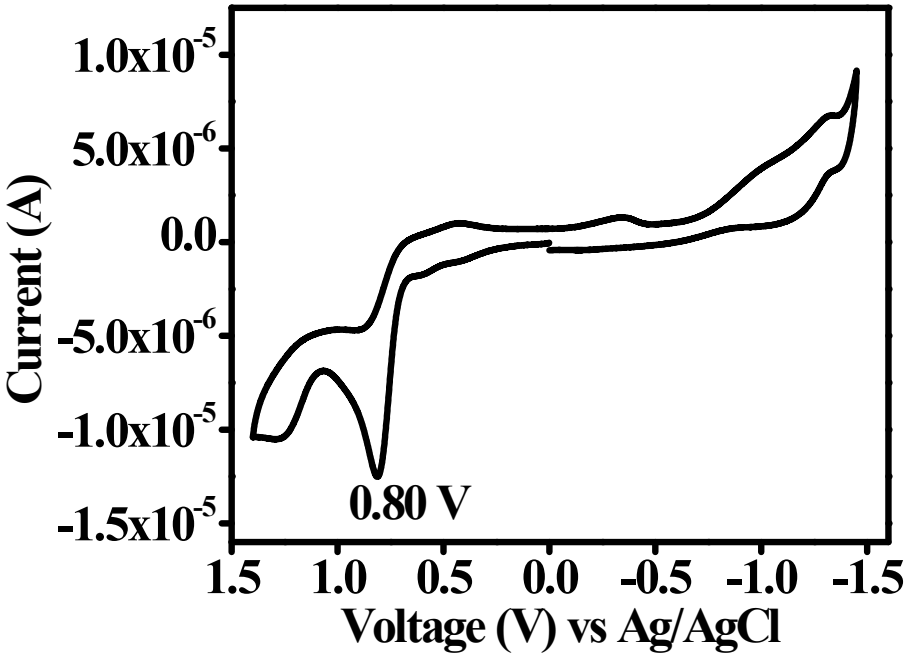

Figure S12. Cyclic voltammogram of 2-phenyl-2,3-dihydrobenzo[*d*]thiazole (**5a**) using TBAP (0.1 M) in N_2 saturated CH_3CN. E_{ox} = 0.80 V *vs* Ag/AgCl.

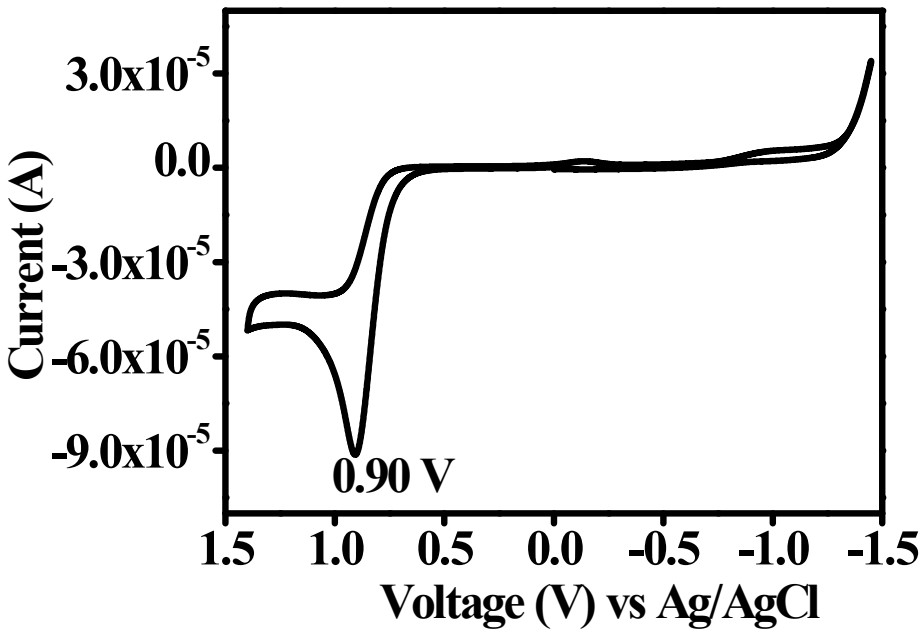

Figure S13. Cyclic voltammogram of 2-(2-chlorophenyl)-2,3-dihydrobenzo[*d*]thiazole (**5b**) using TBAP (0.1 M) in N_2 saturated CH_3CN. E_{ox} = 0.90 V *vs* Ag/AgCl.

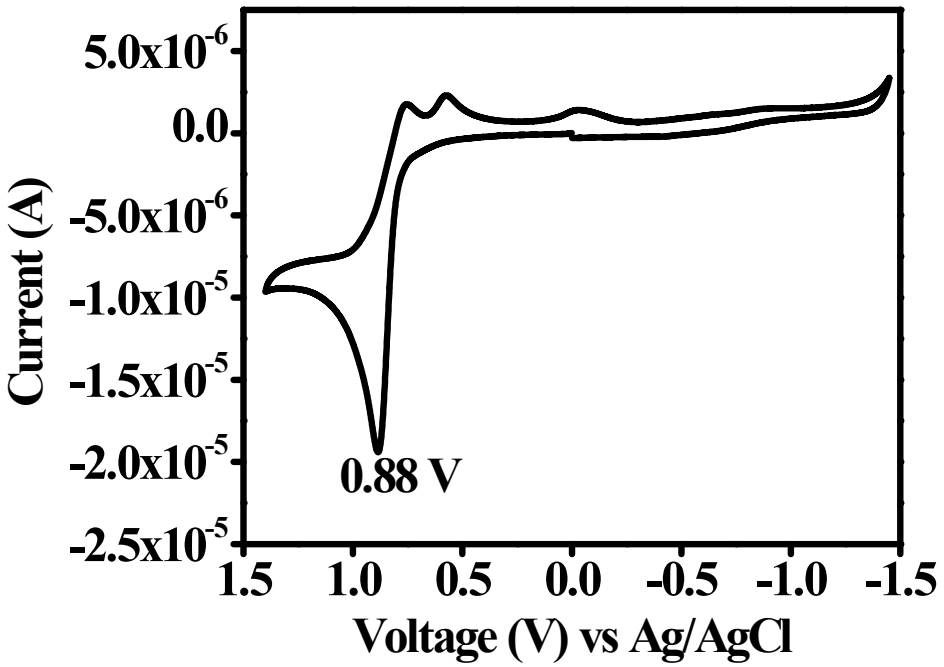

Figure S14. Cyclic voltammogram of 2-(4-methoxyphenyl)-2,3-dihydrobenzo[*d*]thiazole (**5c**) using TBAP (0.1 M) in N_2 saturated CH_3CN. E_{ox} = 0.88 V *vs* Ag/AgCl.

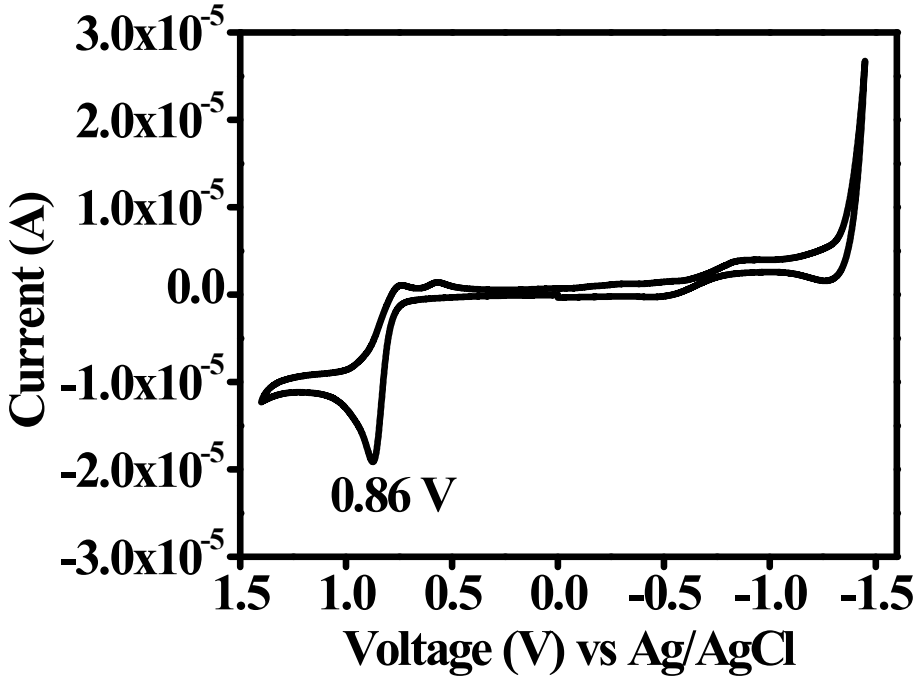

Figure S15. Cyclic voltammogram of 1,3,5-triphenyl-4,5-dihydro-1*H*-pyrazole (**7a**) using TBAP (0.1 M) in d N_2 saturated CH_3CN. E_{ox} = 0.86 V *vs* Ag/AgCl.

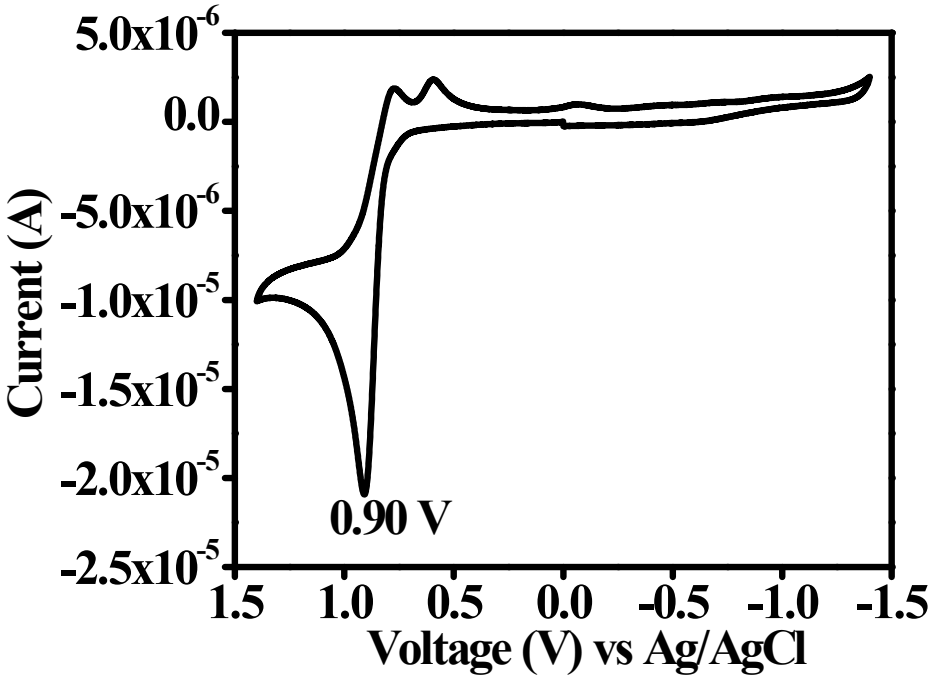

Figure S16. Cyclic voltammogram of 5-(4-chlorophenyl)-1,3-diphenyl-4,5-dihydro-1*H*-pyrazole (**7b**) using TBAP (0.1 M) in N_2 saturated CH_3CN. E_{ox} = 0.90 V *vs* Ag/AgCl.

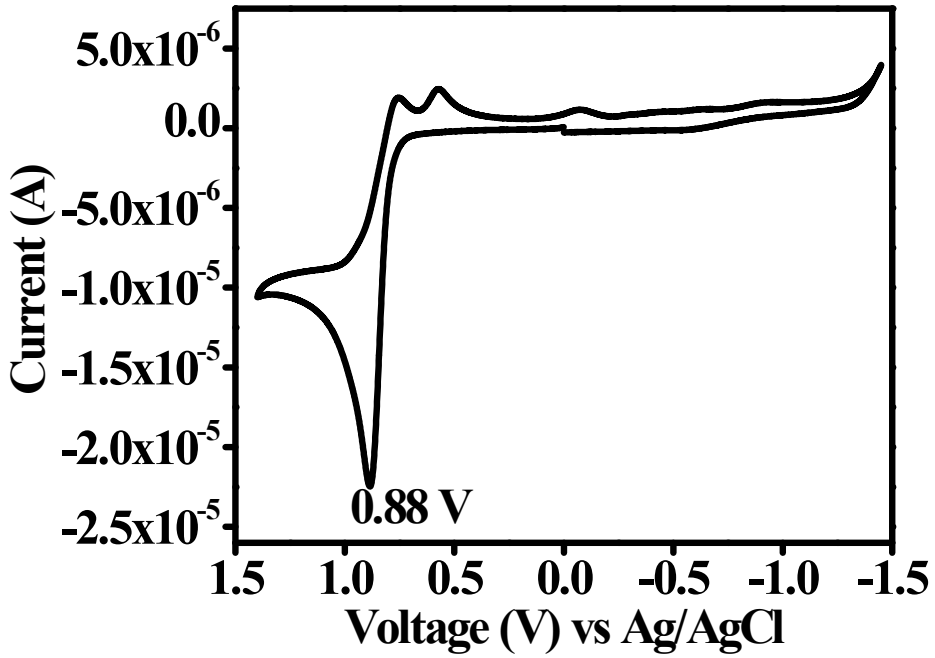

Figure S17. Cyclic voltammogram of 1,3-diphenyl-5-(*p*-tolyl)-4,5-dihydro-1*H*-pyrazole (**7c**) using TBAP (0.1 M) in N_2 saturated CH_3CN. E_{ox} = 0.88 V *vs* Ag/AgCl.

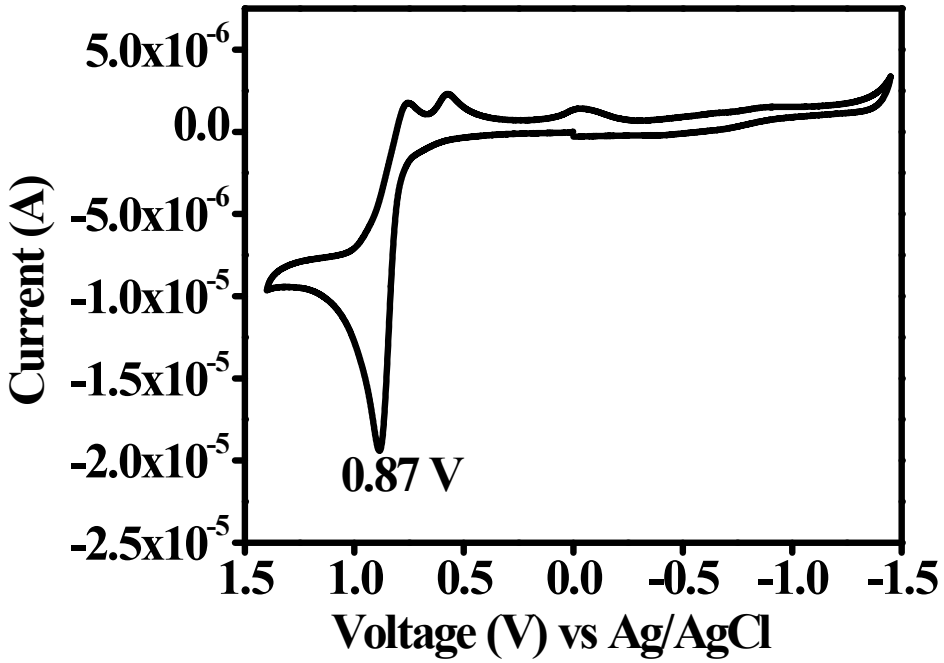

Figure S18. Cyclic voltammogram of 5-(4-methoxyphenyl)-1,3-diphenyl-4,5-dihydro-1*H*-pyrazole (**7d**) using TBAP (0.1 M) in N_2 saturated CH_3CN. E_{ox} = 0.87 V *vs* Ag/AgCl.

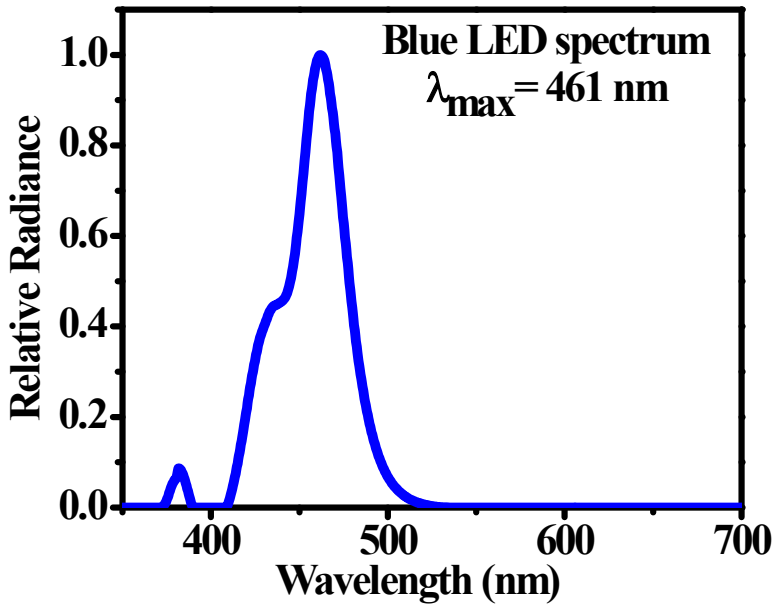

Figure S19. The spectrum of blue LED lamp (40W) employed for performing photocatalytic reaction. The maximum absorption wavelength and the illumination intensity of the blue LED Light are 461 nm and 0.363mW/cm^2 at a distance of 100 cm respectively.

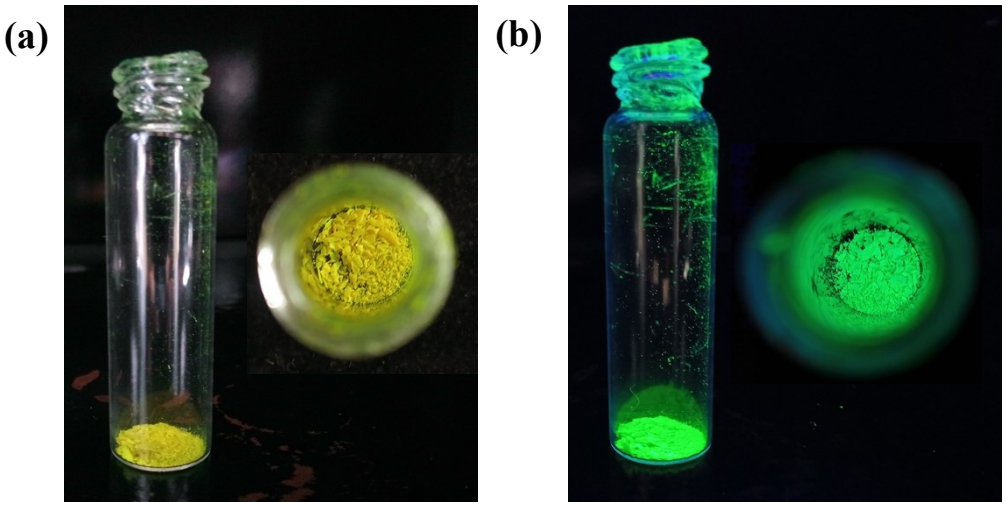

Figure S20. Photographic images (side and top view) of powdered form of purified $CsPbBr_3$ QDs **(QD1)** taken in 4 mL glass vial: (a) Under ambient light; (b) Under UV lamp.

7. Photoluminescence quenching experiment:

$CsPbBr_3$ NCs **(QD1)** emission quenching experiments were performed and the quenching constant (K_{sv}) was calculated using the Stern-Volmer equation,[12]

$$I_0/I = 1 + K_{sv}[Q]$$

where I_0 and I are the highest photoluminescence intensity in the absence and presence of the quencher [Q]. The slope of [I_0/I - 1] vs [Q] plot gives the value of the Stern-Volmer quenching constant (K_{sv}).

The Stern-Volmer kinetics study was performed using a standard fluorometer setup with an excitation wavelength of 400 nm. Similar to the volume of reaction solution, 1 mg of **QD1** was taken in 3 mL DCM solvent. The total volume of 3 mL was taken for study by adding solutions of **QD1**, quencher (**1c**), and solvent. The excitation wavelength was 400 nm and the emission intensity was observed at 517 nm.

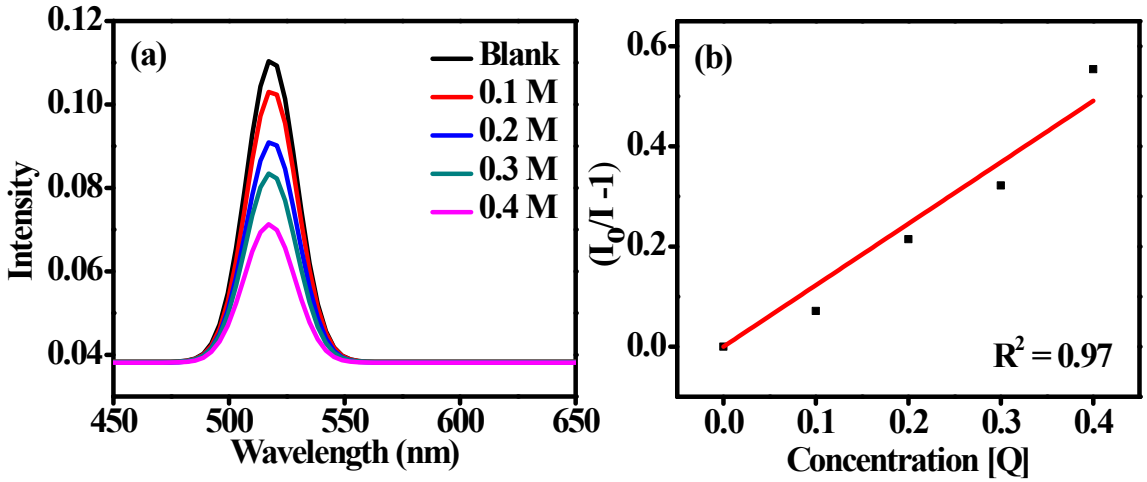

Figure S21. Photoluminescence quenching of **QD1** in the presence of diethyl 2,6-dimethyl-4-phenylpyridine-3,5-dicarboxylate (**1c**) (a) PL spectra of **QD1** with the addition of (**1c**). (b) Stern-Volmer plot, k_{sv} = 1.227 M^{-1}

8. Probable mechanistic pathways:

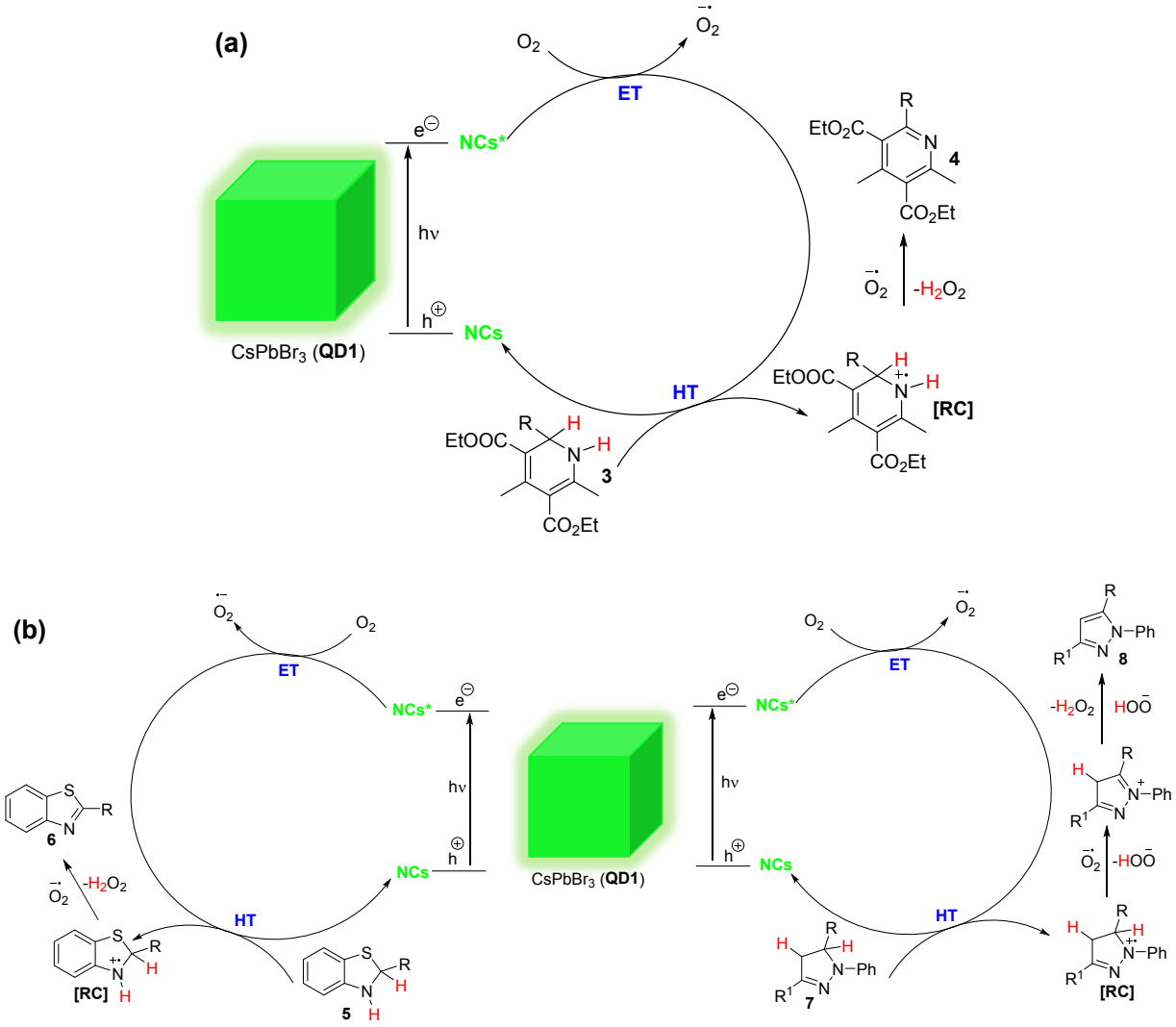

Figure S22. (a) Plausible mechanistic pathway for the formation of aromatized products (**4**) in the presence of **QD1** as photocatalyst under blue irradiation; (b) Plausible mechanistic pathway for the formation of aromatized products (**6 and 8**) in the presence of **QD1** as photocatalyst under blue irradiation. (**RC** = Radical cation, ET = Electron Transfer and HT = Hole Transfer).

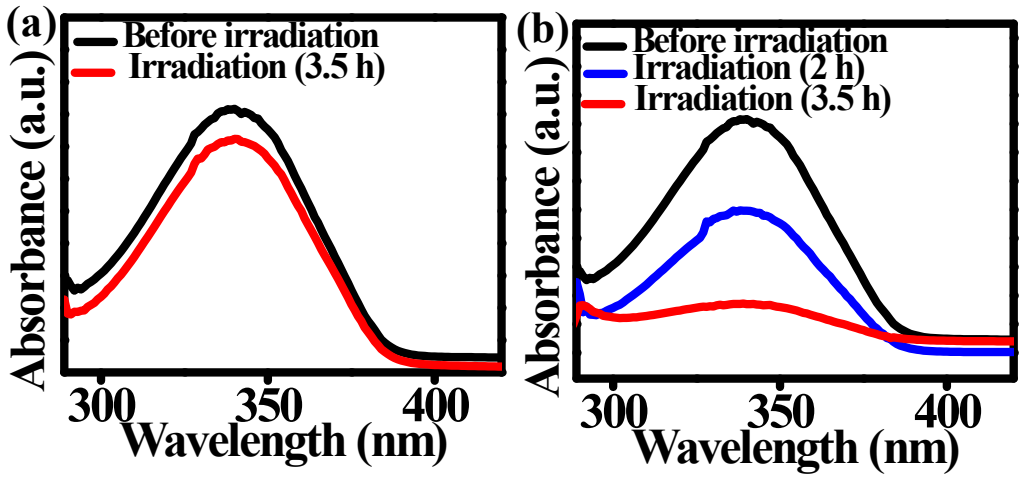

Figure S23. UV–Vis spectra of the successive oxidative aromatization of **1c** in the presence of **QD1** in DCE solvent under blue light irradiation. (a) strictly air-free condition (nitrogen atmosphere) suppresses the formation of product **2c**; (b) under open air condition, the **1c** undergoes complete aromatization to **2c** in 3.5 h.

9. H_2O_2 detection study:

Procedure for the detection of hydrogen peroxide: 100 µL of 3,3',5,5'-Tetramethylbenzidine (TMB, 15 mM) and 400 µL 30% H_2O_2 (33 mM) were added to 2500 µL acetate buffer taken into a cuvette and the UV-Visible spectrum was recorded after 2 h. As expected, the color of the solution turned blue with an absorbance maximum at 652 nm (blue curve, Figure S24) indicating the formation of the diimine complex of TMB. When the UV-Visible spectrum was recorded after 12 h with 100 µL TMB (15 mM) and 2900 µL acetate buffer, no color change was observed indicating the importance of H_2O_2 for promoting the formation of the diimine complex (black curve). Finally, when the UV-Visible spectrum was recorded after 12 h with 100 µL of TMB (15 mM), 400 µL of aliquots of the reaction mixture of aromatization of **1a** after 1 h and 2500 µL acetate buffer, the absorbance maximum at 652 nm was observed along with the formation of a blue colored solution indicating the presence of H_2O_2 formed as byproduct of the aromatization process (red curve).

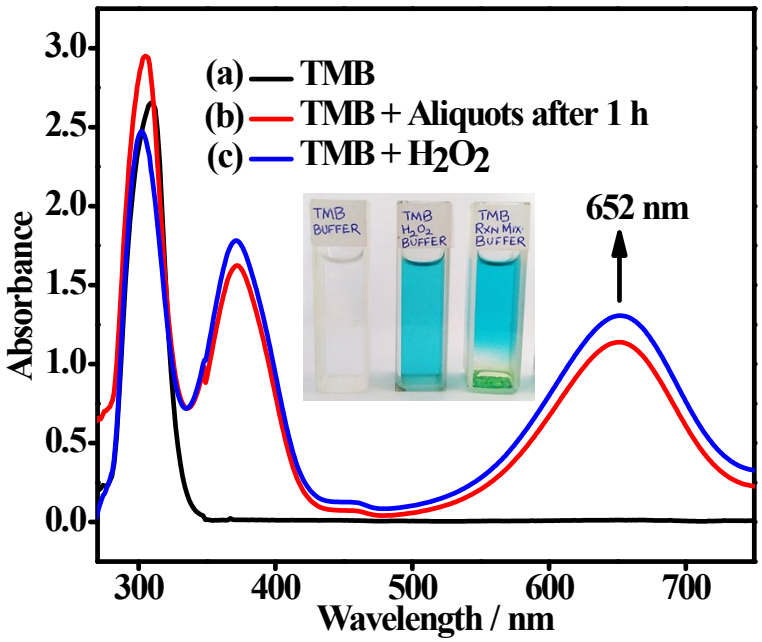

Figure S24. UV–Vis spectra and the photographs of the cuvettes (inset) using TMB under various reaction conditions for the colorimetric detection of H_2O_2. (a) TMB (black); (b) TMB + aliquots of reaction mixture of oxidative aromatization of **1a** after 1h of irradiation (red); (c) TMB + 30 % H_2O_2 (control experiment, blue).

10. Characterization of other photocatalysts:

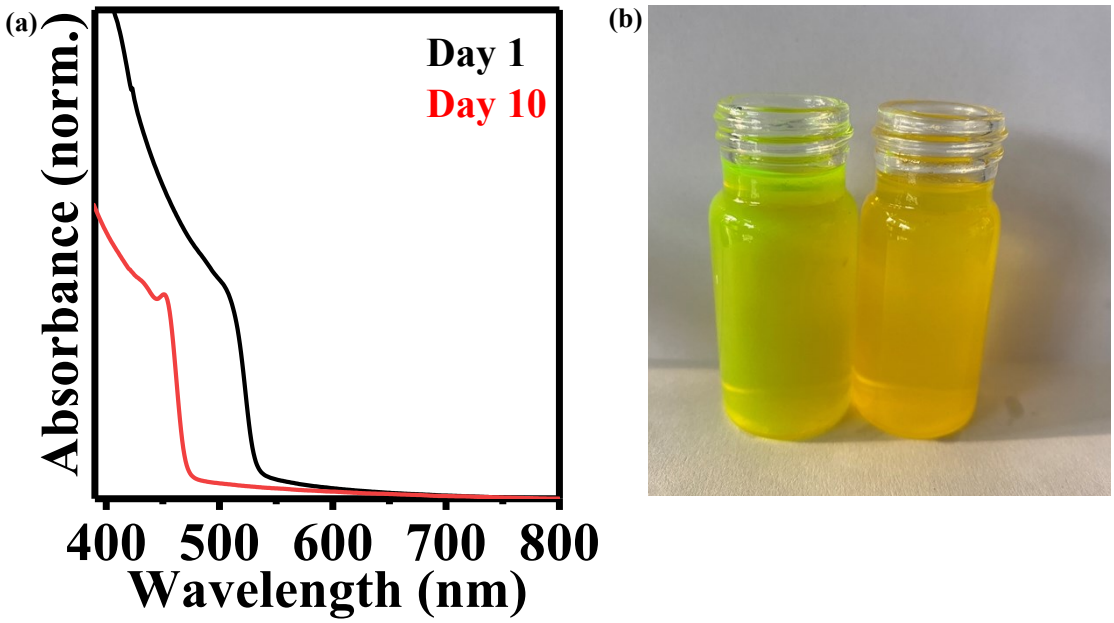

Figure S25. (a) UV-vis absorption of conventionally prepared $CsPbBr_3$ perovskite NCs (**QD4)** dispersed in hexane for day 1 (black) and day 10 (red); (b) corresponding photographs of **QD4** for day 1 and day 10 respectively from left to right.

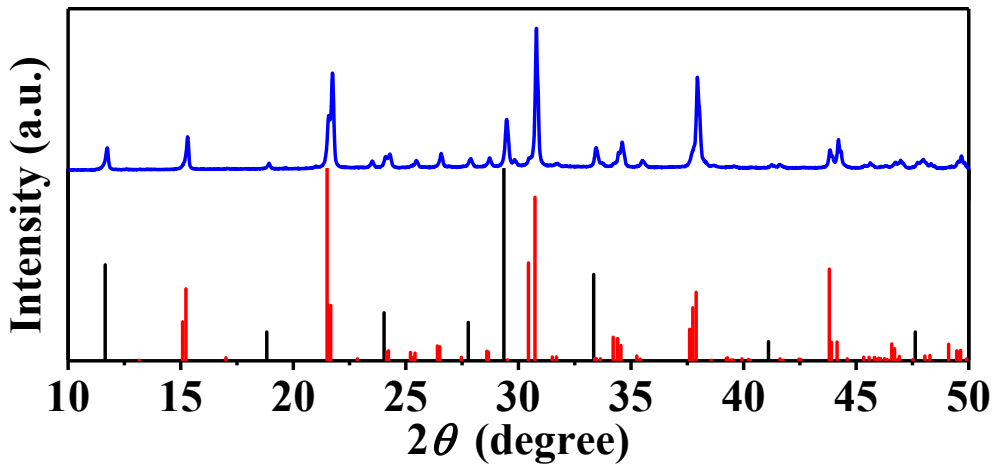

Figure S26. (a) X-ray diffraction patterns of conventionally prepared **QD4** after 10 days. The red and black bars represent orthorhombic $CsPbBr_3$ (JCPDS 96-451-0746) and tetragonal $CsPb_2Br_5$ (JCPDS 00-025-0211).

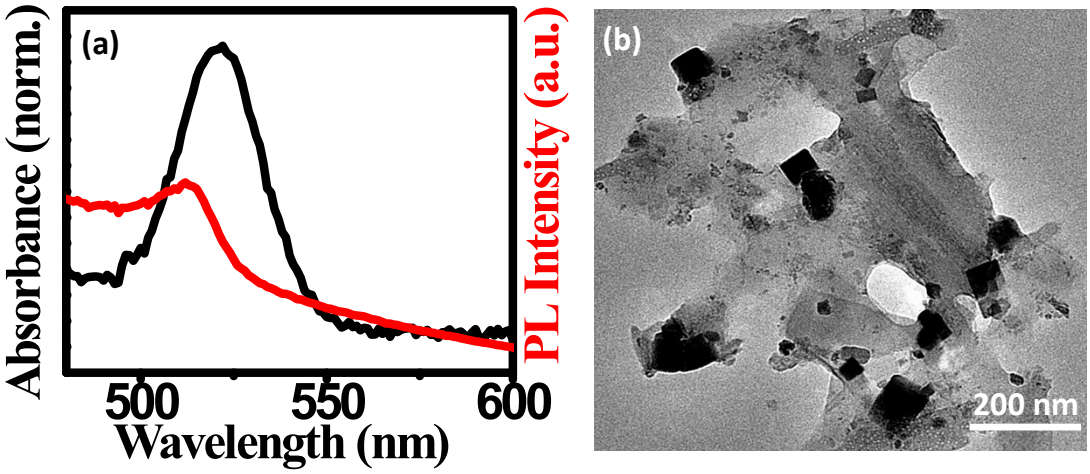

Figure S27. (a) UV-vis absorption and normalised PL spectra of polydisperse bulk $CsPbBr_3$ perovskite NCs (**PNCs**) dispersed in hexane with an emission wavelength of 521 nm; (b) TEM image of the purified **PNCs** revealing their broad size distribution (*ca*. 3~100 nm)

Preparation and UV/vis Spectroscopic characterization of $Ru(bpy)_3(PF_6)_2$:

The $Ru(bpy)_3(PF_6)_2$ complex was prepared by following a previous report[13]. Briefly, the solution of $Ru(bpy)_3Cl_2 \cdot 6H_2O$ (0.866 mmol) in 20 mL of water was added drop wise to another equal volume of a warm aqueous solution of NH_4PF_6 (4.33 mmol) to give an orange product which was kept under stirring for two hours. The orange product was filtered, washed with cold water and dried under vacuum. To purify further, a minimal amount of acetone was taken to dissolve the obtained powder, followed by the precipitation by the addition of diethylether.

Finally, the product was filtered, washed with ether and dried under vacuum overnight.

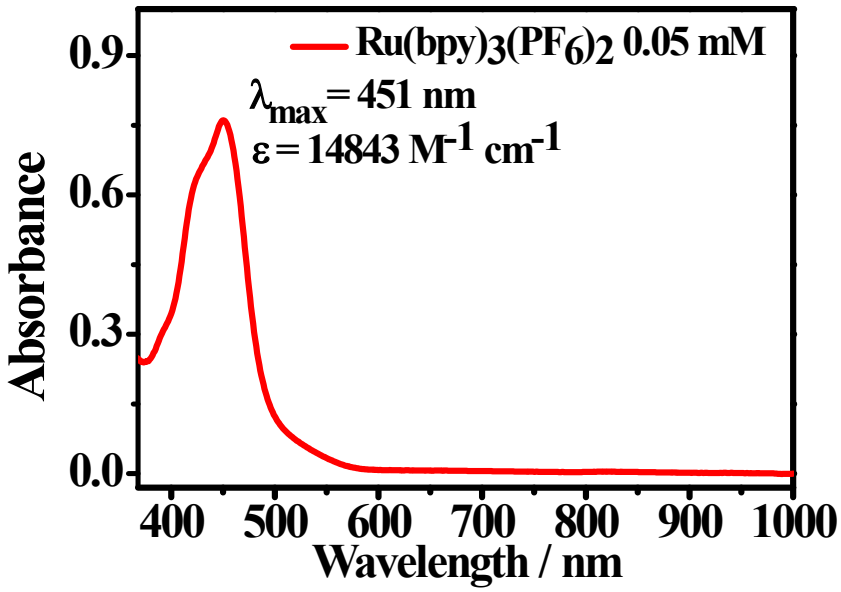

Figure S28. UV/vis absorbance spectrum of purified 0.05 mM $Ru(bpy)_3(PF_6)_2$ in dry CH_3CN having an absorption maximum band (λ_{max}) at 451 nm.

11. UV–Vis spectra of the aromatization of 1b by QD1

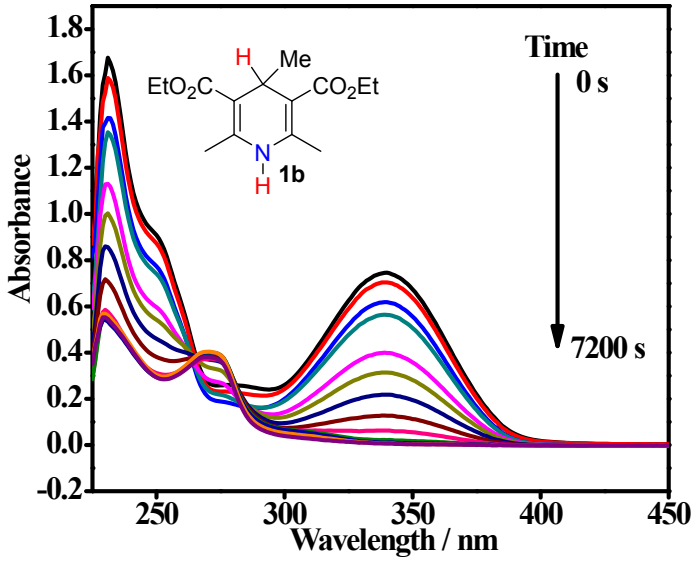

Figure S29. UV–Vis spectra of the successive oxidative aromatization of **1b** in the presence of **QD1** photocatalyst under optimized reaction condition.

12. Catalyst reusability test

For oxidative aromatization of 1a. The catalyst recyclability test was performed following the reported literature protocol.[14] To a 4 mL glass vial, **QD1** (1 mg), **1a** (0.1 mmol) and 3 mL 1,2-dichloroethane (DCE) were taken under open air at a distance of 6 cm away from the light source and subjected to irradiation with the blue LED for 1 h. The product yield was calculated by ^{1}H NMR using acetophenone as an internal standard. The yield of the corresponding aromatized product **2a** for the 1st cycle was 96%. For the 2nd cycle, 0.1 mmol of **1a** was added into the same glass vial and irradiated with the blue light for another 1 h. The overall yield for the 2nd cycle was 93%. The above step was repeated for the 3rd and 4th cycle thereby delivering overall yields of **2a** in 86% and 70% respectively as depicted in Figure S30. This indicates that at least for four cycles, the catalytic activity of **QD1** is still robust. Similar experiments were conducted with the bulk counterpart and **QD4** to compare their recyclability and TON with respect to **QD1**. Notably, we collected **QD1** after 1st and the 4th catalytic cycle via centrifugation. The recycled **QD1** was redispersed in hexane solvent and their PL data is shown in Figure S31a.

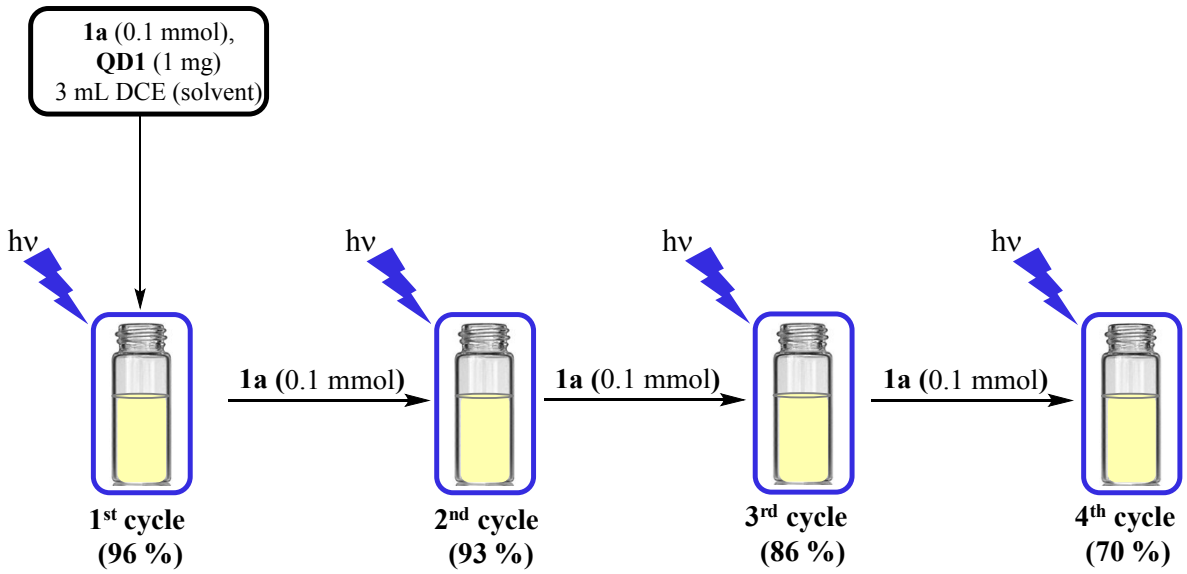

Figure S30. Representation of the recyclability test of **QD1** for the oxidative aromatization of **1a** using four cycles.

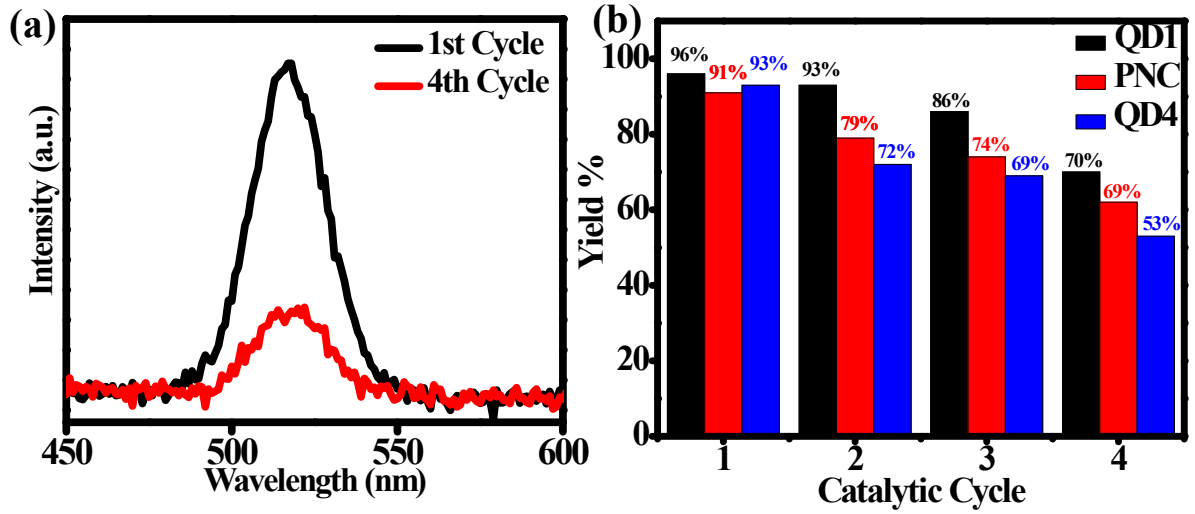

Figure S31. (a) The PL of the recycled **QD1** dispersed in hexane solvent after 1st and 4th catalytic cycle obtained *via* centrifugation; (b) Recycling experiment of $CsPbBr_3$ perovskite photocatalysts in the oxidative aromatization of **1a** for up to 4 cycles: (black) with **QD1**, (red) with **PNCs** and (blue) with conventional $CsPbBr_3$ perovskite nanocrystals (**QD4**). The percentage yield was calculated by ^1H NMR analysis of the crude reaction mixture.

13. Supplementary Note:

13.1 Calculation of the Turnover Number (TON):

a) TON for the oxidative aromatization of 1a using QD1: The TON of QD1 catalysis for 0.1 mmol scale reaction for 4 cycles can be calculated using the following equation

$$TON = \frac{total\ mol\ of\ produt\ 2a\ in\ 4\ cycles}{total\ mol\ of\ catalyst\ employed}$$

$$= \frac{\{0.1\ mmol \times (0.96 + 0.93 + 0.86 + 0.70)\}}{(1.0\ mg \div 579.8\ g\ mol^{-1})} \approx 200$$

b) TON for the oxidative aromatization of 1a using bulk perovskite (PNCs):

$$TON = \frac{\{0.1\ mmol \times (0.91 + 0.79 + 0.74 + 0.62)\}}{(1\ mg \div 579.8\ g\ mol^{-1})} \approx 177$$

c) TON for the oxidative aromatization of 1a using conventional $CsPbBr_3$ perovskite NCs (QD4):

$$TON = \frac{\{0.1\ mmol \times (0.93 + 0.72 + 0.69 + 0.53)\}}{(1\ mg \div 579.8\ g\ mol^{-1})} \approx 166$$

13.2 Calculation of the CBM and VBM energy levels of QD1:

The cyclic voltammogram of **QD1** displayed the anodic peak (A) at 1.23 V and cathodic peak (C) at -1.27 V for one complete cycle (Figure 1c, manuscript). The formal redox potential of Fc/Fc+ couple (reference) vs Ag/AgCl in 1:4 v/v mixture of acetonitrile and toluene using 0.1 M TBAP as supporting electrolyte was 0.47 V (Figure S8b). Based on literature reports, the energy levels (eV) were estimated from $-E_{HOMO/LUMO} = E^{redox}$ (*vs* Ag/AgCl) + 4.44 eV = E^{redox} (*vs* Fc/Fc^{+}) + 4.8 eV.[5–7]

For photocatalyst **QD1**:

To calculate CBM in eV, use cathodic peak (C) at -1.27 V

E_{LUMO} = [-e(E_{red} -0.47 + 4.8)] eV = [-e(-1.27 - 0.47 + 4.8)] eV = -3.06 eV;

To calculate VBM in eV, use anodic peak (A) at 1.23 V

E_{HOMO} = [-e(E_{ox} -0.47 + 4.8)] eV = [-e(1.23 - 0.47 + 4.8)] eV = -5.56 eV

14. Comparative efficiency of the three different sized CQDs

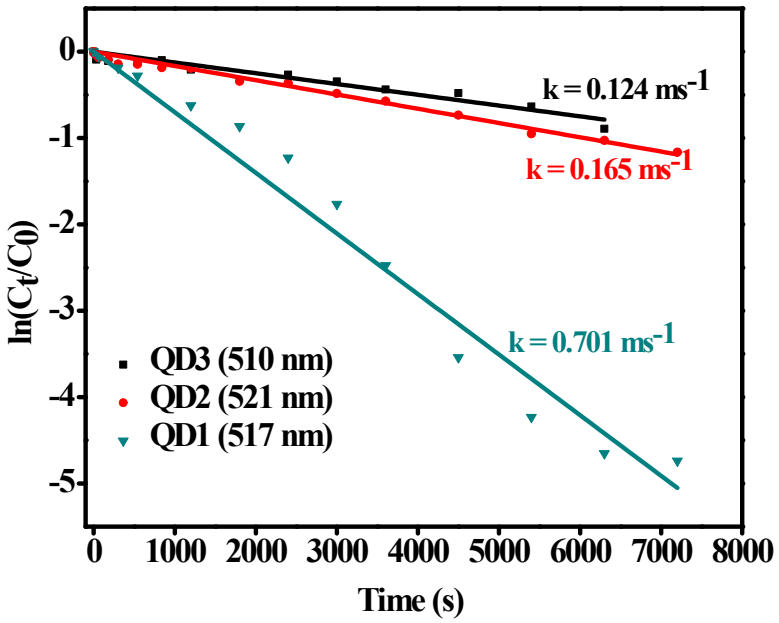

Figure S32. Comparative efficiency of the three different sized CQDs in the aromatization of **1b**: (black) with **QD3**, (red) with **QD2** and (green) with **QD1**.

15. Spectral Data of products

Diethyl 2,6-dimethylpyridine-3,5-dicarboxylate (2a).

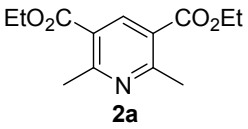

2a

Following the general procedure, $CsPbBr_3$ perovskite NCs (**QD1**, 1 mg), **1a** (0.1 mmol) and 3 mL 1,2-dichloroethane solvent (DCE) were subjected to irradiation to afford the pure product **2a** (23.8 mg, 0.095 mmol) as a thick liquid in 95% yield. ^{1}H NMR (400 MHz, $CDCl_3$) δ 8.64 (s, 1H), 4.37 (q, J = 7.16 Hz, 4H), 2.81 (s, 6H), 1.38 (t, J = 7.16 Hz, 6H); ^{13}C{^{1}H} NMR (100 MHz, $CDCl_3$) δ 165.8, 162.1, 140.8, 123.0, 61.3, 24.8, 14.2.

Diethyl 2,4,6-trimethylpyridine-3,5-dicarboxylate (2b).

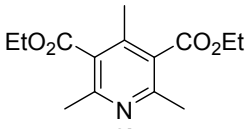

2b

Following the general procedure, $CsPbBr_3$ perovskite NCs (**QD1**, 1 mg), **1b** (0.1 mmol) and 3 mL 1,2-dichloroethane solvent (DCE) were subjected to irradiation to afford the pure product **2b** (24.6 mg, 0.093 mmol) as a thick liquid in 93% yield. ^{1}H NMR (400 MHz, $CDCl_3$) δ 4.39 (q, J = 7.16 Hz, 4H), 2.50 (s, 6H), 2.25 (s, 3H), 1.37 (t, J = 7.12 Hz, 6H); ^{13}C{^{1}H} NMR (100 MHz, $CDCl_3$) δ 168.2, 154.8, 142.2, 127.6, 61.5, 22.8, 16.9, 14.1.

Diethyl 2,6-dimethyl-4-phenylpyridine-3,5-dicarboxylate (2c).

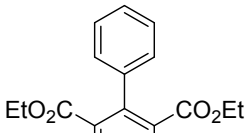

2c

Following the general procedure, $CsPbBr_3$ perovskite NCs (**QD1**, 1 mg), **1c** (0.1 mmol) and 3 mL 1,2-dichloroethane solvent (DCE) were subjected to irradiation to afford the pure product **2c** (30.1 mg, 0.092 mmol) as a thick liquid in 92% yield. ^{1}H NMR (400 MHz, $CDCl_3$) δ 7.35–7.33 (m, 3H), 7.24–7.22 (m, 2H), 3.98 (q, J = 7.12 Hz, 4H), 2.58 (s, 6H), 0.87 (t, J = 7.16 Hz, 6H); ^{13}C{^{1}H} NMR (100 MHz, $CDCl_3$) δ 167.8, 155.3, 146.1, 136.5, 128.4, 128.0, 126.9, 61.3, 22.8, 13.5.

Diethyl 4-(4-chlorophenyl)-2,6-dimethylpyridine-3,5-dicarboxylate (2d).

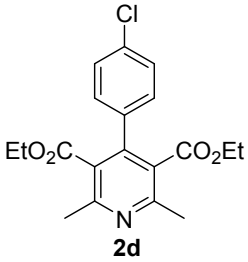

2d

Following the general procedure, $CsPbBr_3$ perovskite NCs (**QD1**, 1 mg), **1d** (0.1 mmol) and 3 mL 1,2-dichloroethane solvent (DCE) were subjected to irradiation to afford the pure product **2d** (32.5 mg, 0.09 mmol) as a thick liquid in 90% yield. ^{1}H NMR (400 MHz, $CDCl_3$) δ 7.36 (d, J = 8.36 Hz, 2H), 7.20 (d, J = 8.40 Hz, 2H), 4.04 (q, J = 7.16 Hz, 4H),

2.60 (s, 6H), 0.98 (t, J = 7.12 Hz, 6H); $^{13}C\{^{1}H\}$ NMR (100 MHz, $CDCl_3$) δ 167.6, 155.6, 144.8, 134.9, 134.7, 129.5, 128.3, 126.8, 61.4, 22.8, 13.6.

Diethyl 2,6-dimethyl-4-(*p*-tolyl)pyridine-3,5-dicarboxylate (2e).

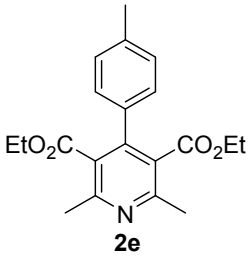

2e

Following the general procedure, $CsPbBr_3$ perovskite NCs (**QD1**, 1 mg), **1e** (0.1 mmol) and 3 mL 1,2-dichloroethane solvent (DCE) were subjected to irradiation to afford the pure product **2e** (31.7 mg, 0.093 mmol) as a thick liquid in 93% yield. ^{1}H NMR (400 MHz, $CDCl_3$) δ 7.19–7.13 (m, 4H), 4.04 (q, J = 7.16 Hz, 4H), 2.60 (s, 6H), 2.37 (s, 3H), 0.96 (t, J = 7.12 Hz, 6H); $^{13}C\{^{1}H\}$ NMR (100 MHz, $CDCl_3$) δ 167.9, 155.2, 146.2, 138.3, 133.5, 128.8, 127.9, 127.1, 61.3, 22.8, 21.2, 13.6.

Diethyl 4-(4-methoxyphenyl)-2,6-dimethylpyridine-3,5-dicarboxylate (2f).

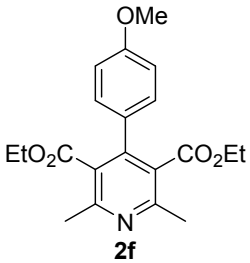

2f

Following the general procedure, $CsPbBr_3$ perovskite NCs (**QD1**, 1 mg), **1f** (0.1 mmol) and 3 mL 1,2-dichloroethane solvent (DCE) were subjected to irradiation to afford the pure product **2f** (33.6 mg, 0.094 mmol) as a thick liquid in 94% yield. ^{1}H NMR (400 MHz, $CDCl_3$) δ 7.19 (d, J = 8.64 Hz, 2H), 6.99 (d, J = 8.64 Hz, 2H), 4.05 (q, J = 7.08 Hz, 4H), 3.82 (s, 3H), 2.58 (s, 6H), 0.98 (t, J = 7.16 Hz, 6H); $^{13}C\{^{1}H\}$ NMR (100 MHz, $CDCl_3$) δ 168.0, 159.8, 155.1, 129.4, 128.6, 127.2, 113.5, 61.3, 55.2, 22.7, 13.7.

Diethyl 2,6-dimethyl-4-(4-nitrophenyl)pyridine-3,5-dicarboxylate (2g).

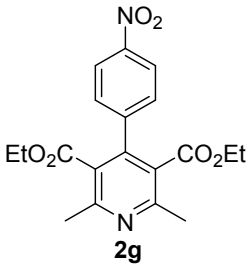

2g

Following the general procedure, $CsPbBr_3$ perovskite NCs (**QD1**, 1 mg), **1g** (0.1 mmol) and 3 mL 1,2-dichloroethane solvent (DCE) were subjected to irradiation to afford the pure product **2g** (32.4 mg, 0.087 mmol) as a yellow solid in 87% yield. ^{1}H NMR (400 MHz, $CDCl_3$) δ 8.27 (d, J = 8.60 Hz, 2H), 7.46 (d, J = 8.52 Hz, 2H), 4.04 (q, J = 7.16 Hz, 4H), 2.65 (s, 6H), 0.98 (t, J = 7.16 Hz, 6H); $^{13}C\{^{1}H\}$ NMR (100 MHz, $CDCl_3$) δ 167.1, 156.1, 147.8, 144.0, 143.2, 129.3, 126.2, 123.2, 61.7, 23.0, 13.7.

9-(4-Chlorophenyl)-3,4,6,7-tetrahydroacridine-1,8(2*H*,5*H*)-dione (2h).

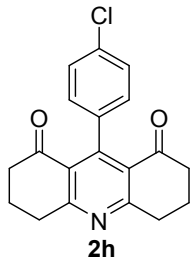

2h

Following the general procedure, $CsPbBr_3$ perovskite NCs (**QD1**, 1 mg), **1h** (0.1 mmol) and 3 mL 1,2-dichloroethane solvent (DCE) were subjected to irradiation to afford the pure product **2h** (28.0 mg, 0.086 mmol) as a thick liquid in 86% yield. ^{1}H NMR (400 MHz, $CDCl_3$) δ 7.36 (d, J = 8.32 Hz, 2H), 6.95 (d, J = 8.32 Hz, 2H), 3.22 (t, J = 6.24 Hz, 4H), 2.61 (t, J = 6.72 Hz, 4H), 2.22–2.15 (m, 4H); ^{13}C{^{1}H} NMR (100 MHz, $CDCl_3$) δ 197.0, 167.0, 151.6, 137.1, 133.0, 128.0, 126.5, 40.2, 34.1, 21.0.

9-(4-Methoxyphenyl)-3,4,6,7-tetrahydroacridine-1,8(2*H*,5*H*)-dione (2i).

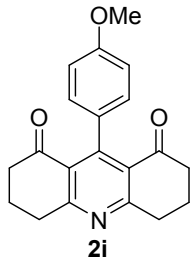

2i

Following the general procedure, $CsPbBr_3$ perovskite NCs (**QD1**, 1 mg), **1i** (0.1 mmol) and 3 mL 1,2-dichloroethane solvent (DCE) were subjected to irradiation to afford the pure product **2i** (28.9 mg, 0.090 mmol) as a white solid in 90% yield. ^{1}H NMR (400 MHz, $CDCl_3$) δ 6.96–6.92 (m, 4H), 3.86 (s, 3H), 3.20 (t, J = 6.28 Hz, 4H), 2.62 (t, J = 6.72 Hz, 4H), 2.21–2.14 (m, 4H); ^{13}C{^{1}H} NMR (100 MHz, $CDCl_3$) δ 197.3, 166.7, 158.8, 152.8, 130.5, 127.9, 127.0, 55.0, 40.3, 34.0, 21.1.

3,3,6,6-Tetramethyl-9-(*p*-tolyl)-3,4,6,7-tetrahydroacridine-1,8(2*H*,5*H*)-dione (2j).

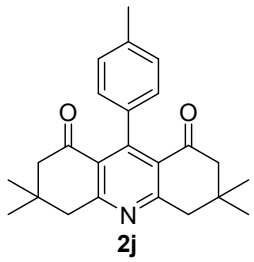

2j

Following the general procedure, $CsPbBr_3$ perovskite NCs (**QD1**, 1 mg), **1j** (0.1 mmol) and 3 mL 1,2-dichloroethane solvent (DCE) were subjected to irradiation to afford the pure product **2j** (33.2 mg, 0.092 mmol) as a solid in 92% yield. ^{1}H NMR (400 MHz, $CDCl_3$) δ 7.22 (d, J = 7.88 Hz, 2H), 6.92 (d, J = 8.08 Hz, 2H), 3.11 (s, 4H), 2.48 (s, 4H), 2.43 (s, 3H), 1.13 (s, 12H); ^{13}C{^{1}H} NMR (100 MHz, $CDCl_3$) δ 197.2, 165.7, 152.3, 136.5, 135.4, 128.5, 126.4, 125.7, 54.0, 47.9, 32.3, 28.2, 21.4.

Diethyl 2,4-dimethyl-6-phenylpyridine-3,5-dicarboxylate (4a).

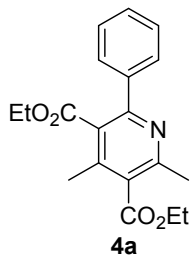

4a

Following the general procedure, $CsPbBr_3$ perovskite NCs (**QD1**, 1 mg), **3a** (0.1 mmol) and 3 mL 1,2-dichloroethane solvent (DCE) were subjected to irradiation to afford the pure product **4a** (29.7 mg, 0.091 mmol) as a thick liquid in 91% yield. ^{1}H NMR (400 MHz, $CDCl_3$) δ 7.56–7.53 (m, 2H) 7.42–7.38 (m, 3H), 4.43 (q, J = 7.20 Hz, 2H), 4.09 (q, J = 7.08 Hz, 2H), 2.60 (s,

3H), 2.35 (s, 3H), 1.40 (t, J = 7.08 Hz, 3H), 0.97 (t, J = 7.08 Hz, 3H); $^{13}C\{^1H\}$ NMR (100 MHz, $CDCl_3$) δ168.3, 156.4, 155.2, 142.7, 139.6, 128.8, 128.4, 128.3, 128.2, 127.2, 61.7, 61.5, 23.1, 16.8, 14.1, 13.5.

Diethyl 2-(4-chlorophenyl)-4,6-dimethylpyridine-3,5-dicarboxylate (4b).

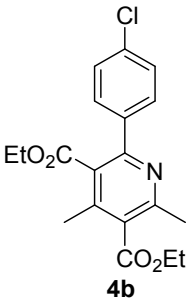

4b

Following the general procedure, $CsPbBr_3$ perovskite NCs (**QD1**, 1 mg), **3b** (0.1 mmol) and 3 mL 1,2-dichloroethane solvent (DCE) were subjected to irradiation to afford the pure product **4b** (32.2 mg, 0.089 mmol) as a thick liquid in 89% yield. ^1H NMR (400 MHz, $CDCl_3$) δ7.50 (d, J = 8.40 Hz, 2H), 7.38–7.35 (m, 2H), 4.42 (q, J = 7.08 Hz, 2H), 4.12 (q, J = 7.08 Hz, 2H), 2.58 (s, 3H), 2.33 (s, 3H), 1.38 (t, J = 7.04 Hz, 3H), 1.03 (t, J = 7.20 Hz, 3H); $^{13}C\{^1H\}$ NMR (100 MHz, $CDCl_3$) δ168.34, 168.30, 155.5, 155.1, 143.1, 138.2, 135.2, 129.8, 128.8, 128.7, 127.3, 61.9, 61.8, 23.2, 17.0, 14.3, 13.8.

Diethyl 2-(2-chlorophenyl)-4,6-dimethylpyridine-3,5-dicarboxylate (4c).

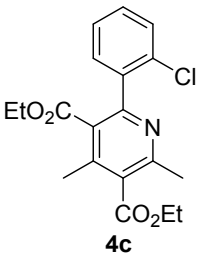

4c

Following the general procedure, $CsPbBr_3$ perovskite NCs (**QD1**, 1 mg), **3c** (0.1 mmol) and 3 mL 1,2-dichloroethane solvent (DCE) were subjected to irradiation to afford the pure product **4c** (31.4 mg, 0.087 mmol) as a thick liquid in 87% yield. ^1H NMR (400 MHz, $CDCl_3$) δ7.39 (d, J = 6.96 Hz, 1H), 7.31–7.25 (m, 3H), 4.43 (q, J = 7.12 Hz, 2H), 3.98 (q, J = 7.12 Hz, 2H), 2.57 (s, 3H), 2.37 (s, 3H), 1.39 (t, J = 7.12 Hz, 3H), 0.86 (t, J = 7.12 Hz, 3H); $^{13}C\{^1H\}$ NMR (100 MHz, $CDCl_3$) δ 168.1, 166.9, 155.3, 143.2, 138.6, 132.7, 130.3, 129.7, 129.5, 129.4, 127.8, 126.4, 61.7, 61.3, 22.9, 17.1, 14.1, 13.4.

Diethyl 2-(4-bromophenyl)-4,6-dimethylpyridine-3,5-dicarboxylate (4d).

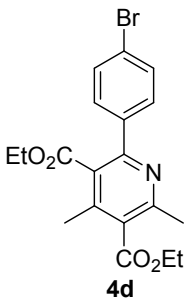

4d

Following the general procedure, $CsPbBr_3$ perovskite NCs (**QD1**, 1 mg), **3d** (0.1 mmol) and 3 mL 1,2-dichloroethane solvent (DCE) were subjected to irradiation to afford the pure product **4d** (36.5 mg, 0.090 mmol) as a thick liquid in 90% yield. ^1H NMR (400 MHz, $CDCl_3$) δ7.53 (d, J = 8.48 Hz, 2H), 7.44 (d, J = 8.52 Hz, 2H), 4.43 (q, J = 7.08 Hz, 2H), 4.13 (q, J = 7.20 Hz, 2H), 2.58 (s, 3H), 2.34 (s, 3H), 1.40 (t, J = 7.20 Hz, 3H), 1.05 (t, J = 7.08 Hz, 3H); $^{13}C\{^1H\}$ NMR (100 MHz, $CDCl_3$) δ 168.1, 155.4, 155.0, 143.0, 138.5, 131.5, 129.9, 128.7, 127.1, 123.3, 61.7, 61.6, 23.0, 16.8, 14.1, 13.6.

Diethyl 2,4-dimethyl-6-(*p*-tolyl)pyridine-3,5-dicarboxylate (4e).

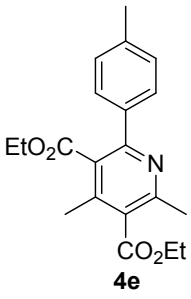

4e

Following the general procedure, $CsPbBr_3$ perovskite NCs (**QD1**, 1 mg), **3e** (0.1 mmol) and 3 mL 1,2-dichloroethane solvent (DCE) were subjected to irradiation to afford the pure product **4e** (31.7 mg, 0.093 mmol) as a thick liquid in 93% yield. ^{1}H NMR (400 MHz, $CDCl_3$) δ 7.46 (d, J = 7.84 Hz, 2H), 7.20 (d, J = 7.80 Hz, 2H), 4.43 (q, J = 7.12 Hz, 2H), 4.12 (q, J = 7.04 Hz, 2H), 2.59 (s, 3H), 2.36 (s, 3H), 2.34 (s, 3H), 1.40 (t, J = 7.12 Hz, 3H), 1.03 (t, J = 7.16 Hz, 3H); ^{13}C{^{1}H} NMR (100 MHz, $CDCl_3$) δ 168.5, 168.4, 156.3, 155.1, 142.6, 138.7, 136.8, 129.0, 128.2, 127.1, 61.6, 61.4, 23.1, 21.2, 16.8, 14.1, 13.6.

Diethyl 2-(4-methoxyphenyl)-4,6-dimethylpyridine-3,5-dicarboxylate (4f).

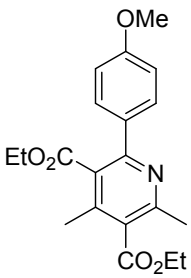

4f

Following the general procedure, $CsPbBr_3$ perovskite NCs (**QD1**, 1 mg), **3f** (0.1 mmol) and 3 mL 1,2-dichloroethane solvent (DCE) were subjected to irradiation to afford the pure product **4f** (33.6 mg, 0.094 mmol) as a thick liquid in 94% yield. ^{1}H NMR (400 MHz, $CDCl_3$) δ 7.52 (d, J = 8.72 Hz, 2H), 6.92 (d, J = 8.76 Hz, 2H), 4.43 (q, J = 7.20 Hz, 2H), 4.14 (q, J = 7.16 Hz, 2H), 3.82 (s, 3H), 2.58 (s, 3H), 2.33 (s, 3H), 1.40 (t, J = 7.00 Hz, 3H), 1.06 (t, J = 7.24 Hz, 3H); ^{13}C{^{1}H} NMR (100 MHz, $CDCl_3$) δ 168.6, 168.4, 160.3, 155.8, 155.1, 142.6, 132.1, 129.7, 127.9, 126.9, 113.8, 61.6, 61.5, 55.3, 23.1, 16.8, 14.1, 13.7.

2-Phenylbenzo[*d*]thiazole (6a).

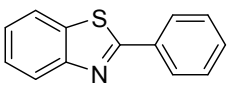

6a

Following the general procedure, $CsPbBr_3$ perovskite NCs (**QD1**, 1 mg), **5a** (0.1 mmol) and 3 mL 1,2-dichloroethane solvent (DCE) were subjected to irradiation to afford the pure product **6a** (20.0 mg, 0.095 mmol) as a white solid in 95% yield. ^{1}H NMR (400 MHz, $CDCl_3$) δ 8.13–8.09 (m, 3H), 7.92 (d, J = 7.88 Hz, 1H), 7.52–7.50 (m, 4H), 7.42–7.39 (m, 1H); ^{13}C{^{1}H} NMR (100 MHz, $CDCl_3$) δ 168.1, 154.2, 135.0, 133.6, 131.0, 129.0, 127.5, 126.3, 125.2, 123.2, 121.6.

2-(2-Chlorophenyl)benzo[*d*]thiazole (6b).

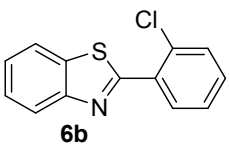

6b

Following the general procedure, $CsPbBr_3$ perovskite NCs (**QD1**, 1 mg), **5b** (0.1 mmol) and 3 mL 1,2-dichloroethane solvent (DCE) were subjected to irradiation to afford the pure product **6b** (22.6 mg, 0.092 mmol) as a white solid in 92% yield. ^{1}H NMR (400 MHz, $CDCl_3$) δ 8.25–8.23 (m, 1H), 8.17 (d, J = 8.12

Hz, 1H), 7.96 (d, J = 7.92 Hz, 1H), 7.57–7.53 (m, 2H), 7.47–7.41 (m, 3H); $^{13}C\{^1H\}$ NMR (100 MHz, $CDCl_3$) δ 164.2, 152.5, 136.1, 132.7, 132.2, 131.7, 131.1, 130.8, 127.1, 126.3, 125.4, 123.4, 121.4.

2-(4-Methoxyphenyl)benzo[d]thiazole (6c).

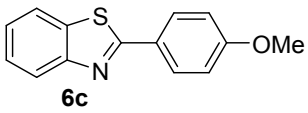

6c

Following the general procedure, $CsPbBr_3$ perovskite NCs (**QD1**, 1 mg), **5c** (0.1 mmol) and 3 mL 1,2-dichloroethane solvent (DCE) were subjected to irradiation to afford the pure product **6c** (22.6 mg, 0.094 mmol) as a white solid in 94% yield. ^1H NMR (400 MHz, $CDCl_3$) δ 8.07–8.04 (m, 3H), 7.89 (d, J = 7.96 Hz, 1H), 7.49 (t, J = 7.84 Hz, 1H), 7.37 (t, J = 7.64 Hz, 1H), 7.01 (d, J = 7.96 Hz, 2H), 3.88 (s, 3H); $^{13}C\{^1H\}$ NMR (100 MHz, $CDCl_3$) δ 167.9, 161.9, 154.2, 134.8, 129.1, 126.4, 126.2, 124.8, 122.8, 121.5, 114.3, 55.4.

1,3,5-Triphenyl-1*H*-pyrazole (8a).

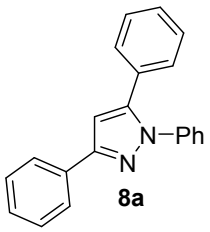

8a

Following the general procedure, $CsPbBr_3$ perovskite NCs (**QD1**, 1 mg), **7a** (0.1 mmol) and 3 mL 1,2-dichloroethane solvent (DCE) were subjected to irradiation to afford the pure product **8a** (27.2 mg, 0.092 mmol) as a thick liquid in 92% yield. ^1H NMR (400 MHz, $CDCl_3$) δ 8.00 (d, J = 7.52 Hz, 2H), 7.51–7.35 (m, 13H), 6.89 (s, 1H); $^{13}C\{^1H\}$ NMR (100 MHz, $CDCl_3$) δ 152.0, 144.4, 140.1, 133.0, 130.6, 128.9, 128.8, 128.7, 128.5, 128.3, 128.0, 127.5, 125.8, 125.3, 105.2.

5-(4-Chlorophenyl)-1,3-diphenyl-1*H*-pyrazole (8b).

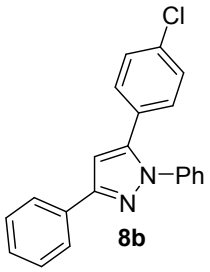

8b

Following the general procedure, $CsPbBr_3$ perovskite NCs (**QD1**, 1 mg), **7b** (0.1 mmol) and 3 mL 1,2-dichloroethane solvent (DCE) were subjected to irradiation to afford the pure product **8b** (29.7 mg, 0.090 mmol) as a thick liquid in 90% yield. ^1H NMR (400 MHz, $CDCl_3$) δ 7.96 (d, J = 7.52 Hz, 2H), 7.48–7.21 (m, 12H), 6.83 (s, 1H); $^{13}C\{^1H\}$ NMR (100 MHz, $CDCl_3$) δ 152.1, 143.2, 139.9, 134.4, 132.9, 130.0, 129.1, 128.8, 128.7, 128.1, 127.7, 125.8, 125.3, 105.3.

1,3-Diphenyl-5-(*p*-tolyl)-1*H*-pyrazole (8c).

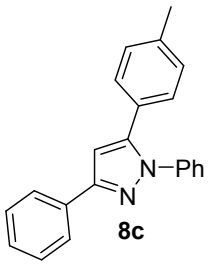

Following the general procedure, $CsPbBr_3$ perovskite NCs (**QD1**, 1 mg), **7c** (0.1 mmol) and 3 mL 1,2-dichloroethane solvent (DCE) were subjected to irradiation to afford the pure product **8c** (28.8 mg, 0.093 mmol) as a thick liquid in 93% yield. ^{1}H NMR (400 MHz, $CDCl_3$) δ 7.97–7.94 (m, 2H), 7.47–7.30 (m, 8H), 7.20–7.13 (m, 4H), 6.82 (s, 1H), 2.37 (s, 3H); $^{13}C\{^1H\}$ NMR (100 MHz, $CDCl_3$) δ 151.9, 144.5, 140.3, 138.2, 133.1, 129.2, 128.9, 128.6, 127.9, 127.7, 127.3, 125.8, 125.3, 105.0, 21.3.

5-(4-Methoxyphenyl)-1,3-diphenyl-1*H*-pyrazole (8d).

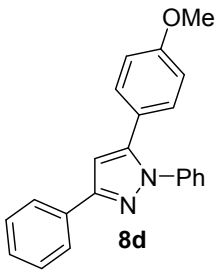

Following the general procedure, $CsPbBr_3$ perovskite NCs (**QD1**, 1 mg), **7d** (0.1 mmol) and 3 mL 1,2-dichloroethane solvent (DCE) were subjected to irradiation to afford the pure product **8d** (30.3 mg, 0.093 mmol) as a thick liquid in 93% yield. ^{1}H NMR (400 MHz, $CDCl_3$) δ 7.96 (d, J = 8.08 Hz, 2H), 7.47–7.31 (m, 8H), 7.22 (d, J = 8.72 Hz, 2H), 6.86 (d, J = 8.72 Hz, 2H), 6.79 (s, 1H), 3.80 (s, 3H); $^{13}C\{^1H\}$ NMR (100 MHz, $CDCl_3$) δ 159.6, 151.9, 144.3, 140.3, 133.2, 130.0, 128.9, 128.6, 127.9, 127.3, 125.8, 125.3, 123.0, 113.9, 104.7, 55.2.

3-(4-Chlorophenyl)-1,5-diphenyl-1*H*-pyrazole (8e).

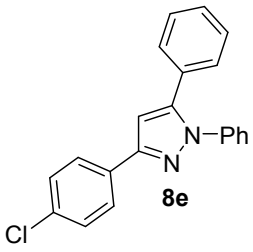

Following the general procedure, $CsPbBr_3$ perovskite NCs (**QD1**, 1 mg), **7e** (0.1 mmol) and 3 mL 1,2-dichloroethane solvent (DCE) were subjected to irradiation to afford the pure product **8e** (29.4 mg, 0.089 mmol) as a thick liquid in 89% yield. ^{1}H NMR (400 MHz, $CDCl_3$) δ 7.87 (d, J = 8.44 Hz, 2H), 7.42–7.27 (m, 12H), 6.80 (s, 1H); $^{13}C\{^1H\}$ NMR (100 MHz, $CDCl_3$) δ 150.8, 144.6, 140.0, 133.7, 131.6, 130.4, 128.9, 128.8, 128.7, 128.5, 128.4, 127.5, 127.0, 125.3, 105.1.

16. References:

(1) Yang, J.; Jiang, C.; Yang, J.; Qian, C.; Fang, D.; Taylor, P. Green Chemistry Letters and Reviews A Clean Procedure for the Synthesis of 1 , 4- Dihydropyridines via Hantzsch Reaction in Water. *Green Chem. Lett. Rev.* **2013**, *6*, 262–267.

(2) Ananthakrishnan, R.; Gazi, S. [Ru(Bpy)3]2+ Aided Photocatalytic Synthesis of 2-Arylpyridines via Hantzsch Reaction under Visible Irradiation and Oxygen Atmosphere. *Catal. Sci. Technol.* **2012**, *2*, 1463–1471.

(3) Raghav, N.; Singh, M. Bioorganic & Medicinal Chemistry SAR Studies of Differently Functionalized Chalcones Based Hydrazones and Their Cyclized Derivatives as Inhibitors of Mammalian Cathepsin B and Cathepsin H. *Bioorg. Med. Chem.* **2014**, *22*, 4233–4245.

(4) Zhu, C.; Akiyama, T. Benzothiazoline : Highly Efficient Reducing Agent for the Enantioselective Organocatalytic Transfer Hydrogenation of Ketimines. *Org. Lett.* **2009**, *11*, 4180–4183.

(5) Fujisue, C.; Kadoya, T.; Higashino, T.; Sato, R.; Kawamoto, T.; Mori, T. Air-Stable Ambipolar Organic Transistors Based on Charge-Transfer Complexes Containing Dibenzopyrrolopyrrole. *RSC Adv.* **2016**, *6*, 53345–53350.

(6) Tang, M. L.; Reichardt, A. D.; Wei, P.; Bao, Z. Correlating Carrier Type with Frontier Molecular Orbital Functionalized Acene Derivatives. *J. Am. Chem. Soc.* **2009**, *131*, 5264–5273.

(7) Wang, W.; Zhao, N.; Geng, Y.; Cui, S.; Hauser, J.; Decurtins, S.; Liu, S.-X. A Highly Sensitive TTF-Functionalised Probe for the Determination of Physiological Thiols and Its Application in Tumor Cells. *RSC Adv.* **2014**, *4*, 32639–32642.

(8) Thapa, S.; Bhardwaj, K.; Basel, S.; Pradhan, S.; Eling, C. J.; Adawi, A. M.; Bouillard, J.-S. G.; Stasiuk, G. J.; Reiss, P.; Pariyar, A.; et al. Long-Term Ambient Air-Stable Cubic CsPbBr3 Perovskite Quantum Dots Using Molecular Bromine. *Nanoscale Adv.* **2019**, *1*, 3388–3391.

(9) Protesescu, L.; Yakunin, S.; Bodnarchuk, M. I.; Krieg, F.; Caputo, R.; Hendon, C. H.;

Yang, R. X.; Walsh, A.; Kovalenko, M. V. Nanocrystals of Cesium Lead Halide Perovskites (CsPbX3, X = Cl, Br, and I): Novel Optoelectronic Materials Showing Bright Emission with Wide Color Gamut. *Nano Lett.* **2015**, *15*, 3692–3696.

(10) Swarnkar, A.; Chulliyil, R.; Ravi, V. K.; Irfanullah, M.; Chowdhury, A.; Nag, A. Colloidal CsPbBr3 Perovskite Nanocrystals: Luminescence beyond Traditional Quantum Dots. *Angew. Chem. Int. Ed.* **2015**, *54*, 15424–15428.

(11) Zhu, X.; Lin, Y.; Sun, Y.; Beard, M. C.; Yan, Y. Lead-Halide Perovskites for Photocatalytic α-Alkylation of Aldehydes. *J. Am. Chem. Soc.* **2019**, *141*, 733–738.

(12) Luiz, F. C. L.; Garcia, L. S.; Filho, L. S. G.; Teixeira, L. R.; Louro, S. R. W. Fluorescence Studies of Gold (III)-Norfloxacin Complexes in Aqueous Solutions. *J. Fluoresc.* **2011**, *21*, 1933–1940.

(13) Hidalgo-Acosta, J. C.; Méndez, M. A.; Scanlon, M. D.; Vrubel, H.; Amstutz, V.; Adamiak, W.; Opallo, M.; Girault, H. H. Catalysis of Water Oxidation in Acetonitrile by Iridium Oxide Nanoparticles. *Chem. Sci.* **2015**, *6*, 1761–1769.

(14) Wu, W.-B.; Wong, Y.-C.; Tan, Z.-K.; Wu, J. Photo-Induced Thiol Coupling and C−H Activation Using Nanocrystalline Lead-Halide Perovskite Catalysts. *Catal. Sci. Technol.* **2018**, *8*, 4257–4263.

17. Copies of NMR spectra of products:

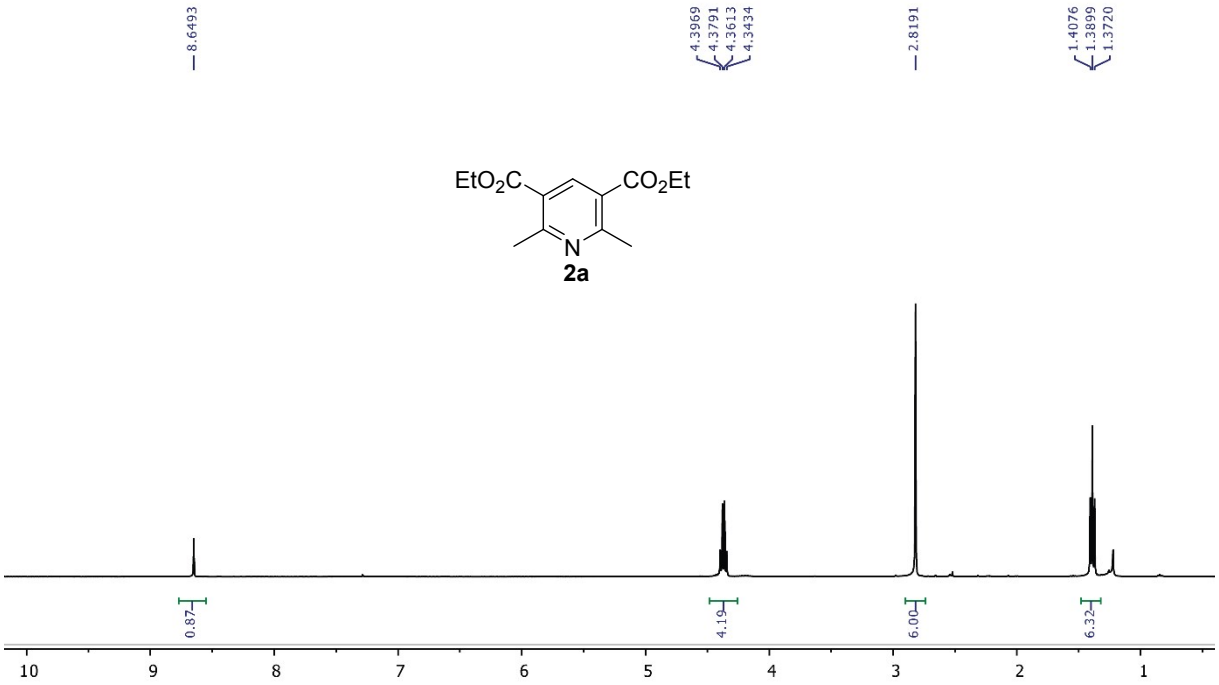

Figure S33. ^{1}H NMR of **2a** (400 MHz, $CDCl_3$)

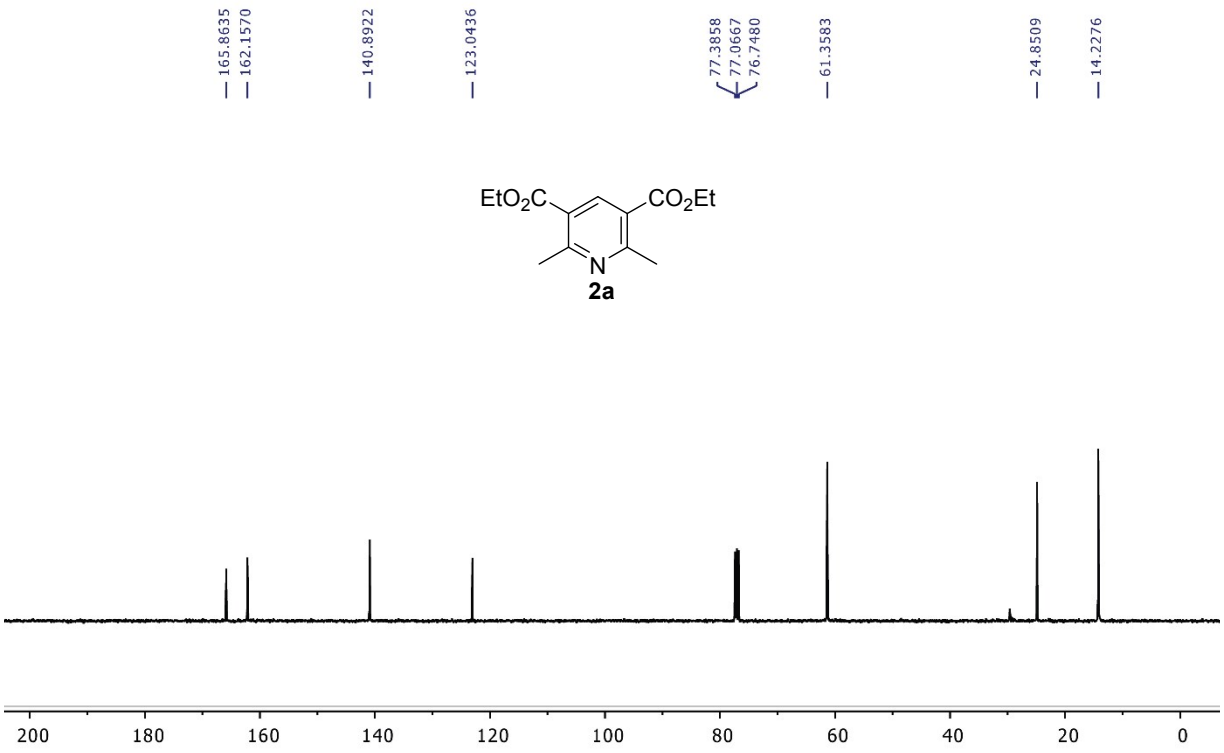

Figure S34. $^{13}C\{^{1}H\}$ NMR of **2a** (100 MHz, $CDCl_3$)

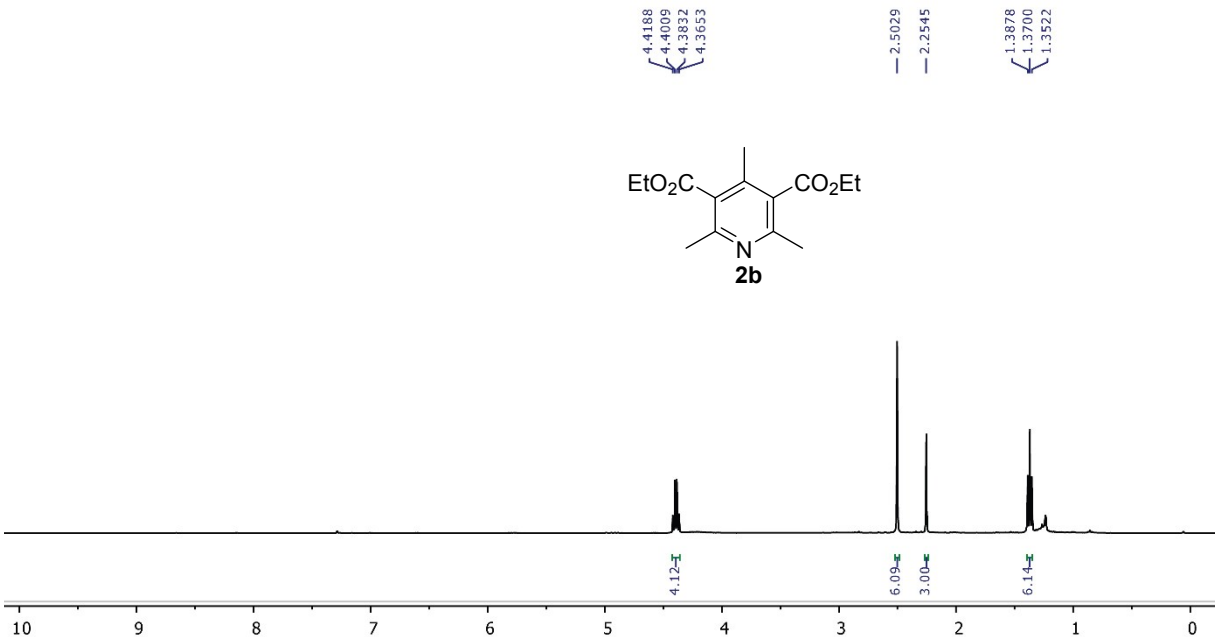

Figure S35. ^{1}H NMR of **2b** (400 MHz, $CDCl_3$)

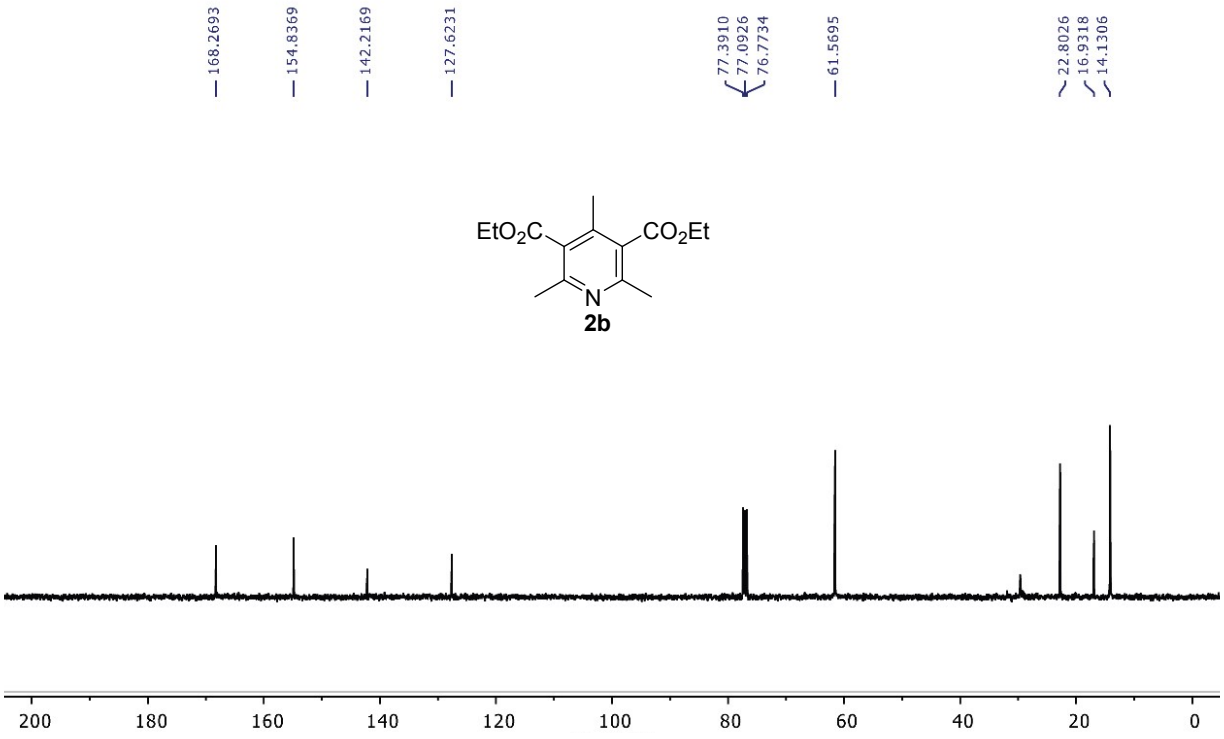

Figure S36. $^{13}C\{^{1}H\}$ NMR of **2b** (100 MHz, $CDCl_3$)

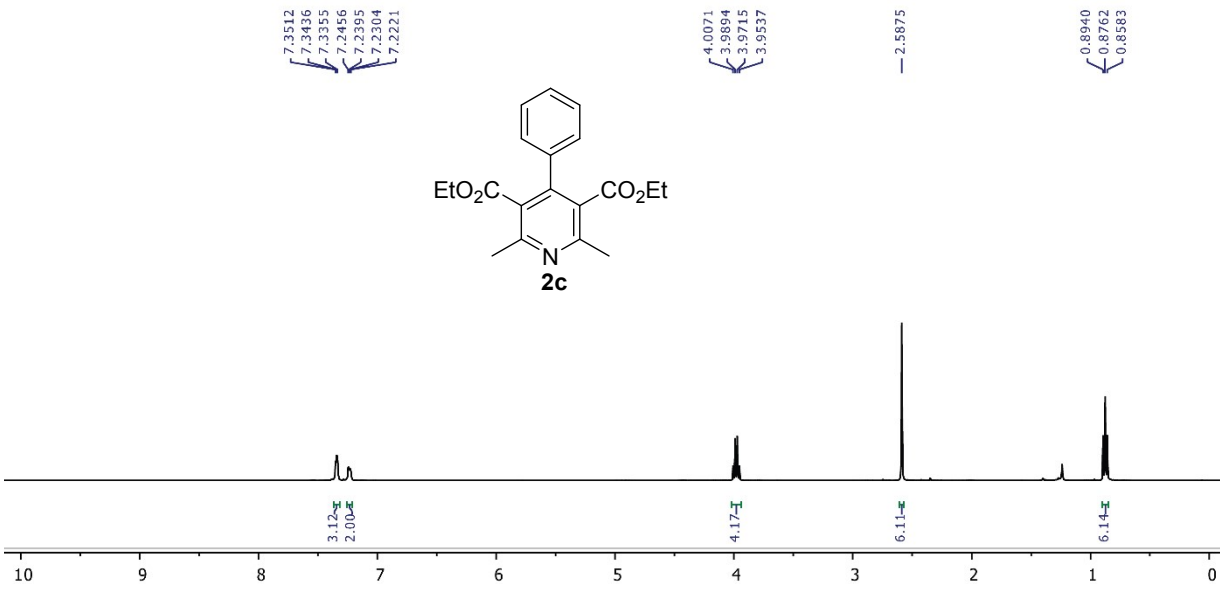

Figure S37. ^{1}H NMR of **2c** (400 MHz, $CDCl_3$)

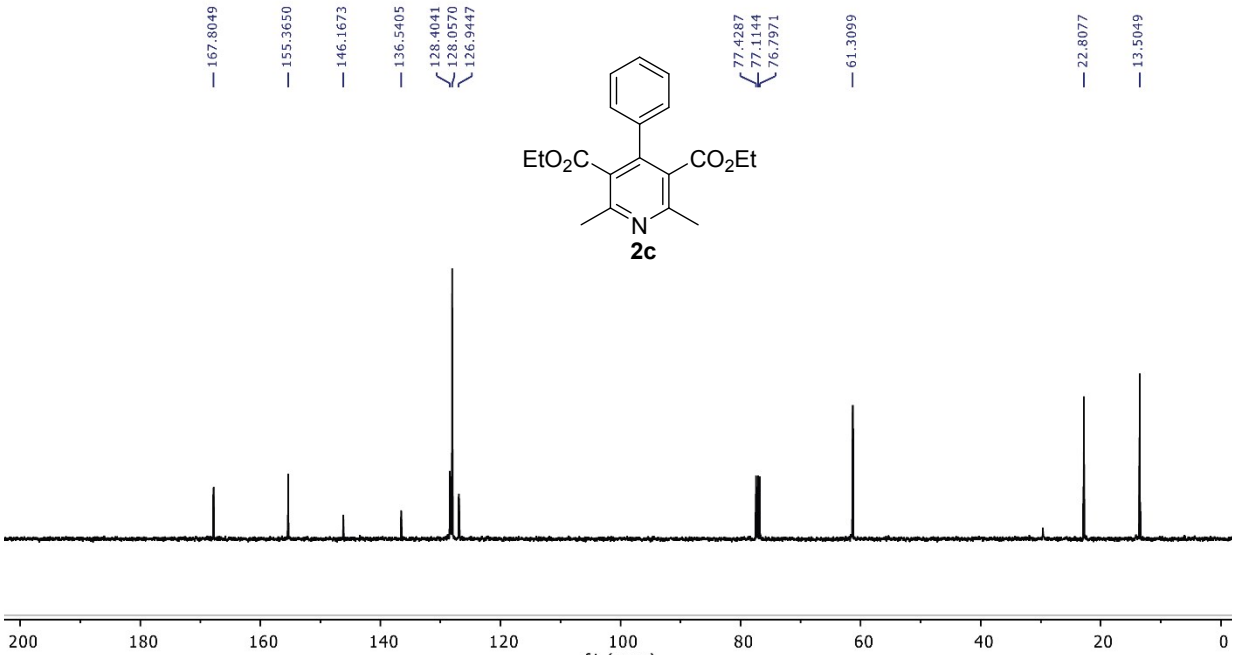

Figure S38. $^{13}C\{^{1}H\}$ NMR of **2c** (100 MHz, $CDCl_3$)

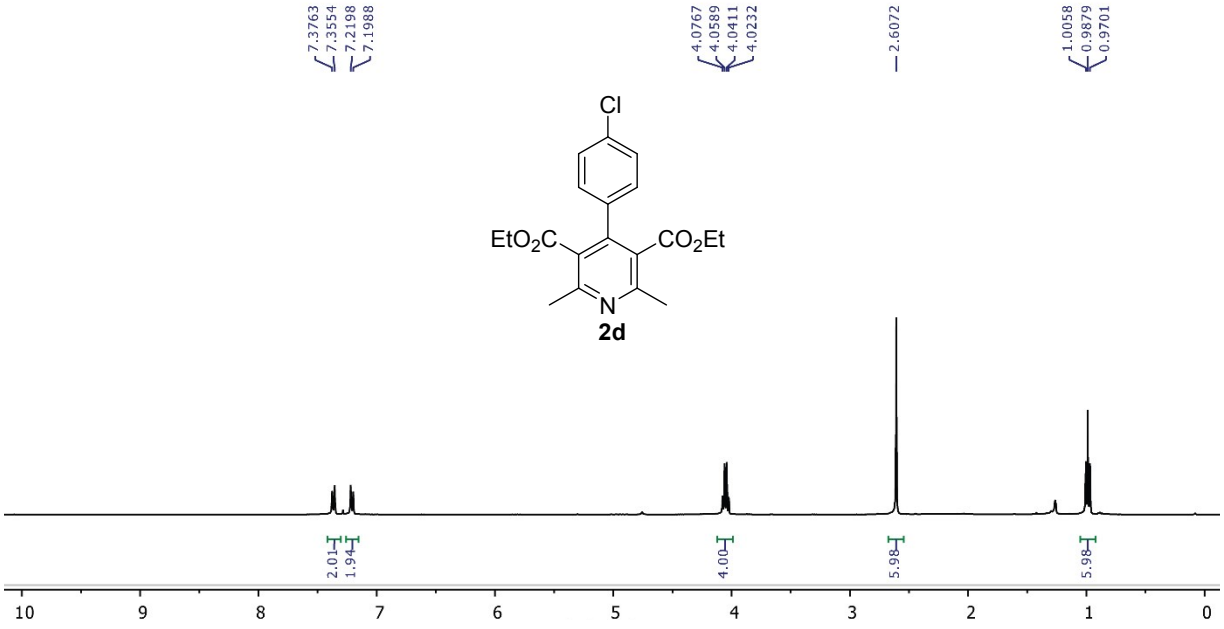

Figure S39. ^{1}H NMR of **2d** (400 MHz, $CDCl_3$)

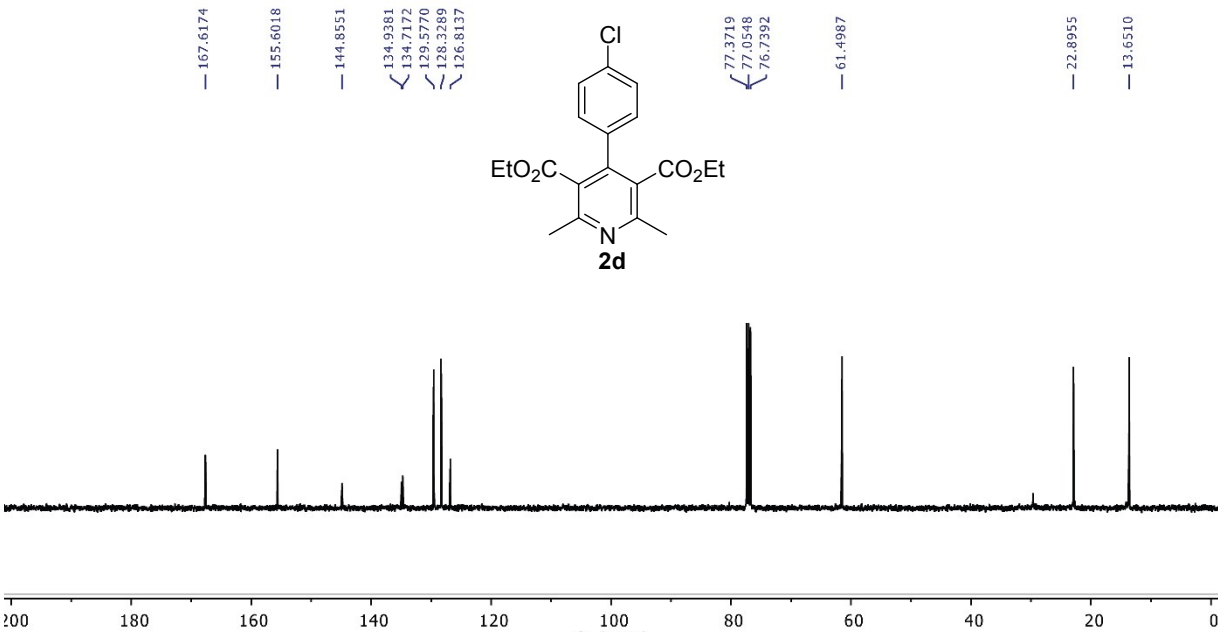

Figure S40. $^{13}C\{^{1}H\}$ NMR of **2d** (100 MHz, $CDCl_3$)

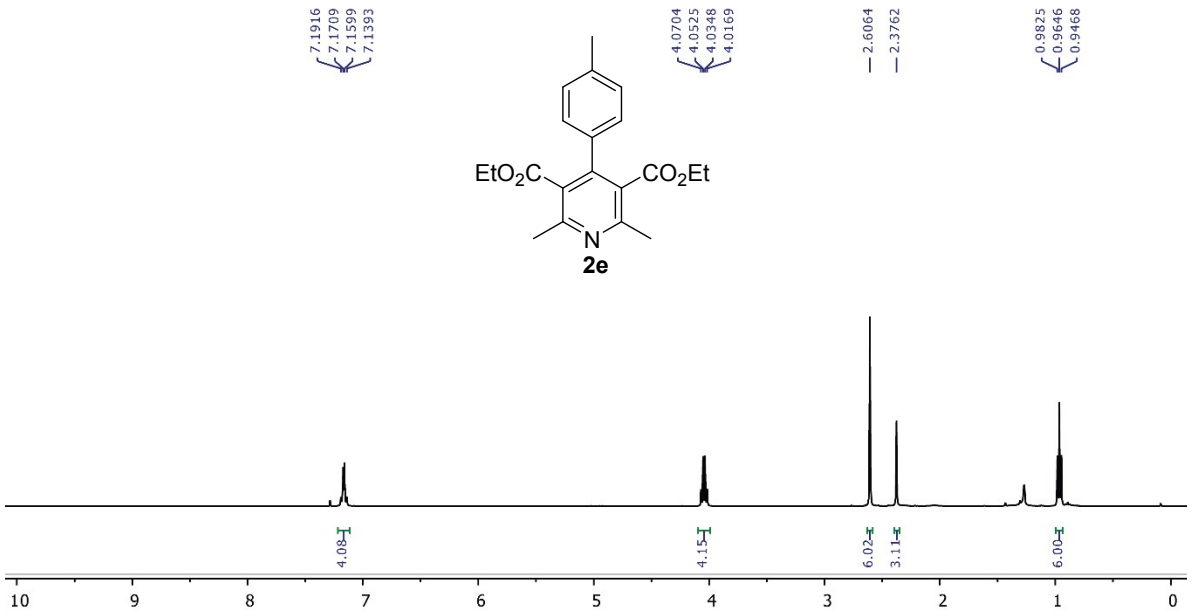

Figure S41. ^{1}H NMR of **2e** (400 MHz, $CDCl_3$)

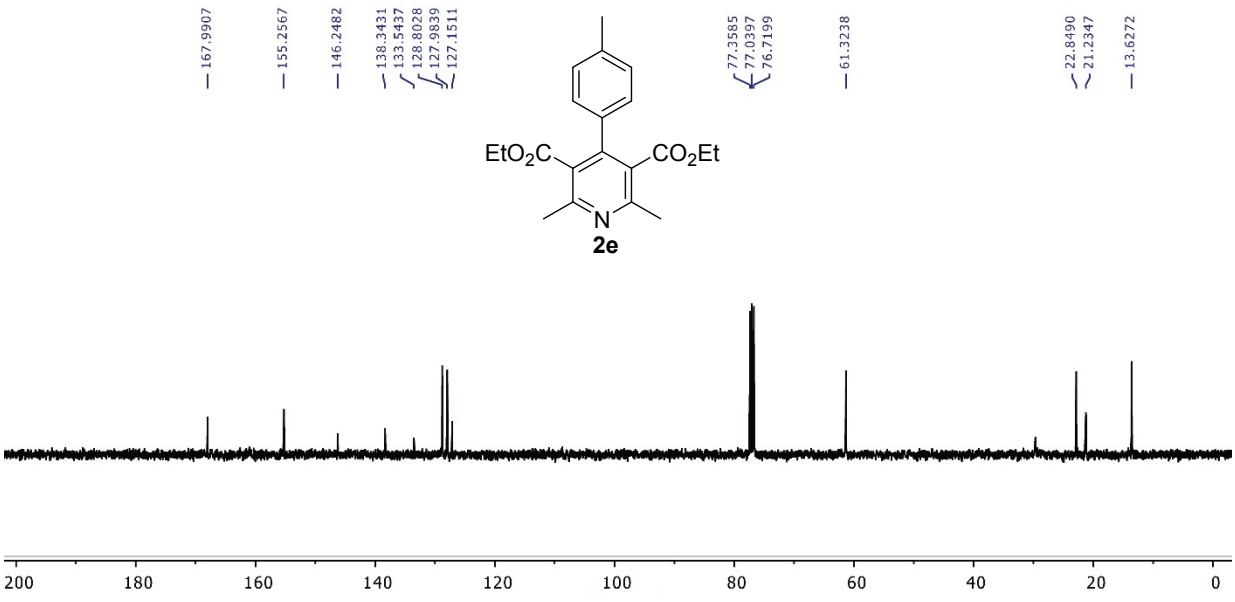

Figure S42. $^{13}C\{^{1}H\}$ NMR of **2e** (100 MHz, $CDCl_3$)

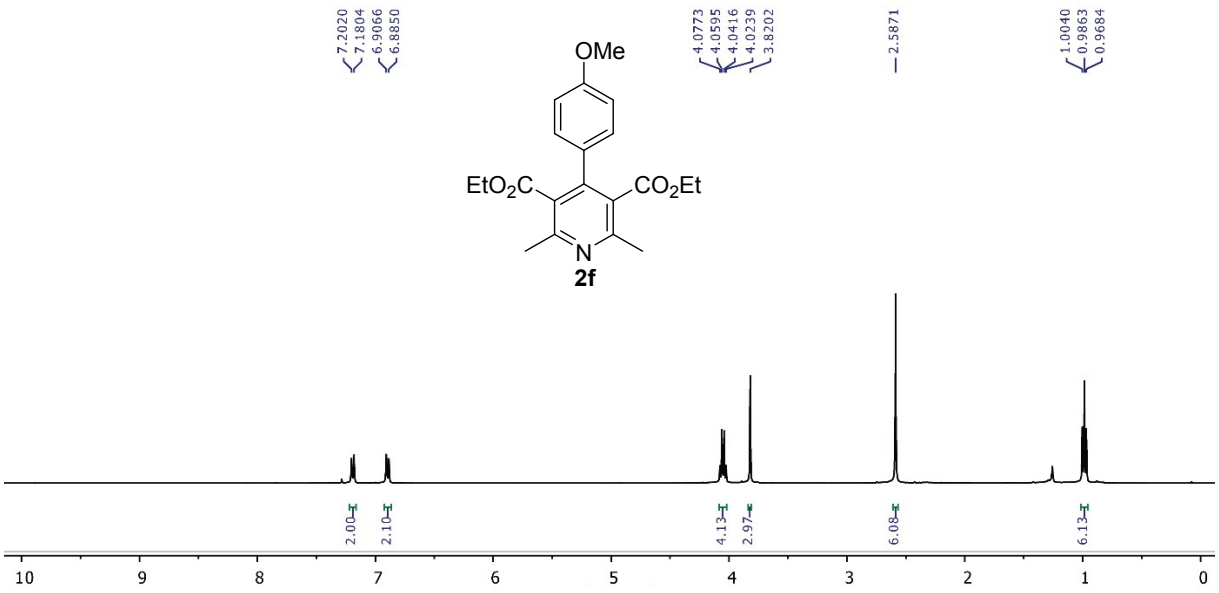

Figure S43. ^{1}H NMR of **2f** (400 MHz, $CDCl_3$)

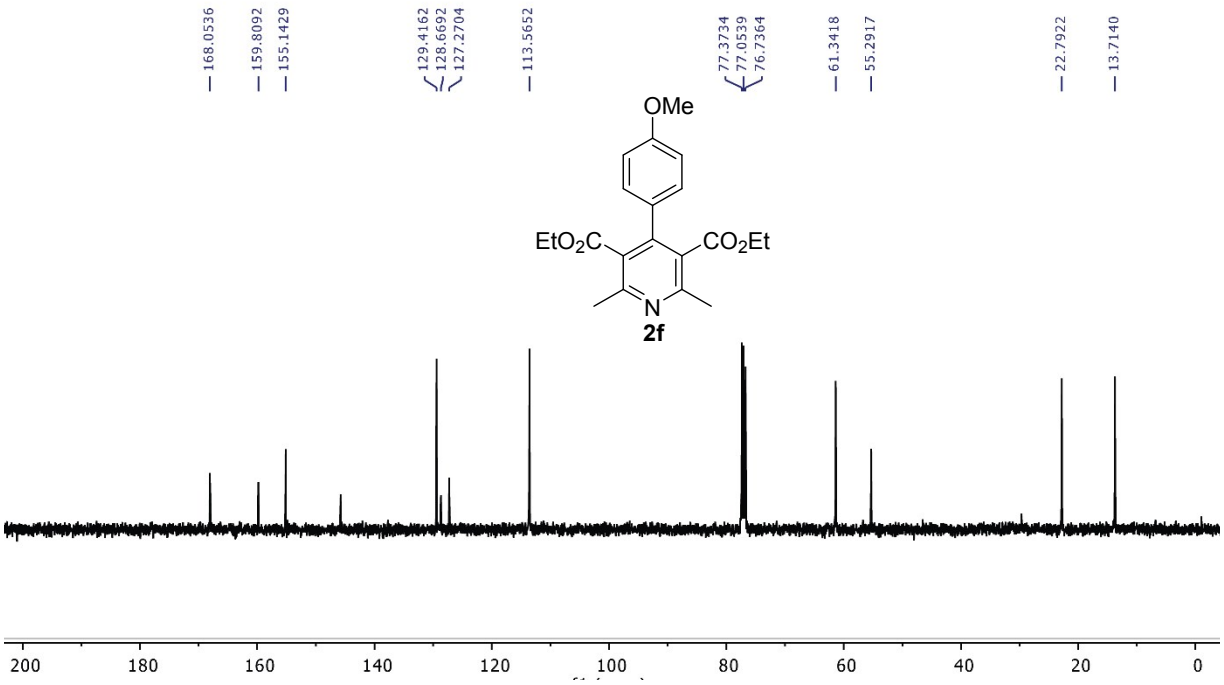

Figure S44. ^{13}C{^{1}H} NMR of **2f** (100 MHz, $CDCl_3$)

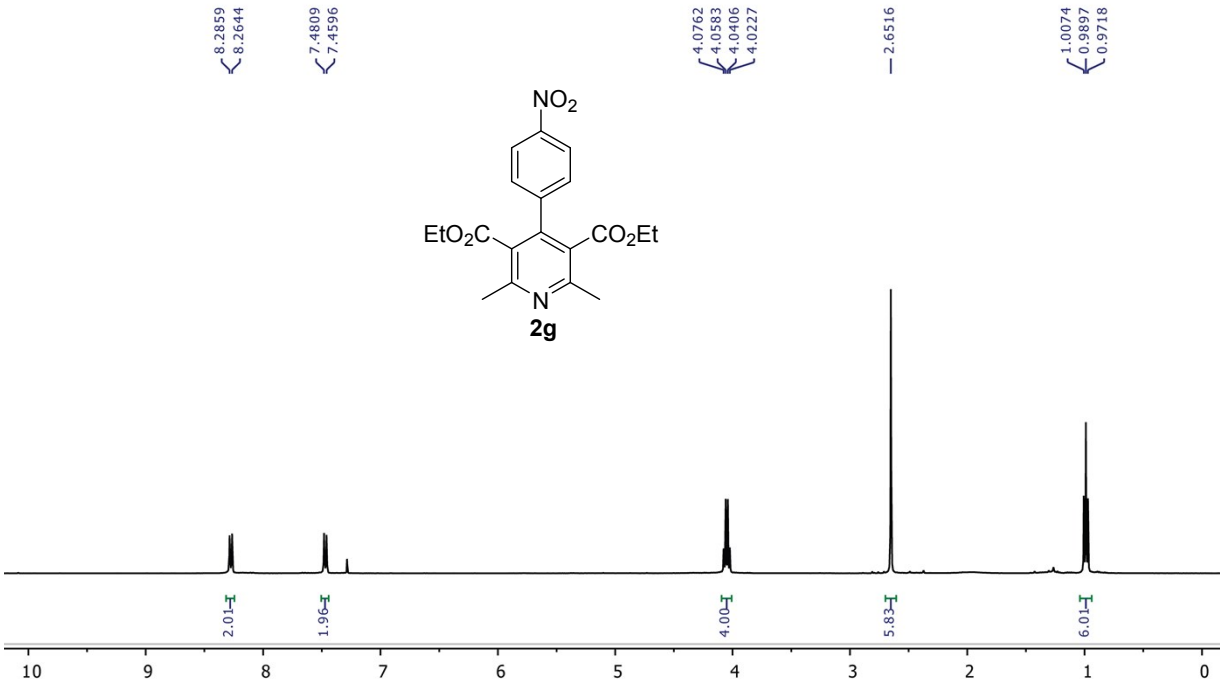

Figure S45. ^{1}H NMR of **2g** (400 MHz, $CDCl_3$)

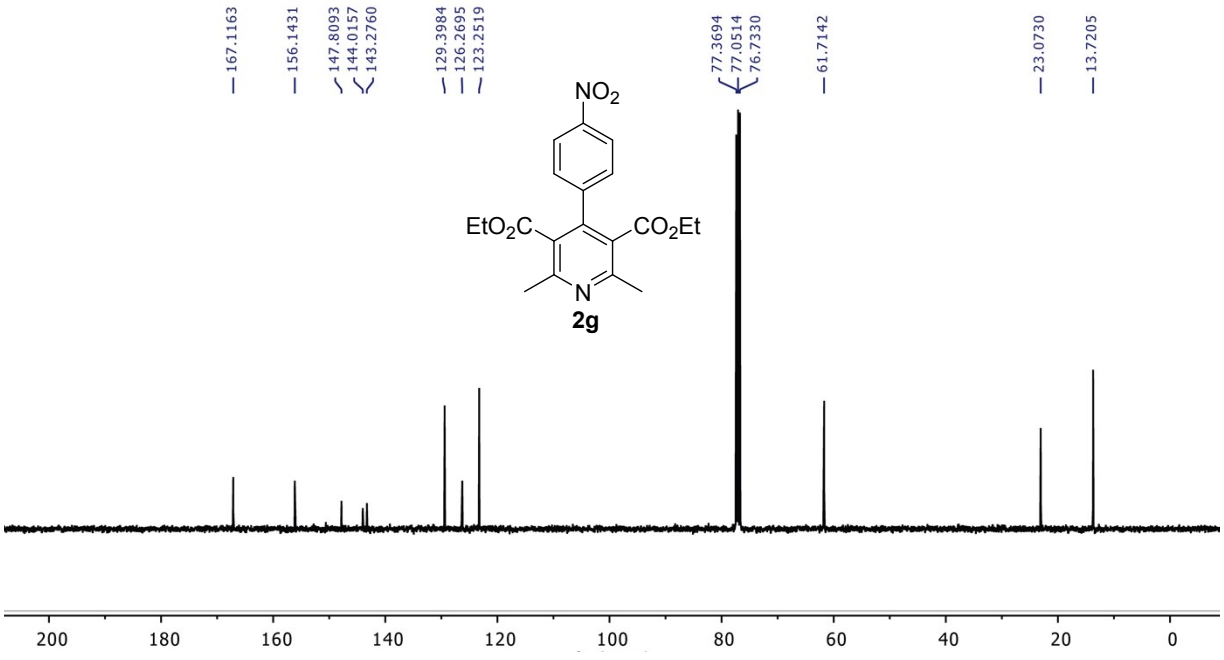

Figure S46. $^{13}C\{^{1}H\}$ NMR of **2g** (100 MHz, $CDCl_3$)

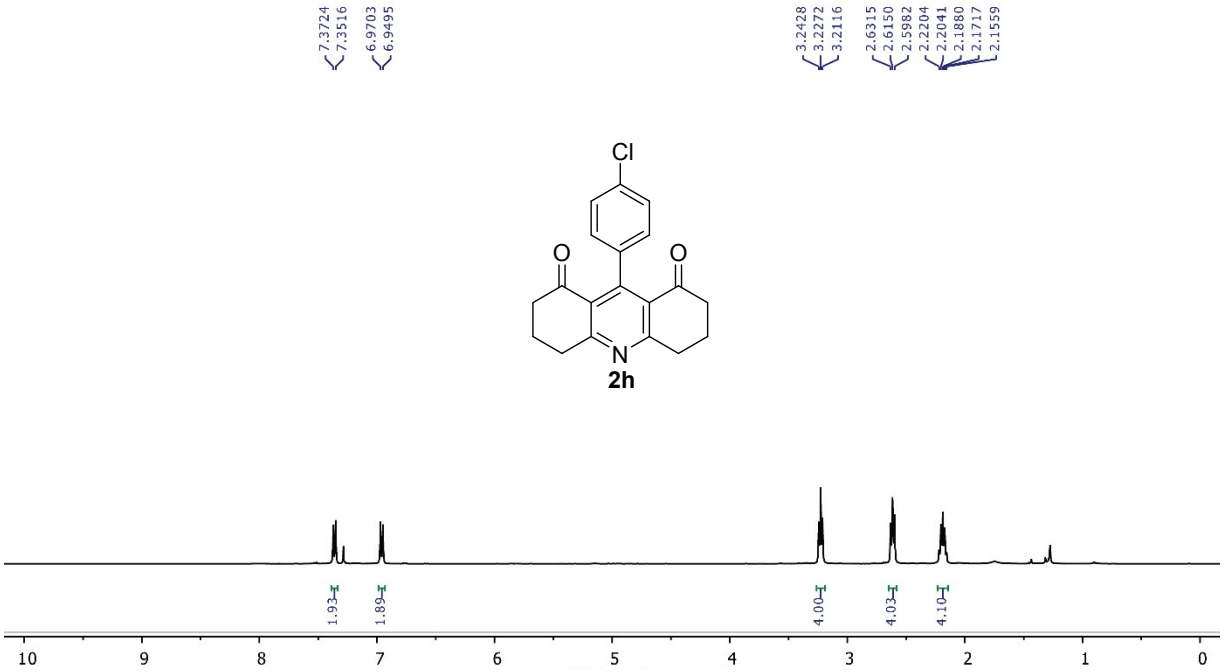

Figure S47. ^{1}H NMR of **2h** (400 MHz, $CDCl_3$)

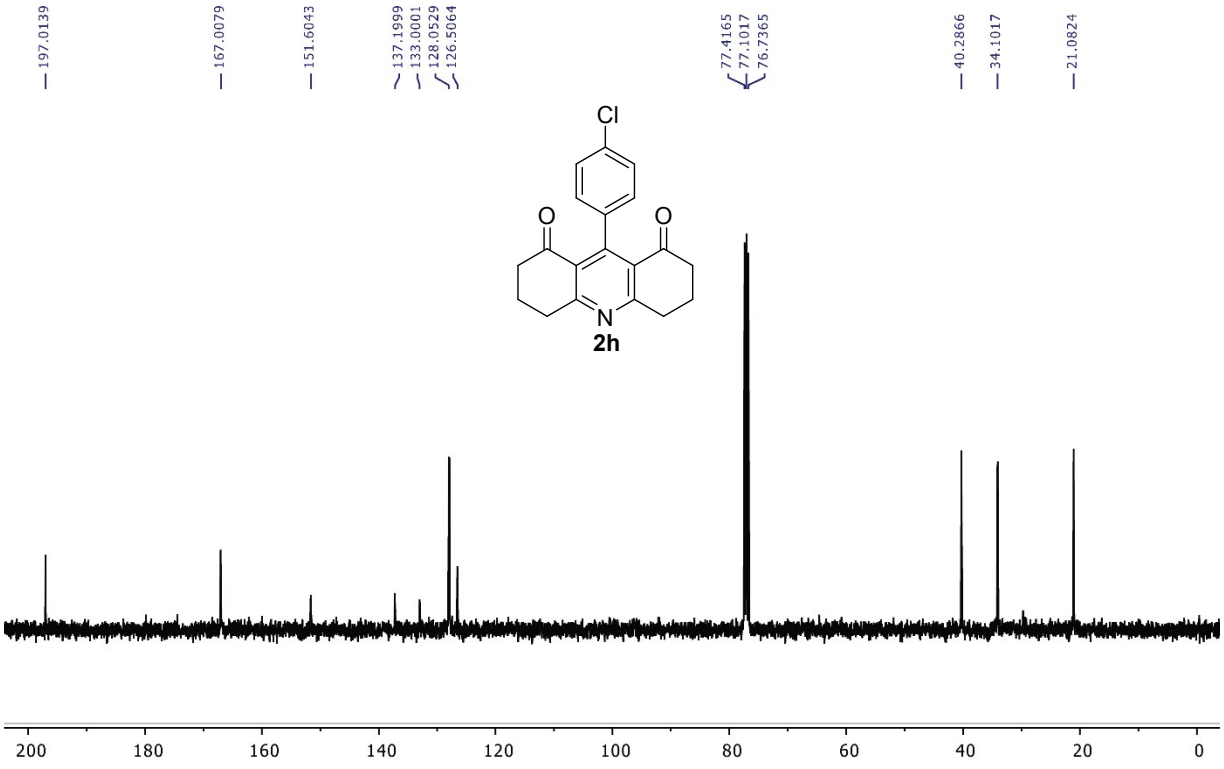

Figure S48. $^{13}C\{^{1}H\}$ NMR of **2h** (100 MHz, $CDCl_3$)

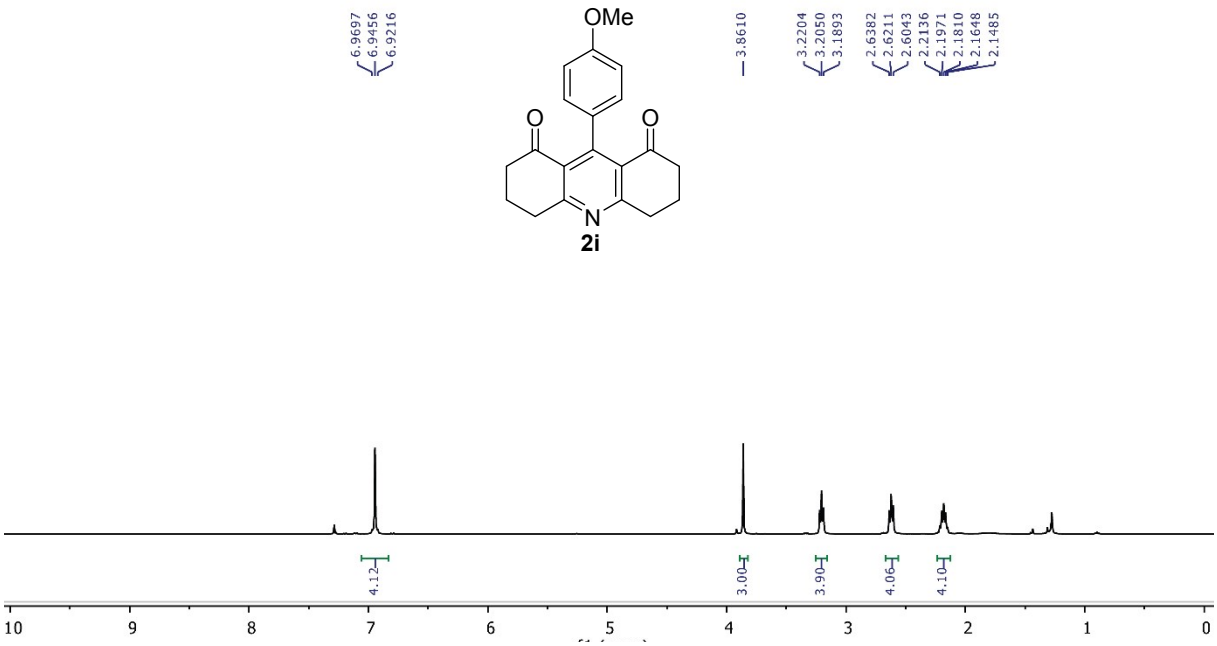

Figure S49. ^{1}H NMR of **2i** (400 MHz, $CDCl_3$)

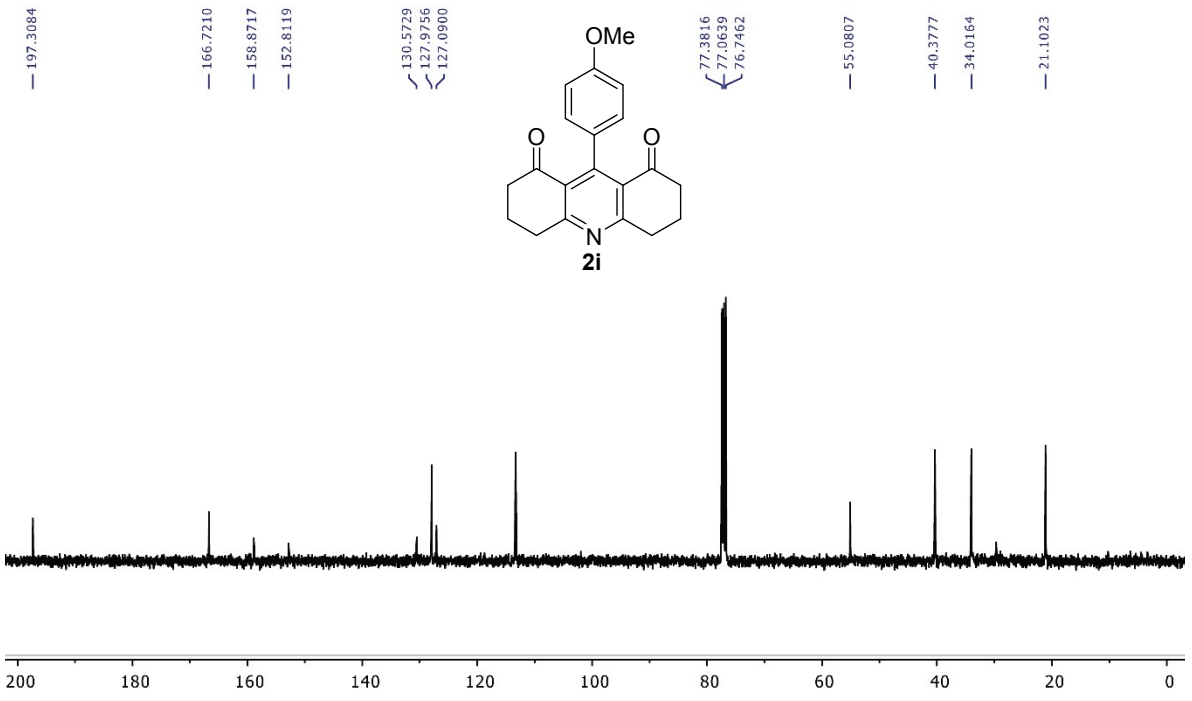

Figure S50. $^{13}C\{^{1}H\}$ NMR of **2i** (100 MHz, $CDCl_3$)

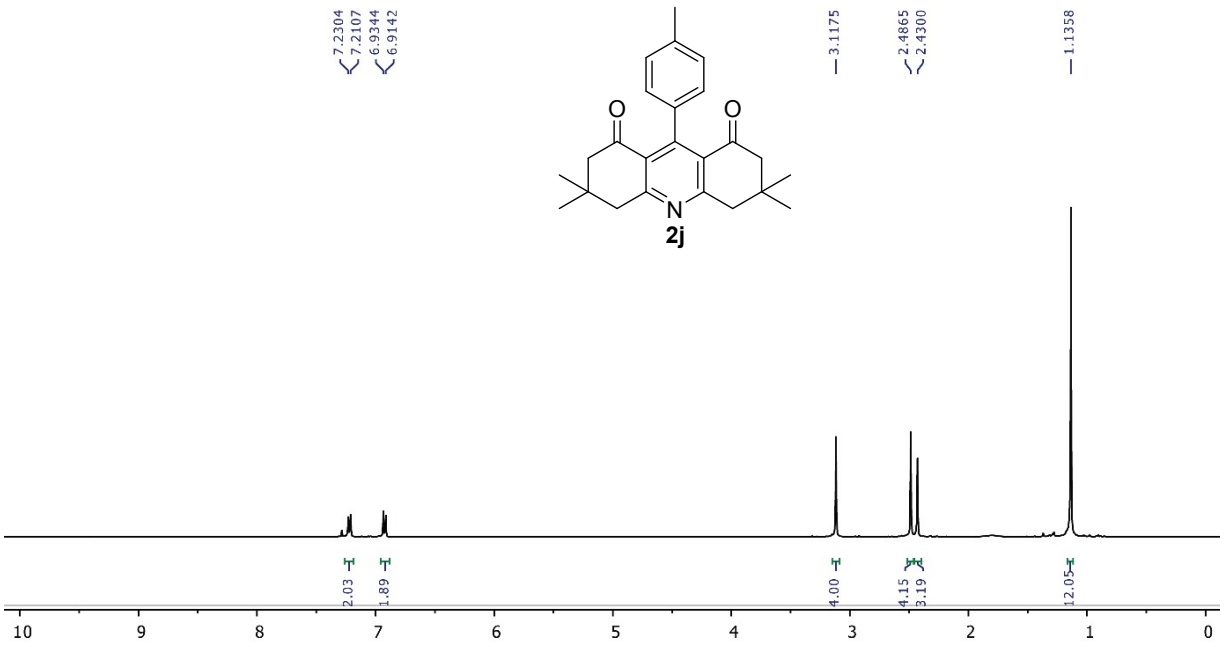

Figure S51. ^{1}H NMR of **2j** (400 MHz, $CDCl_3$)

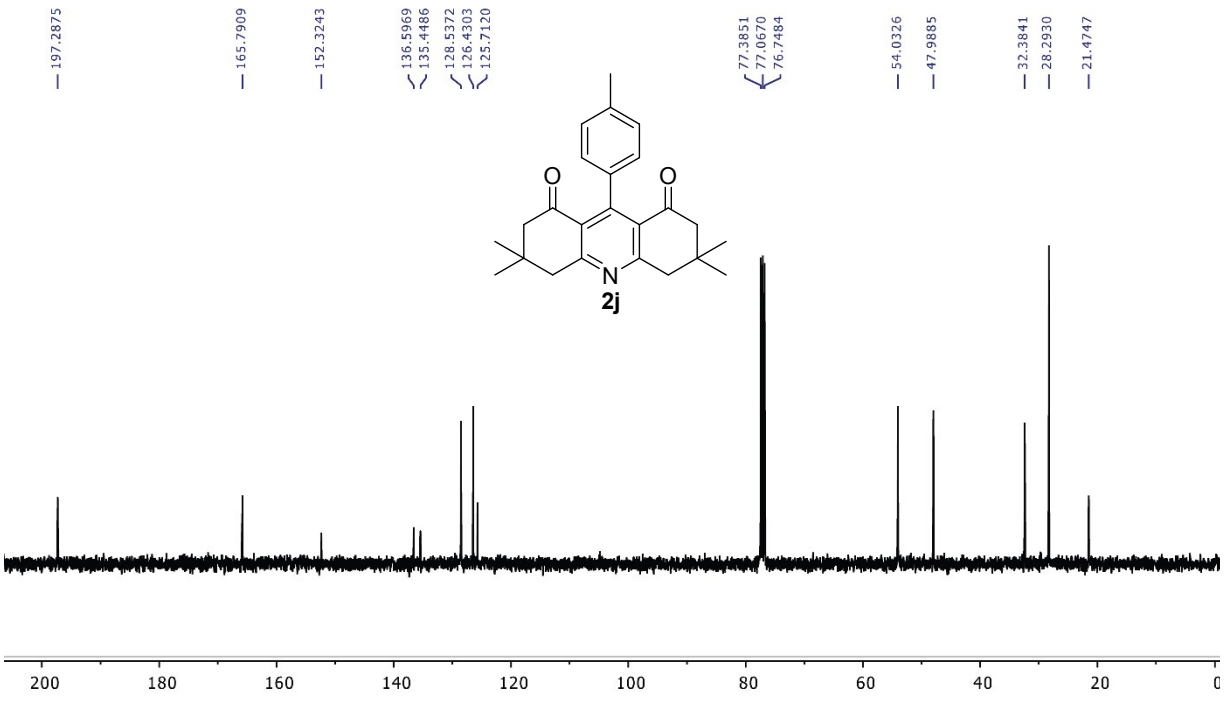

Figure S52. $^{13}C\{^{1}H\}$ NMR of **2j** (100 MHz, $CDCl_3$)

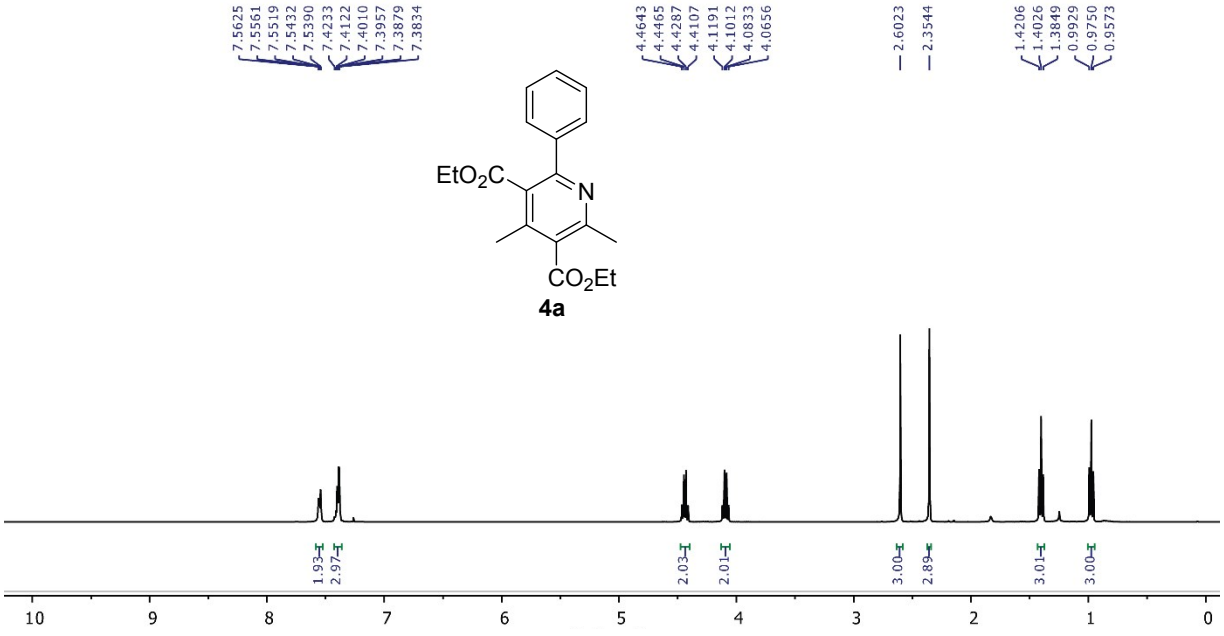

Figure S53. ^{1}H NMR of **4a** (400 MHz, $CDCl_3$)

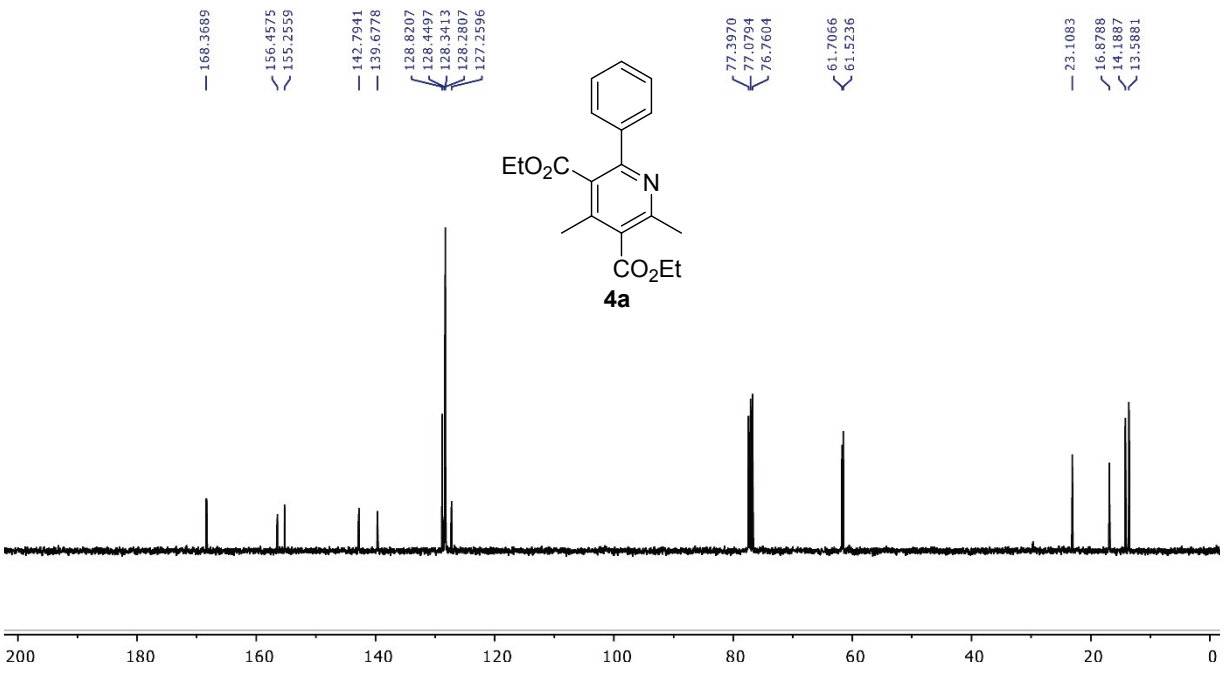

Figure S54. $^{13}C\{^{1}H\}$ NMR of **4a** (100 MHz, $CDCl_3$)

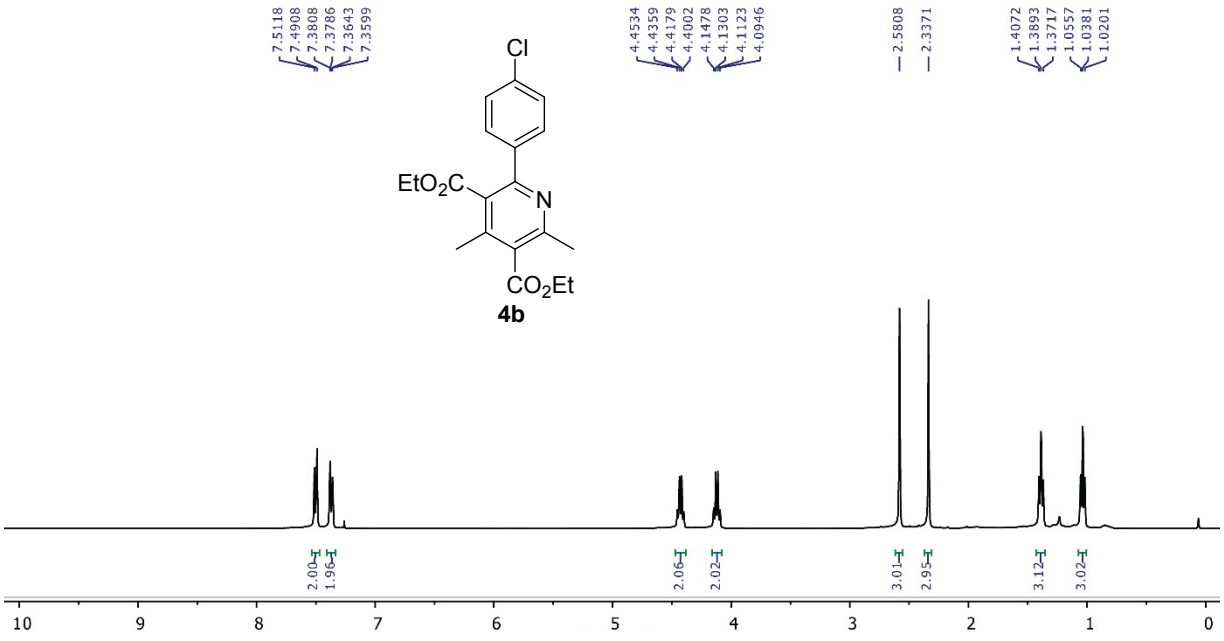

Figure S55. ^{1}H NMR of **4b** (400 MHz, $CDCl_3$)

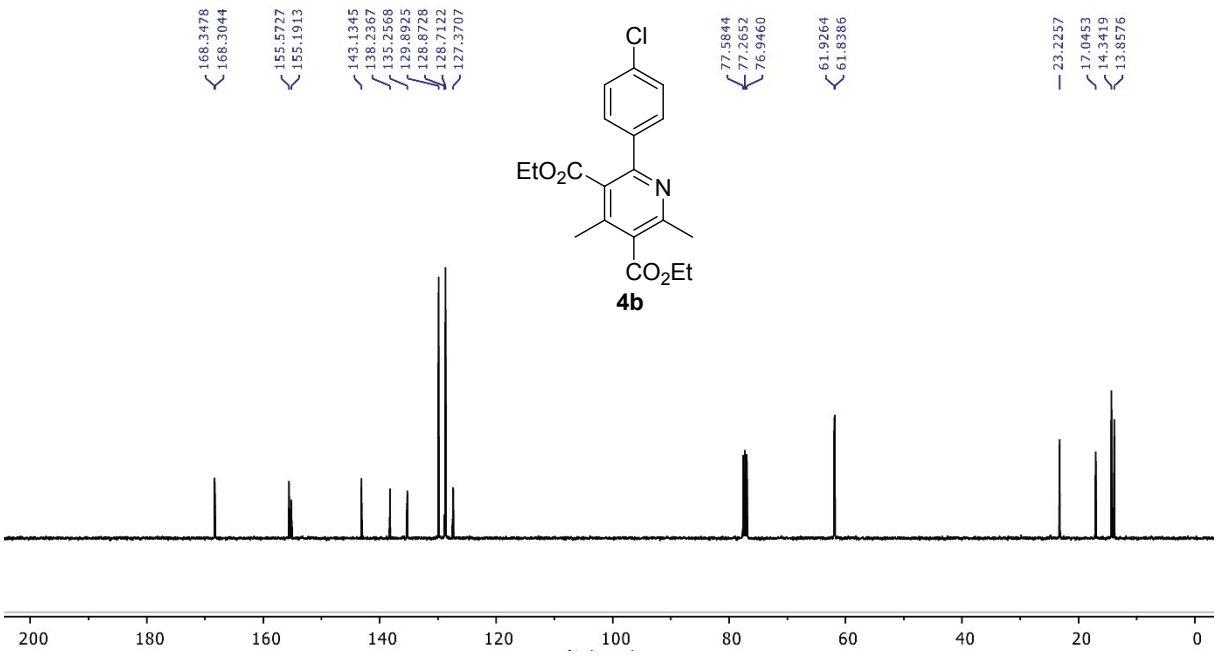

Figure S56. $^{13}C\{^{1}H\}$ NMR of **4b** (100 MHz, $CDCl_3$)

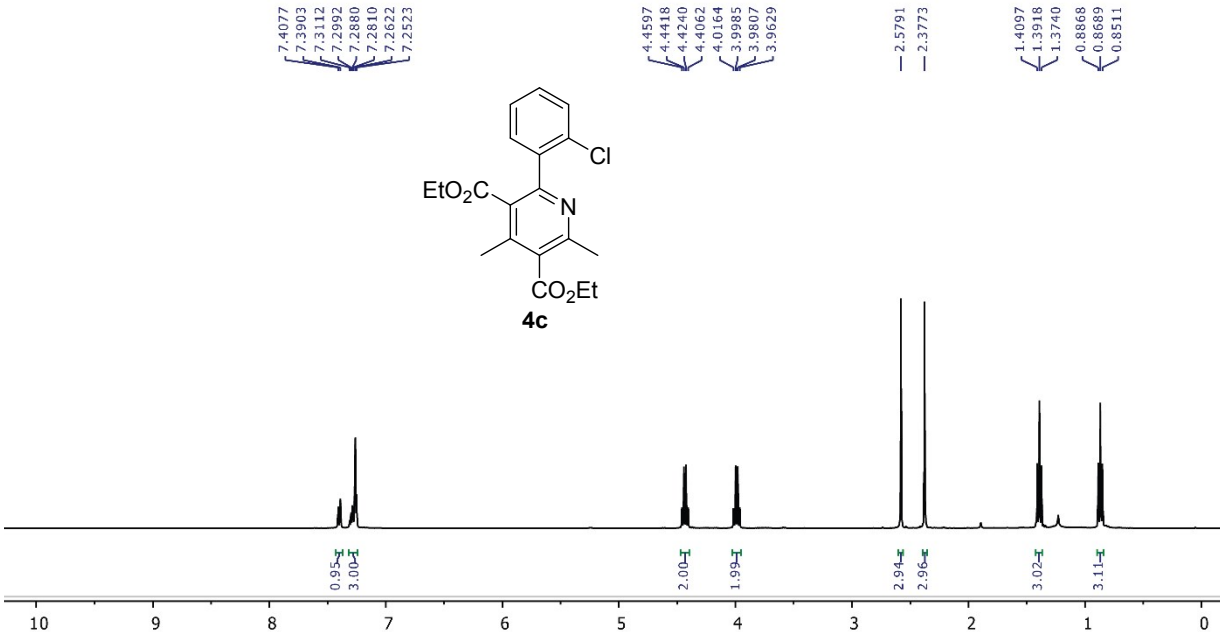

Figure S57. ^{1}H NMR of **4c** (400 MHz, $CDCl_3$)

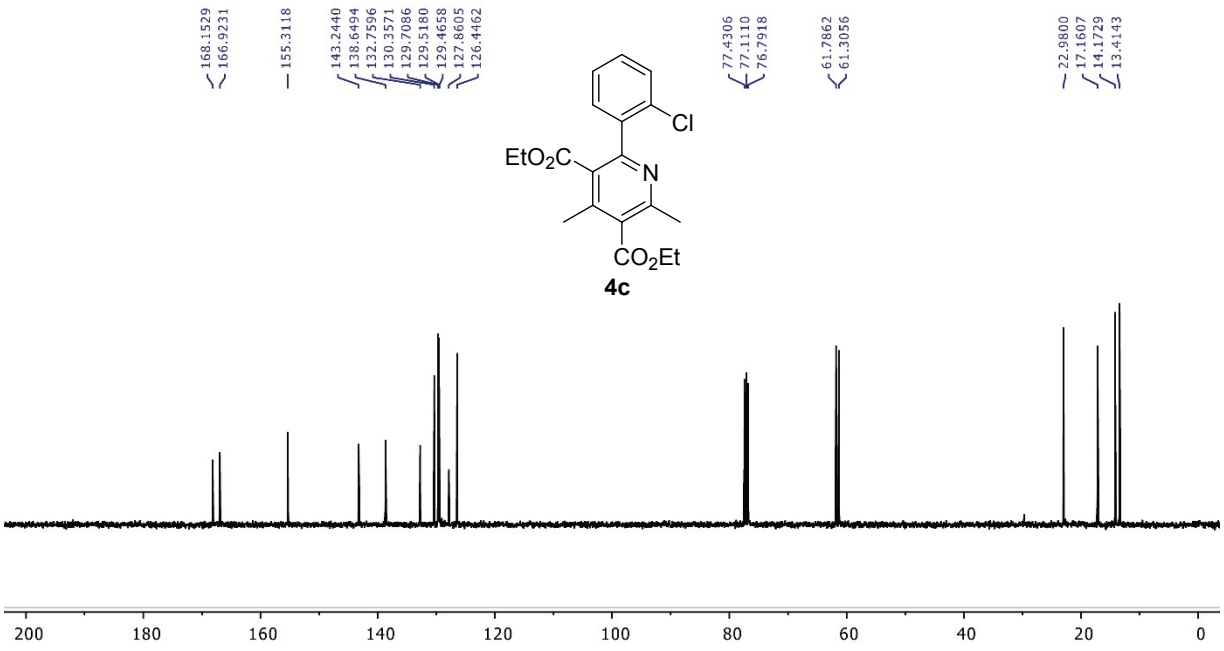

Figure S58. $^{13}C\{^{1}H\}$ NMR of **4c** (100 MHz, $CDCl_3$)

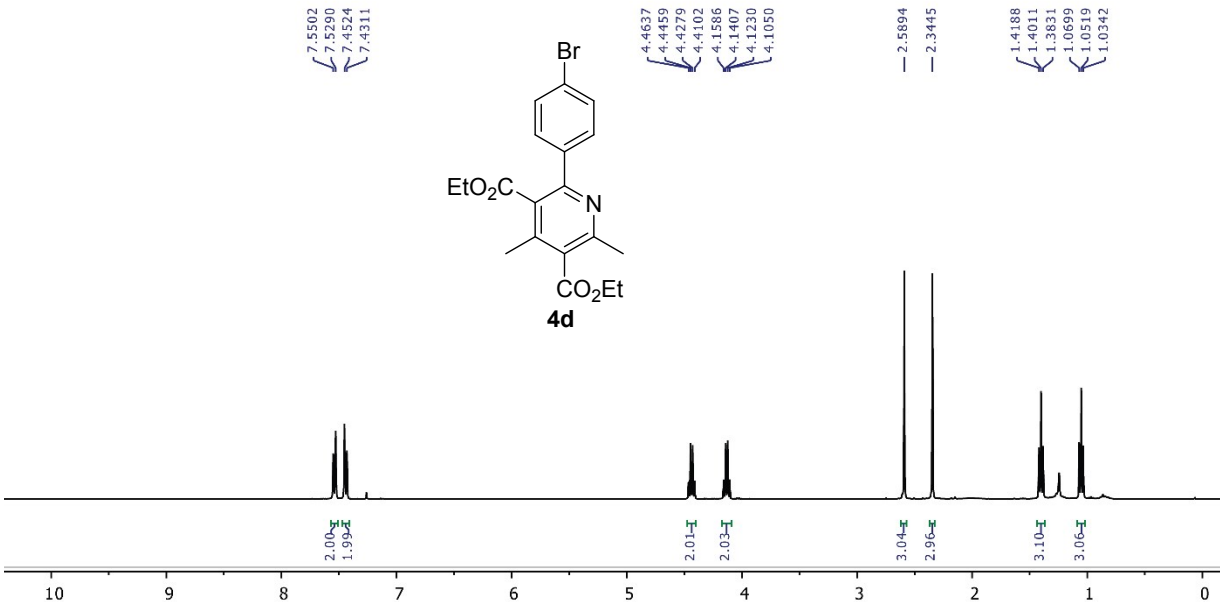

Figure S59. ^{1}H NMR of **4d** (400 MHz, $CDCl_3$)

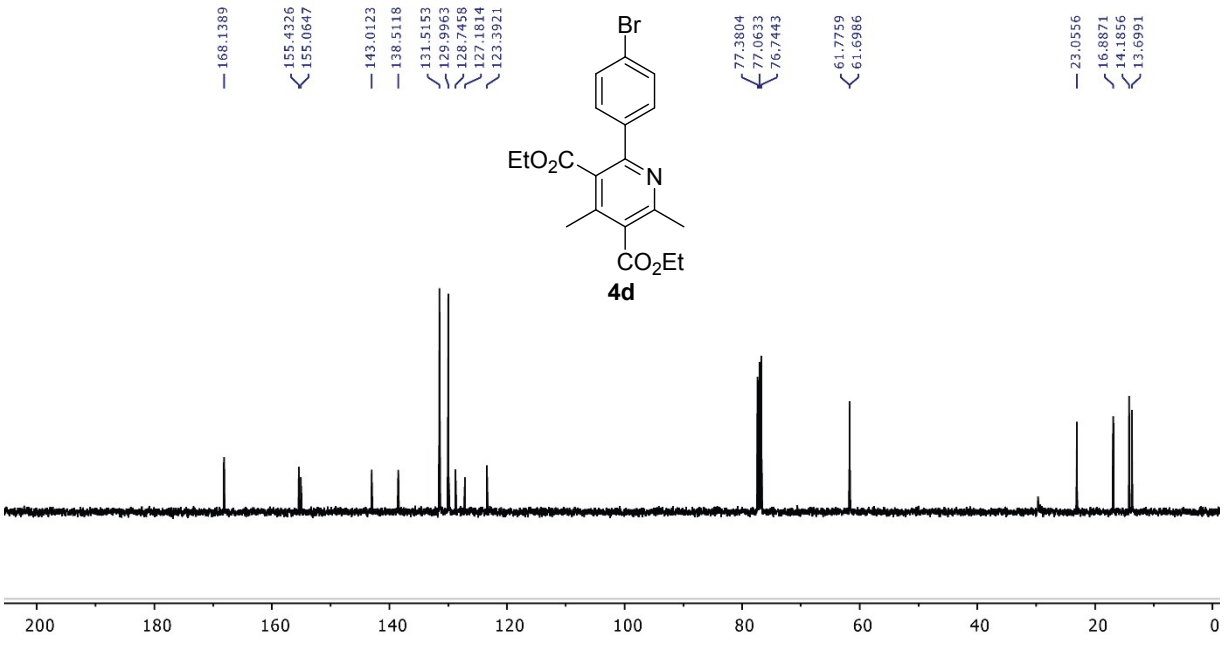

Figure S60. $^{13}C\{^{1}H\}$ NMR of **4d** (100 MHz, $CDCl_3$)

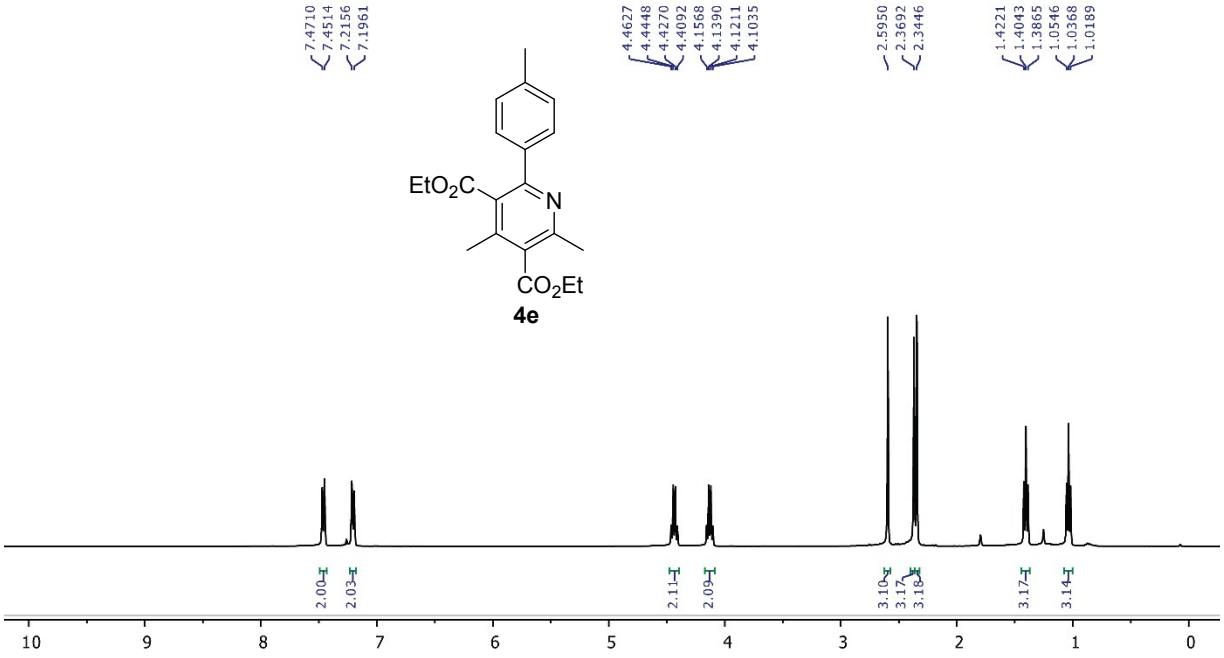

Figure S61. ^{1}H NMR of **4e** (400 MHz, $CDCl_3$)

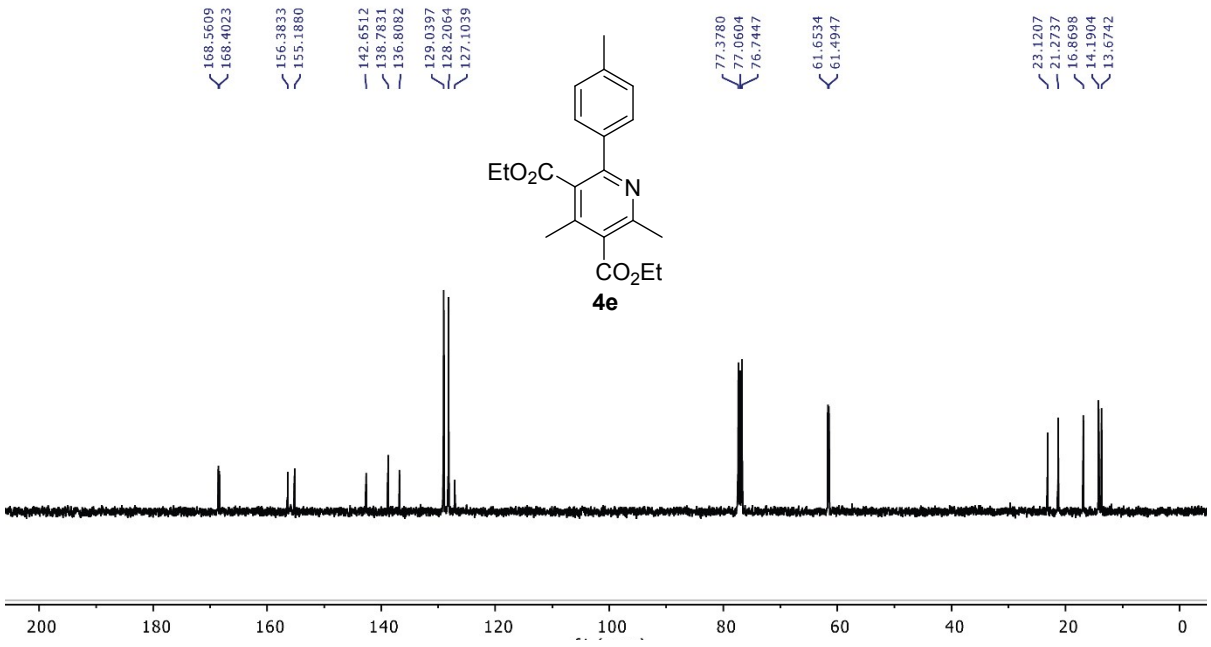

Figure S62. $^{13}C\{^{1}H\}$ NMR of **4e** (100 MHz, $CDCl_3$)

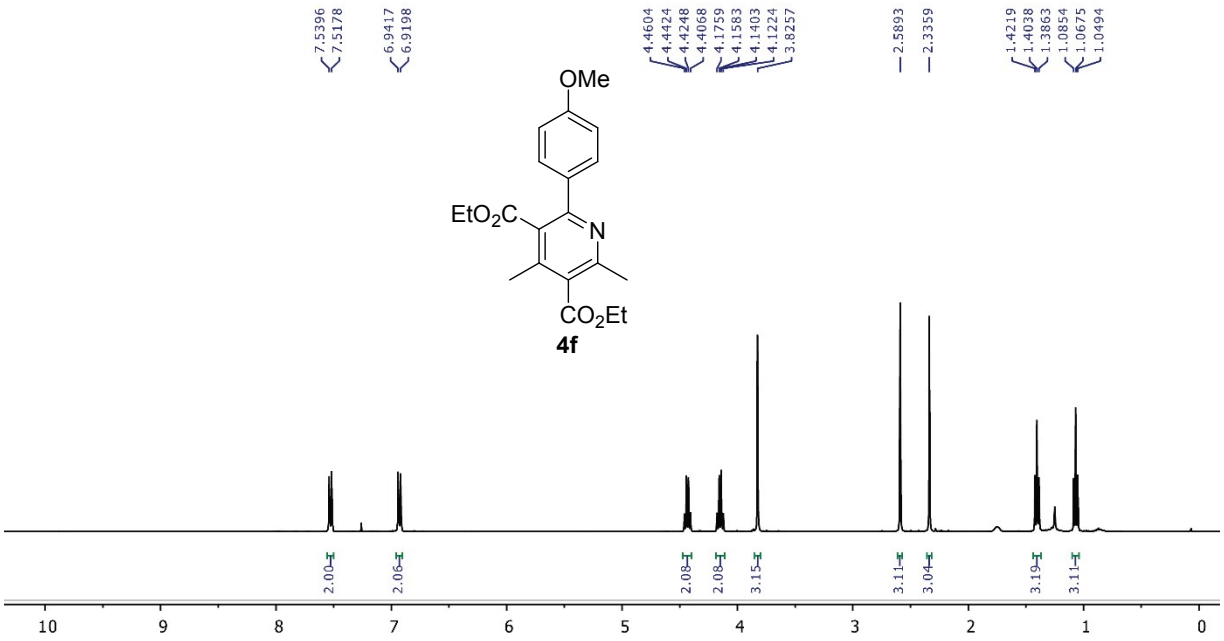

Figure S63. ^{1}H NMR of **4f** (400 MHz, $CDCl_3$)

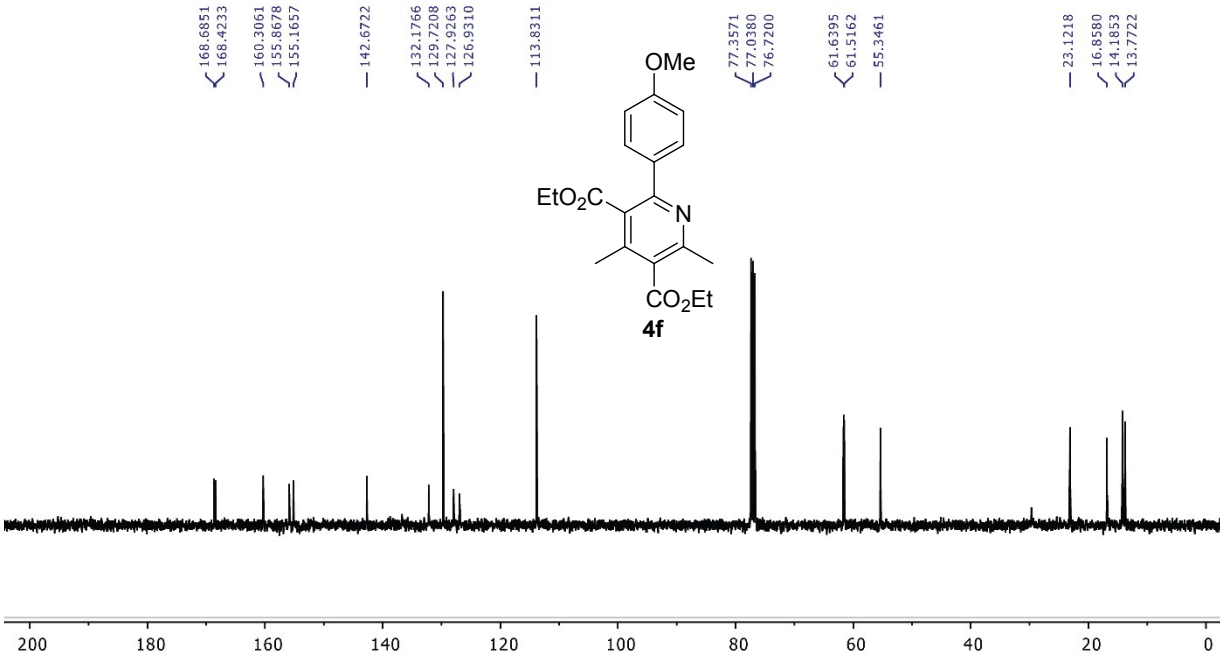

Figure S64. ^{13}C{^{1}H} NMR of **4f** (100 MHz, $CDCl_3$)

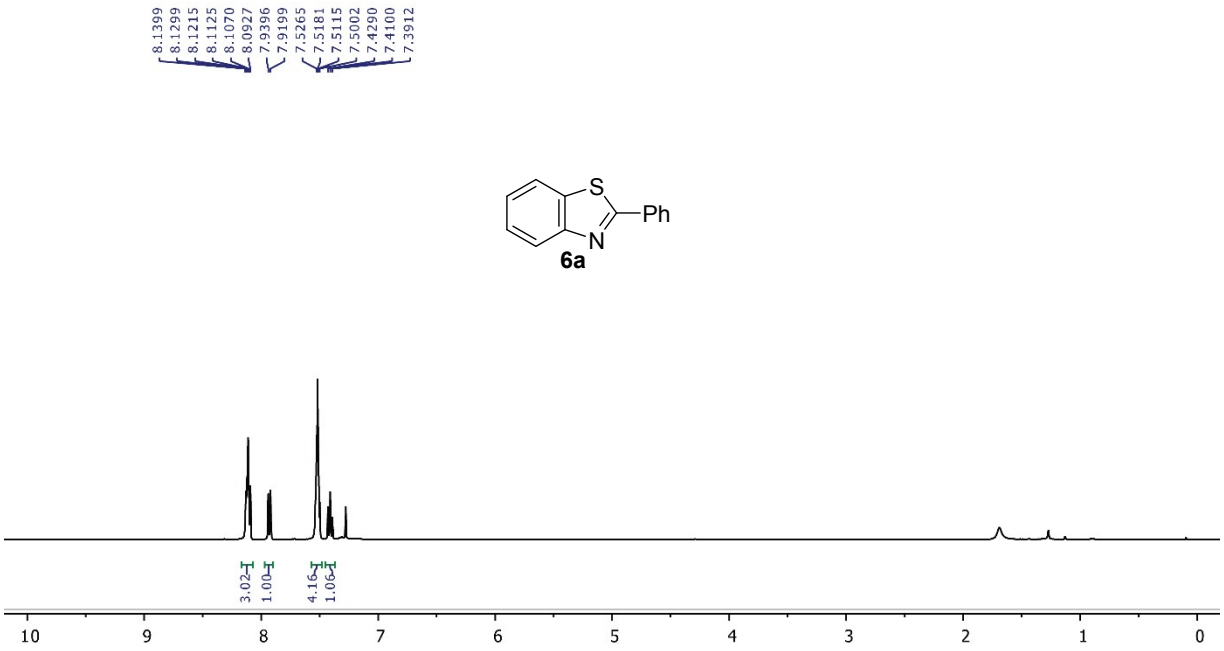

Figure S65. ^{1}H NMR of **6a** (400 MHz, $CDCl_3$)

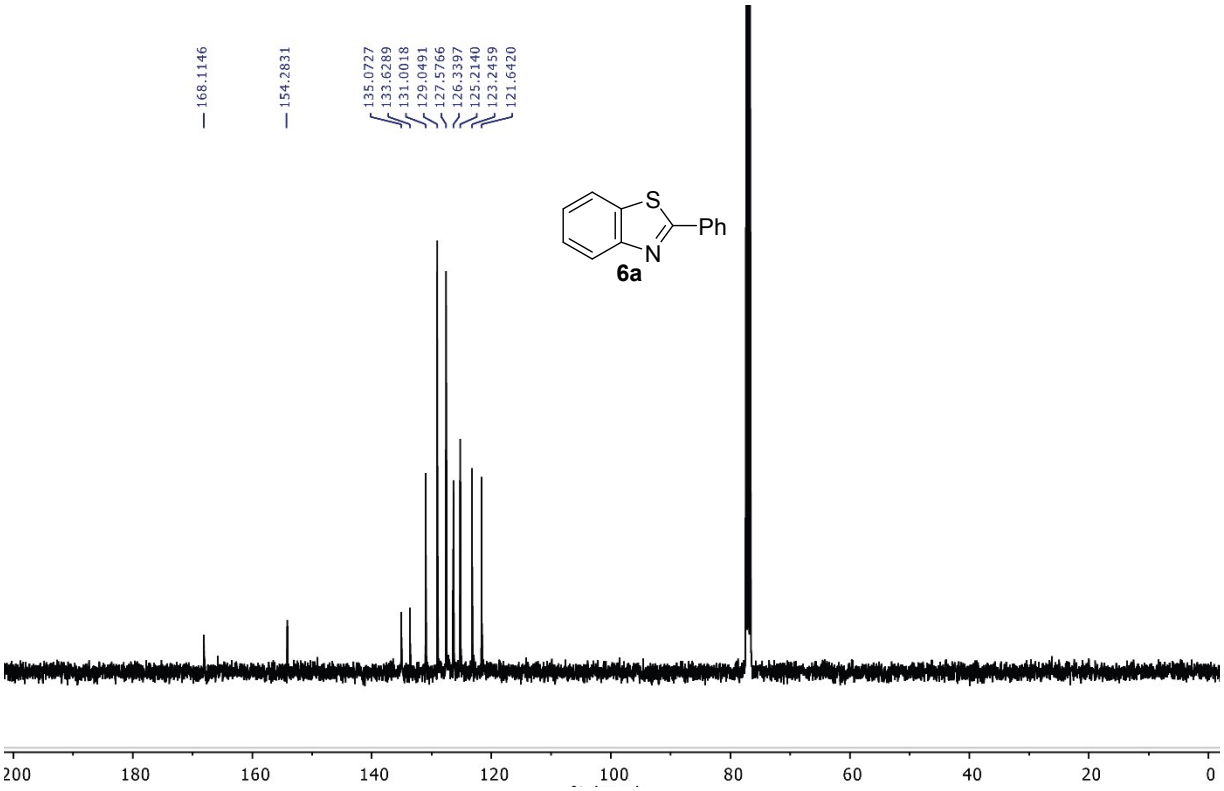

Figure S66. $^{13}C\{^{1}H\}$ NMR of **6a** (100 MHz, $CDCl_3$)

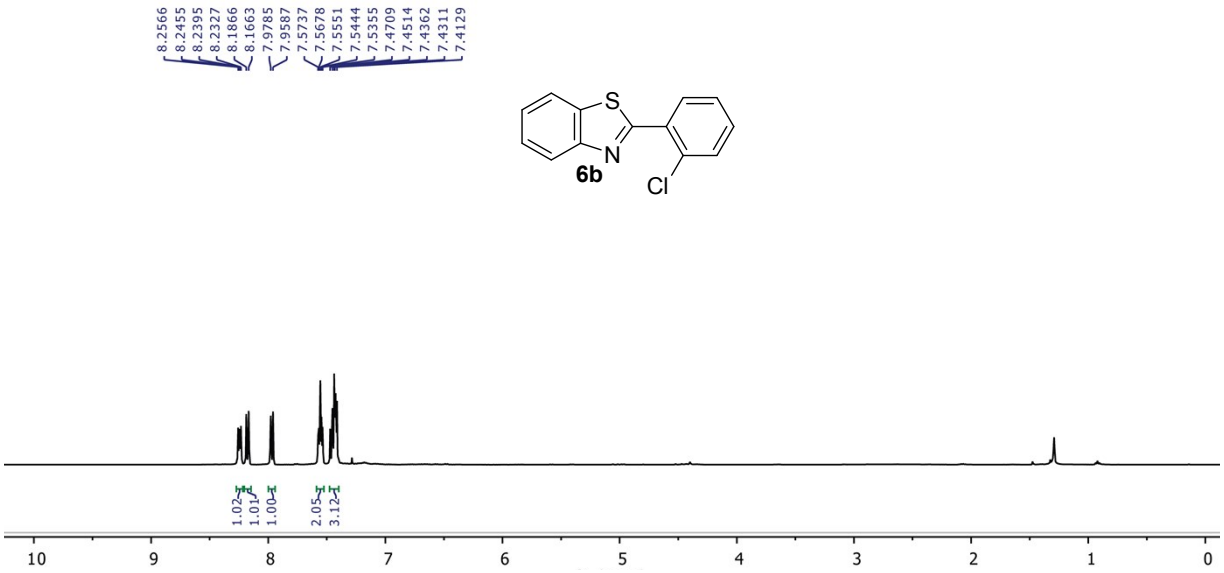

Figure S67. ^{1}H NMR of **6b** (400 MHz, $CDCl_3$)

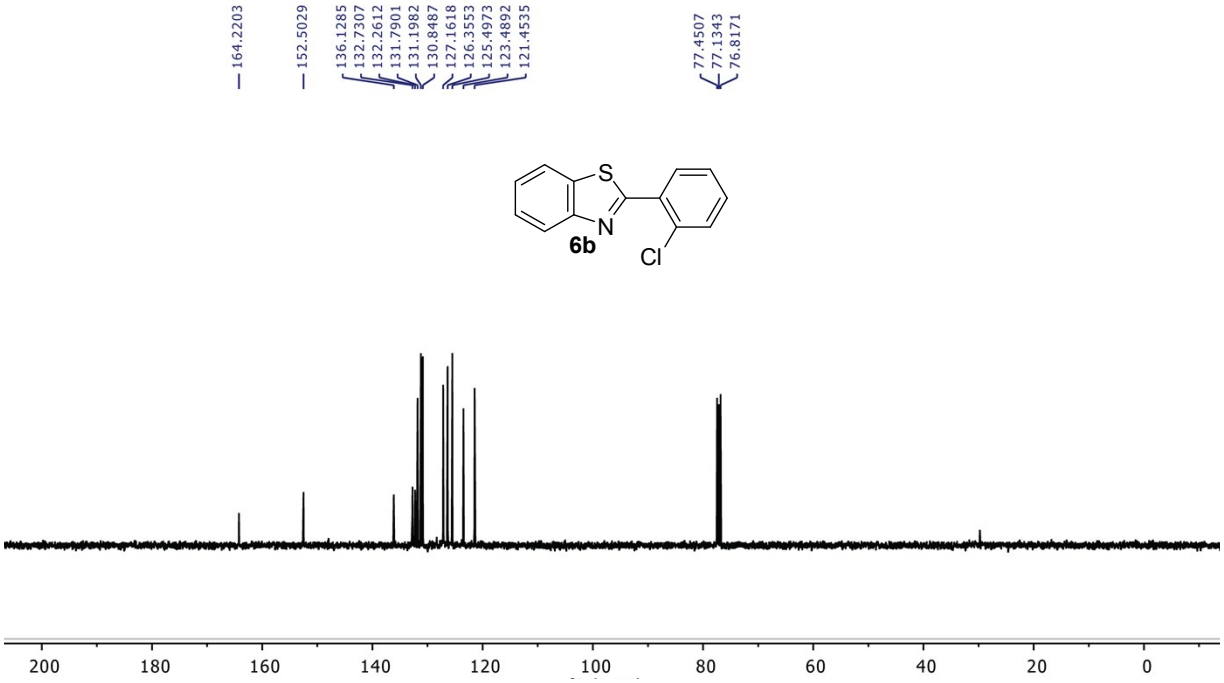

Figure S68. $^{13}C\{^{1}H\}$ NMR of **6b** (100 MHz, $CDCl_3$)

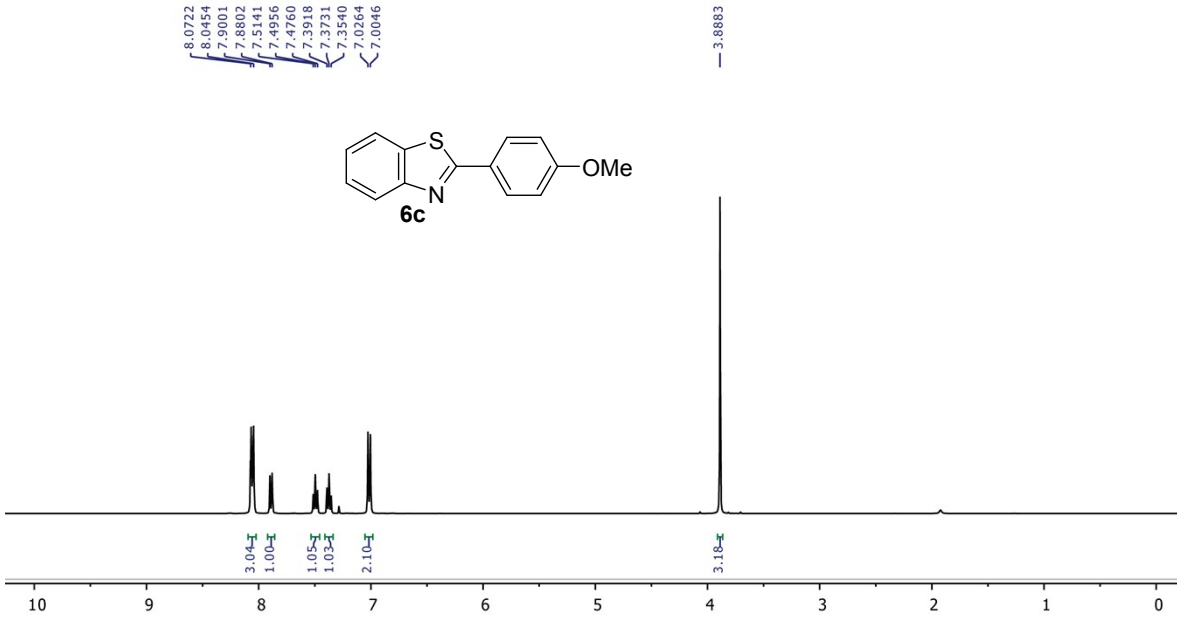

Figure S69. ^{1}H NMR of **6c** (400 MHz, $CDCl_3$)

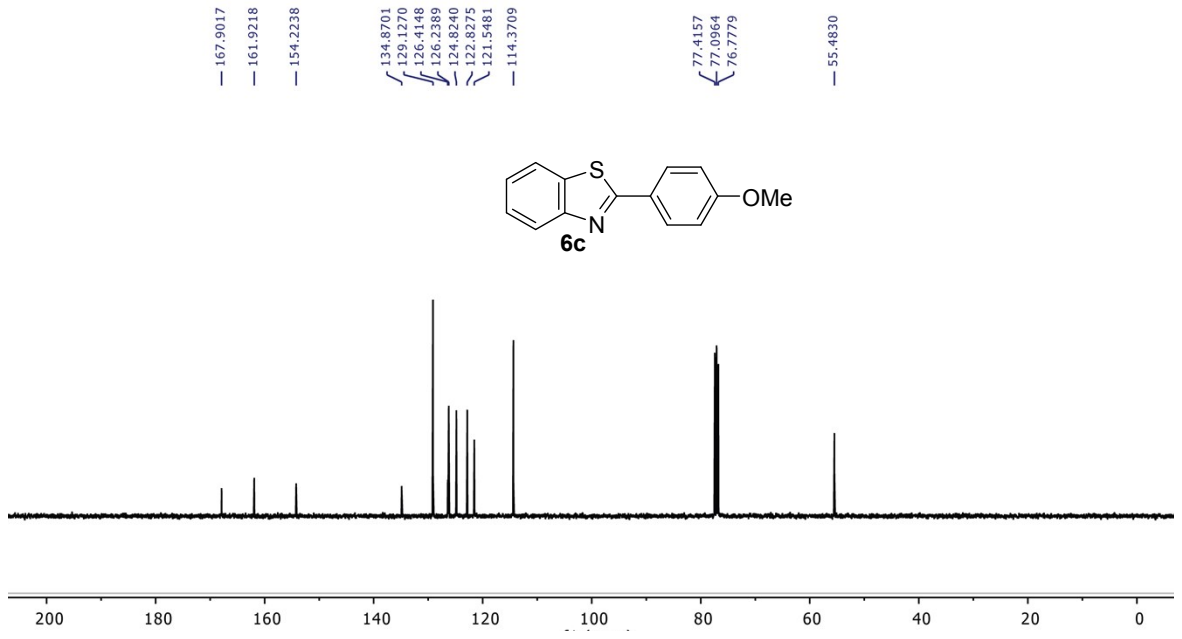

Figure S70. $^{13}C\{^{1}H\}$ NMR of **6c** (100 MHz, $CDCl_3$)

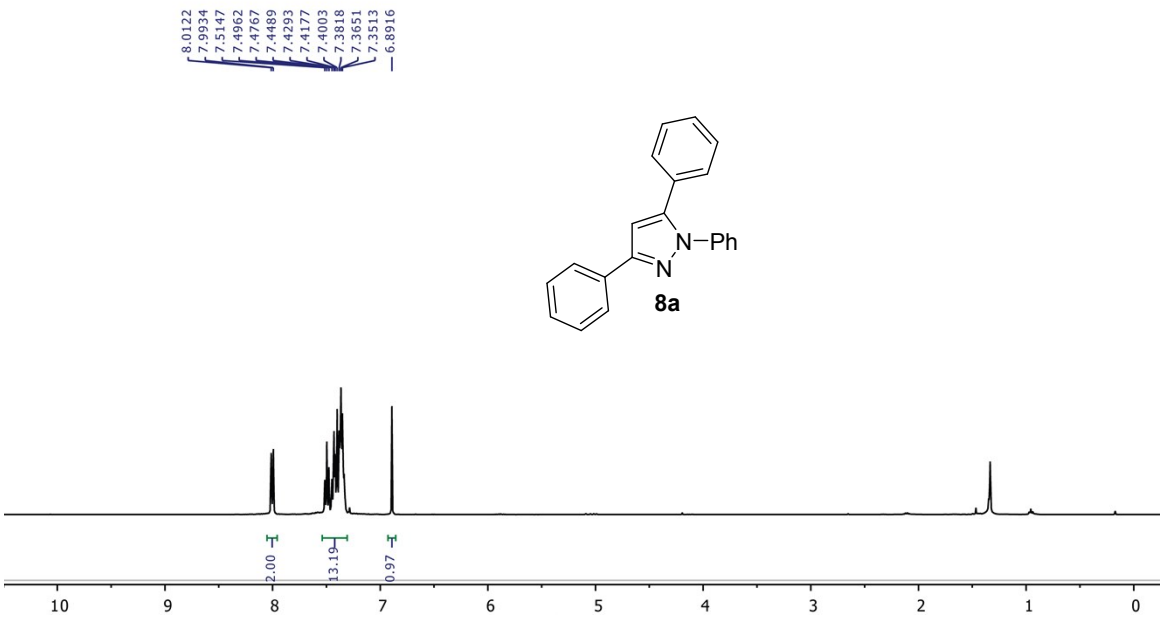

Figure S71. ^{1}H NMR of **8a** (400 MHz, $CDCl_3$)

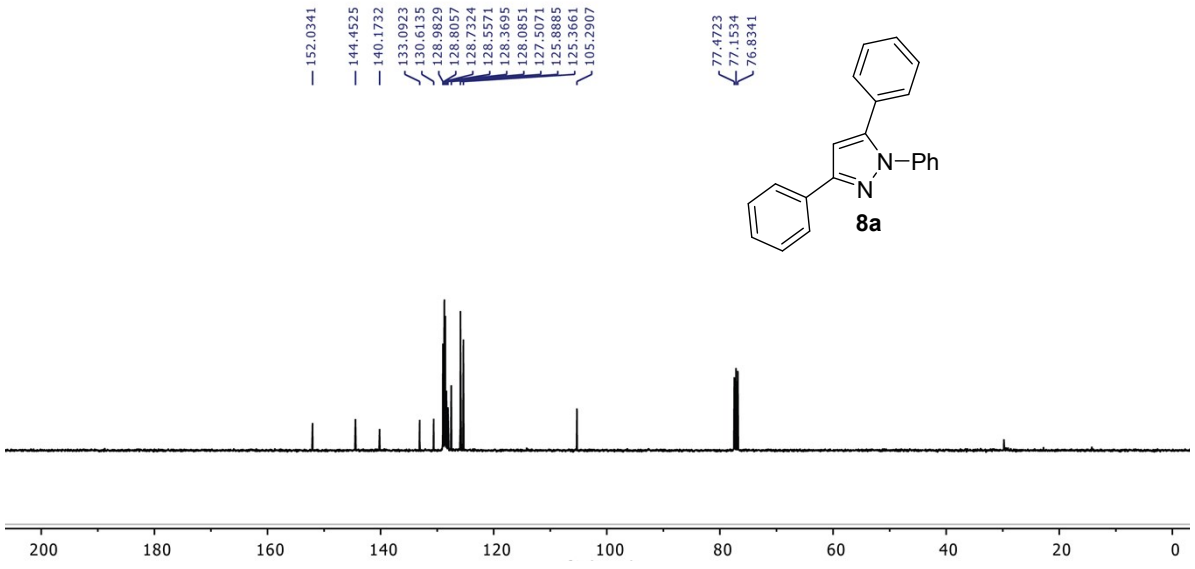

Figure S72. $^{13}C\{^{1}H\}$ NMR of **8a** (100 MHz, $CDCl_3$)

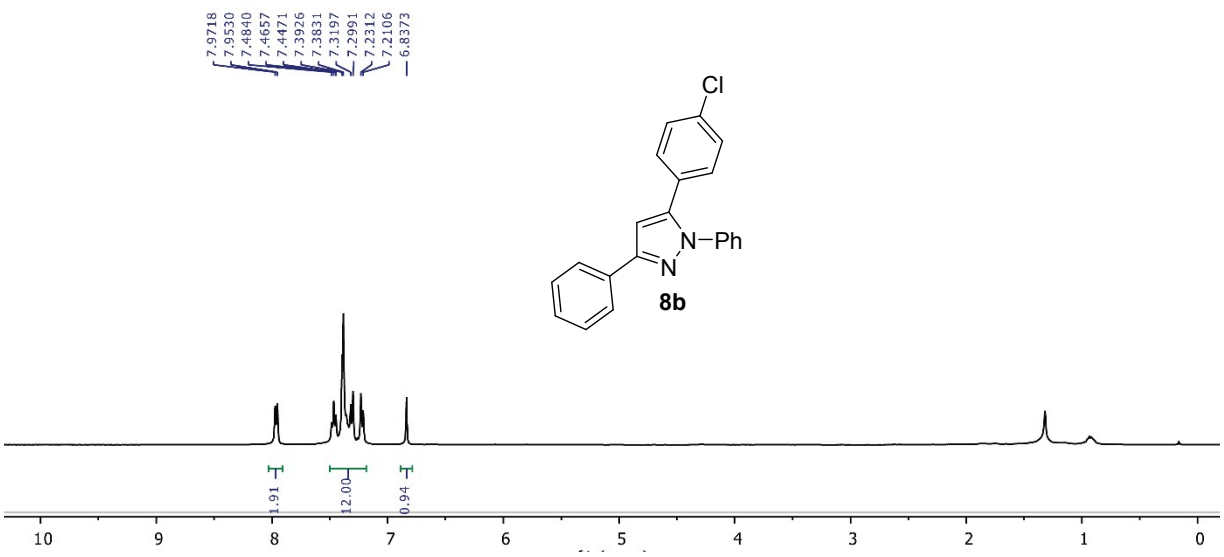

Figure S73. ^{1}H NMR of **8b** (400 MHz, $CDCl_3$)

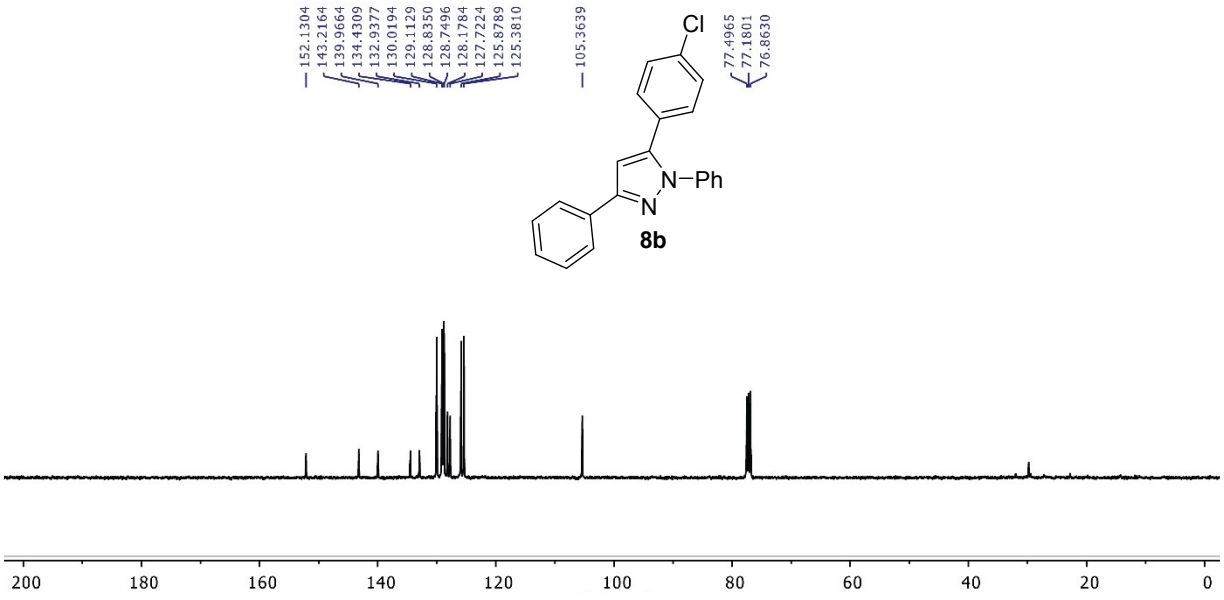

Figure S74. $^{13}C\{^{1}H\}$ NMR of **8b** (100 MHz, $CDCl_3$)

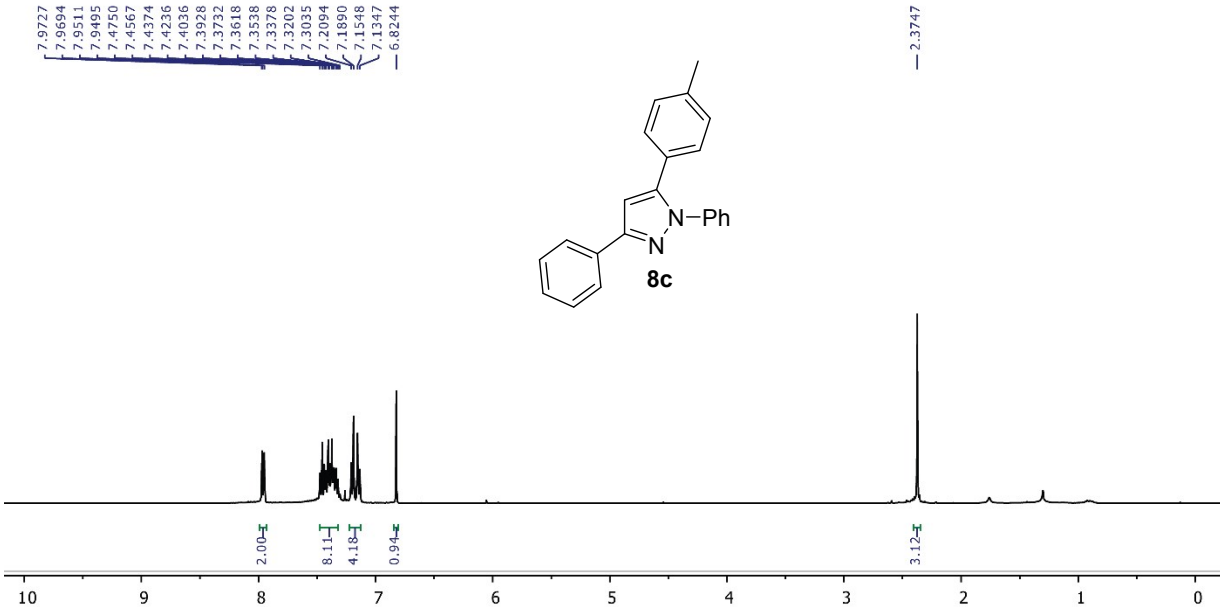

Figure S75. ^{1}H NMR of **8c** (400 MHz, $CDCl_3$)

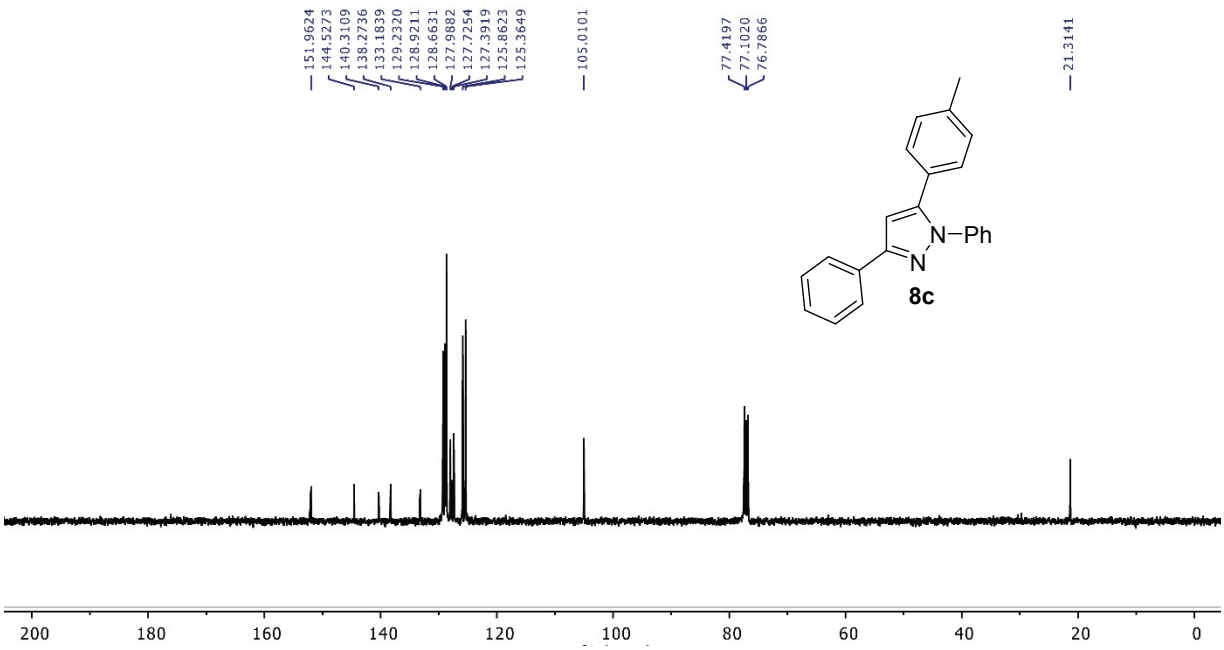

Figure S76. $^{13}C\{^{1}H\}$ NMR of **8c** (100 MHz, $CDCl_3$)

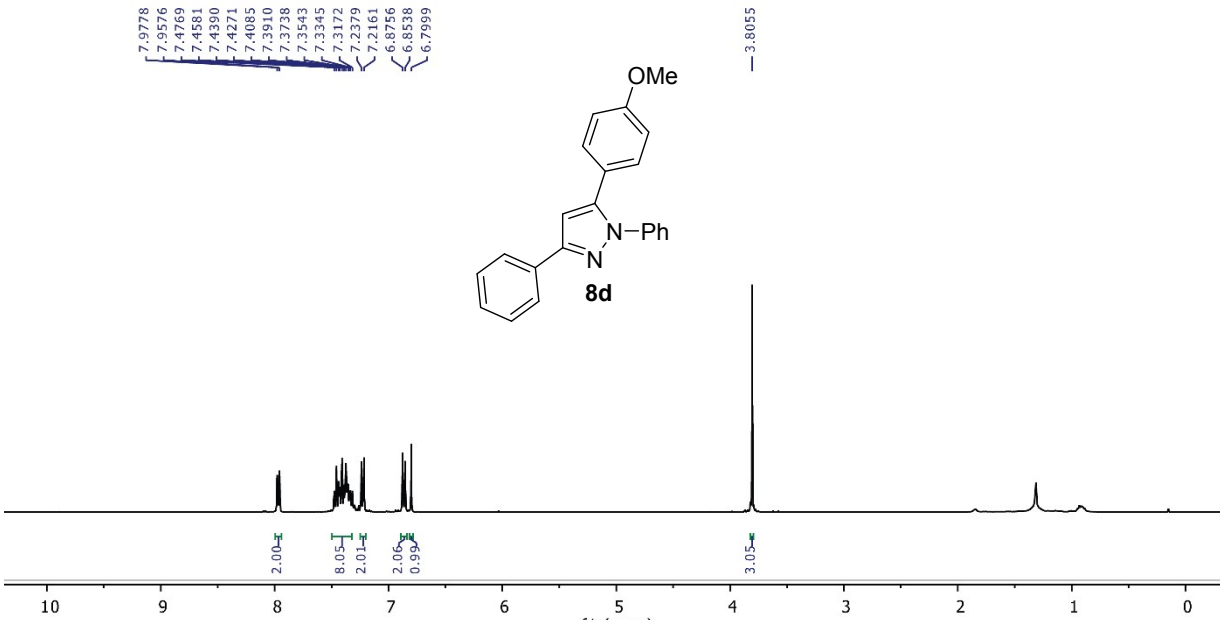

Figure S77. ^{1}H NMR of **8d** (400 MHz, $CDCl_3$)

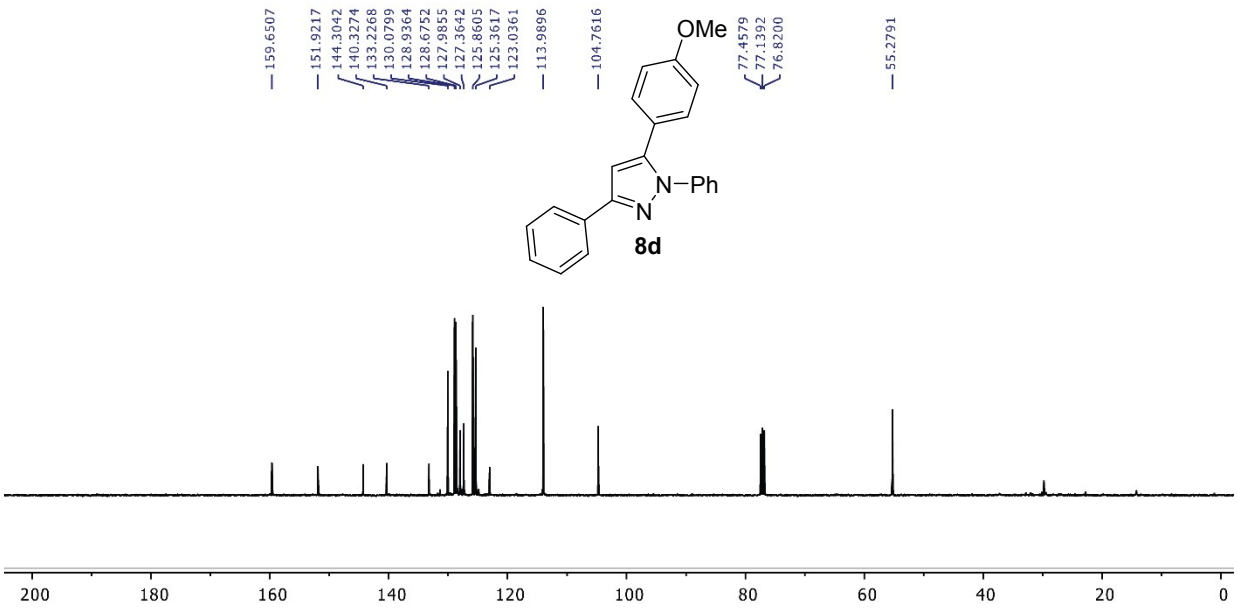

Figure S78. ^{13}C{^{1}H} NMR of **8d** (100 MHz, $CDCl_3$)

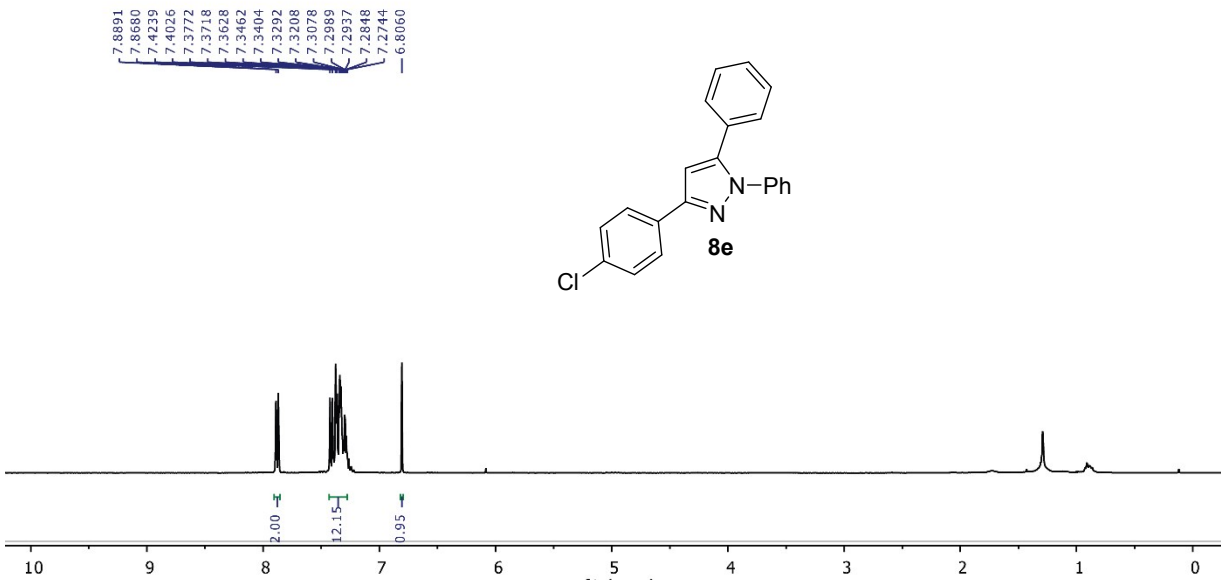

Figure S79. ^{1}H NMR of **8e** (400 MHz, $CDCl_3$)

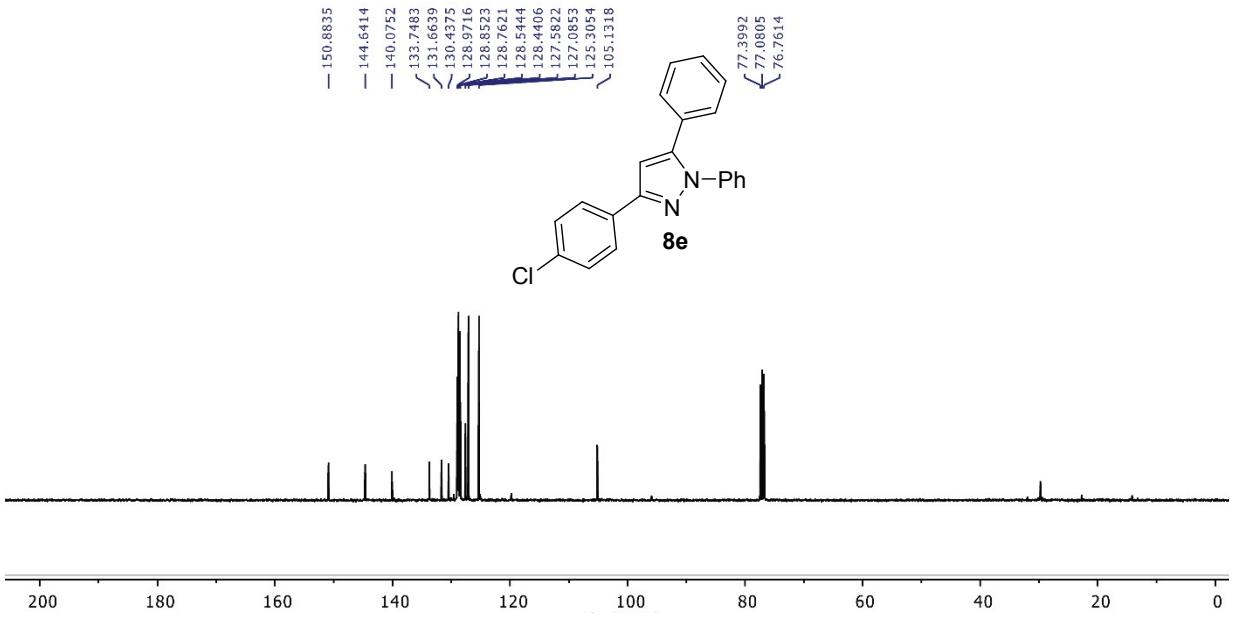

Figure S80. $^{13}C\{^{1}H\}$ NMR of **8e** (100 MHz, $CDCl_3$)